2007

Evaluation of a structural testing system

Anthony Samuelson
Iowa State University

Evaluation of a structural testing system

by

Anthony Samuelson

A thesis submitted to the graduate faculty

in partial fulfillment of the requirements for the degree of

MASTER OF SCIENCE

Major: Civil Engineering (Structural Engineering)

Program of Study Committee:
Terry J. Wipf, Co-major Professor
F. Wayne Klaiber, Co-major Professor
Brent Phares
Lester Schmerr

Iowa State University

Ames, Iowa

2007

TABLE OF CONTENTS

LIST OF FIGURES

LIST OF TABLES

ABSTRACT

According to the 2004 National Bridge Inventory, nearly 28% of Iowa's 25,000 bridges are rated as structurally deficient or functionally obsolete. Many of these structures are rated so by traditional visual bridge inspection and codified rating procedures. With many of these structures needing replaced or repaired, the problem is compounded by increasing bridge project costs and decreasing funding for such projects. A diagnostic tool is often necessary to accurately quantify the actual behavior and load carrying capacity of these deficient structures.

Iowa State University recently completed an evaluation of a commercially available diagnostic load testing system that combines the field testing equipment along with a software package for data interpretation, finite element modeling, and correlation of models to field data. The entire system produces a calibrated model of the load tested bridge for purposes of load rating. The system evaluated as part of this study was the Bridge Diagnostics, Inc. (BDI) Structural Testing System (STS). This paper documents a number of the efforts involved with the evaluation of the BDI system.

1. GENERAL INTRODUCTION

1.1. INTRODUCTION

According to the 2004 National Bridge Inventory (1), of the over 25,000 bridges in the State of Iowa, 27.8%, or around 7,000 bridges, are rated as either structurally deficient or functionally obsolete. A great number of these structurally deficient or functionally obsolete bridges, 85.8%, fall on the county highway system. Many of the bridges rated structurally deficient or functionally obsolete are the result of codified load ratings and visual inspections that place them in these categories.

It has been shown that when bridges are load tested using diagnostic load testing methods, they often exhibit greater strength than standard codified parameters predict (2). This is due to many factors such as unanticipated composite action between bridge girders and bridge decks, girder continuity over piers, and bridge bearing restraint. Often, codified load distribution factors are found to be different when compared to field measured factors. The aim of diagnostic load testing is to more accurately quantify the load carrying capacity of bridges with marginal load ratings through modern load testing techniques, advanced engineering analysis, and computer modeling.

1.2. THESIS ORGANIZATION

This thesis contains three separate papers related to diagnostic load testing and rating of bridges in the state of Iowa. The research was completed between the fall of 2000 and the summer of 2007. The work was funded by the Iowa Highway Research Board Project Development Division through the Iowa Department of Transportation as part of an evaluation of a commercial diagnostic load testing system for load rating purposes. The system investigated was the Bridge Diagnostics, Inc. (BDI) Structural Testing System.

The first paper highlights the modeling and optimization capabilities of the BDI system through a series of optimized models and ratings of three individual steel girder bridges in Iowa tested as part of this research project. The final ‘optimized’ model from each bridge was taken and the optimization limits were removed to uncover the statistical ‘optimized’ model with various Intelliducer configurations. Ratings of the additional models were then calculated to explore the connection between optimized parameters and load ratings. This was done in the hope that the entire testing process could be simplified down to its basics and that the simplest Intelliducer layout could be unveiled and the testing process refined.

The second paper was written for the First International Workshop on Structural Health Monitoring of Innovative Civil Engineering Structures presented by Intelligent Sensing for Innovative Structures of Canada. The paper was presented as a part of a workshop in Winnipeg, Canada in September of 2002. The paper highlights the use of the BDI system on a diagnostic load test of a steel girder bridge in Iowa. The thesis author was the primary author of this paper with guidance and assistance from the other authors listed. Mr. Espen Mellingen completed the modeling and rating of the bridge examined.

The third and final paper was written for the Midwest Transportation Consortium (MTC) student paper competition as part of the MTC scholar program. This paper is an overview and description of the BDI Structural Testing System, its application, and its use on a diagnostic load test. The paper highlights the many uses and tools available with the BDI system. The load test process is described from inception to completion.

1.3. REFERENCES

1. National Bridge Inventory, NBI Report, 2004. http://www.nationalbridgeinventory.com/nbi_report_200414.htm

2. Bridge Diagnostics, Inc., "Load Testing and Load Rating of Eight State Highway Bridges in Iowa," Report submitted to Iowa Department of Transportation, November 1999.

2. TESTING OF THREE BRIDGES AND OPTIMIZATION OF BRIDGE MODELS AND THE MODELING PROCESS

2.1 ABSTRACT

According to the 2004 National Bridge Inventory (1), nearly 28% of Iowa's 25,000 bridges are rated as either structurally deficient or functionally obsolete. Many of these structures are rated so by traditional visual bridge inspections and codified rating procedures. With many of these structures needing replaced or repaired, the problem is compounded by increasing bridge project costs and decreasing funding for such projects. A diagnostic tool is often necessary to accurately quantify the actual behavior and load carrying capacity of these deficient structures.

Iowa State University completed an evaluation of a commercially available diagnostic load testing system that combines field testing equipment along with a software package for data interpretation, finite element modeling, and correlation of models to field data. The entire system produces a calibrated model of the load tested bridge for purposes of load rating.

This paper documents three diagnostic load tests conducted by Iowa State University as part of their evaluation of the system along with further analysis of the field testing and modeling process in an attempt to streamline and simplify the field testing methods.

2.2 INTRODUCTION

There are over 25,000 structures classified as bridges on the highway and secondary road system in the state of Iowa (1). Over 20,000 of these structures fall under the jurisdiction and control of Iowa's 99 counties. Often these structures are in poor visual condition and hence, load rated at well below the structure's actual load capacity. Until recently, visual inspection has been the only cost-effective option for routine inspection and evaluation of a bridge's load carrying capacity. With the recent advent of affordable commercial diagnostic load testing systems, modeling and rating software, such as the Bridge Diagnostics, Inc. (BDI) Structural Testing System (STS) and companion software package, load testing is becoming an option that many local and state agencies can turn to beyond the typical visual inspection.

An Iowa State University research team completed an evaluation of a commercial load testing and rating package produced by Bridge Diagnostics, Inc. (BDI) of Boulder, Colorado (2). The BDI package includes everything needed for load testing, data plotting, finite element modeling, model calibration, and load rating. The BDI system evaluated included 40 strain transducers and associated

hardware to complete a diagnostic load test in minimal time, typically one day (6-10 hours) for a typical (3-span, 200 ft total length) bridge.

The aim of the research documented in this paper was to evaluate the load testing process in the field and minimize the amount of strain transducers needed to properly model and rate bridges. This was accomplished by reviewing three bridges tested through Iowa State's evaluation of the BDI system and further investigating the field data and finite element models to arrive at an efficient solution for the number of strain transducers required on any given bridge.

2.3 OVERVIEW OF THE TESTING AND MODELING PROCESS

The system developed by BDI is a systematic approach to the testing, modeling, and rating of bridges. The system is used in phases, each with their own tools and individual processes. Initially existing data on the bridge being evaluated are examined. Often, previous load rating calculations or visual inspection reports reveal the limiting or critical elements and sections of a bridge. This survey of existing data can then be used to develop an instrumentation plan for the bridge.

Generally, the instrumentation plan is designed to address the issues and concerns identified from the evaluation of the existing condition data. The plan should include the collection of data that may impact the attributes of the finite element model. Common issues include girder end conditions and the presence of composite action between structural members and the bridge deck.

2.3.1 Structural Testing System

Implementing the instrumentation plan in the field is simplified by the BDI Structural Testing System (STS). Installation of the strain transducers simply involves the cleaning of the surface at the transducer location and placement of the transducer using an adhesive and accelerant (3). Each transducer is referred to as an Intelliducer due to its ability to identify itself to the system control unit. This attribute allows for automatic calibration and balancing of the transducers. Each Intelliducer connects to a small box, called an STS Unit, in groups of four. Individual STS Units are connected to one another (typically in series) and finally to the Power Unit. This allows for a minimum number of wires to relay data for up to 64 Intelliducers. The Power Unit is connected to a PC that controls the functions of the system. Data can be collected at rates from 0.01 to 100 Hz.

The system also has a remote load position indicator called the Autoclicker. The Autoclicker uses a reflective strip on the load vehicle wheel, a photo sensor, and a handheld radio to transmit the truck position (in terms of wheel revolution) to the Power Unit.

2.3.2 Software Suite

The BDI Software Suite is used for the analysis, modeling, and rating of the bridge. Included in the package are software for graphing field and analytical data, model generation, and model analysis and calibration.

WinGRF is the first of the software tools used in the analysis of a bridge. WinGRF uses transducer output and load position data to plot load test results verses truck position on the bridge. When the user inputs information related to transducer location (e.g., transducer pairs, vertical distance between transducers, etc.) more advanced plots can be created (4). Results such as strain, neutral axis, and curvature may all be plotted with respect to vehicle position. Options, such as data filtering and offset correction may also be completed in WinGRF. This information can be used to obtain a preliminary understanding of the bridge behavior.

WinGEN is used to create a finite element model of the bridge. The software is limited to beam and shell elements. The initial model is created using the overall bridge geometry and the section properties from the as-built plans. Also, neutral axis location information identified from the field test data can be incorporated. Other significant differences discovered during the investigation of the field results can also be included in the model. The inclusion of rotational and/or translational springs at the supports is a typical model modification. Transducer locations are also input in the model for calibration with the field data.

WinSAC analyzes and calibrates the analytical model. Limits of properties, such as modulus of elasticity, moment of inertia, and spring constants, are input into WinGEN and then analyzed using WinSAC. Within these prescribed limits, the model is calibrated to the field results. WinSAC performs a statistical analysis of the model and analytical results to arrive at a final calibrated model from which load ratings can be calculated.

Final model results may be plotted using the WinGRF program. This will visually verify the analysis results generated from WinSAC.

2.4 BRIDGE DESCRIPTION AND EXPERIMENTAL PROGRAM

Three different bridges, all unique, were field tested with the Bridge Diagnostics, Inc. Structural Testing System (2). Each structure was instrumented with between 32 and 40 BDI Intelliducers. Data were recorded for various vehicle positions on each bridge and the results were plotted and processed.

2.4.1 Bridge #1

Bridge #1, designated by Boone County, Iowa as Boone County Bridge #11, carries secondary road L over Mineral Branch approximately one mile north of County Route E18 in northern Boone County. This 38 ft – 10 in. single span, no skew, non-composite steel girder and timber deck structure rests on steel channel bearings attached to timber piling with a timber backwall as shown in Figure 2.1. The superstructure consists of eight steel girders spaced on 2 ft – 6 3/8 in. centers for a roadway width of 17 ft, single lane loading, and an out to out width of 19 ft – 9 in. The deck consists of 4 in. timber planks laid transversely to the girders with a gravel driving surface over the timbers of roughly 6 in. thickness. The bridge has steel railings as shown in Fig. 2.2.

The bridge girders appear to be in fair condition, based on a visual inspection, with the exception of light rust on all girders. The east exterior girder appears to have been impacted by a large object and is slightly twisted. The bearings and backwall appear to be in good condition. The timber deck also appears to be in good condition.

The bridge girders were instrumented with 40 BDI strain transducers at 20 different locations, as shown in Fig. 2.3. The four westernmost girders were instrumented on the top and bottom flange at 2 ft – 6 in. from each abutment, mid-span, and near ¾ span. The east exterior girder and third girder from the east were instrumented at mid-span and at 2 ft – 6 in. from the north abutment.

The load was applied to the bridge using a loaded tandem-axle dump truck weighing 49.58 k, as shown in Fig. 2.4. Three different load test paths were defined for the bridge, Y1 through Y3, as shown in Fig. 2.3. Tests were run south to north. Y1 placed the passenger side-wheel line 2 ft from the centerline of the east exterior girder. Y3 was symmetrical to Y1 with the driver's side-wheel line 2 ft from the west exterior girder. The Y2 load path placed the passenger side-wheel line directly over the third girder from the east. Data were collected for each load path twice to insure the repeatability and integrity of the data. Given the short span length of the bridge, the use of the Autoclicker was not feasible. (One wheel revolution was around 11 ft.) The data collected included vehicle position 'tick' marks every 5 ft.

2.4.2 Bridge #2

Bridge #2, designated by the Iowa Department of Transportation as bridge number 4821.9O 080, carries secondary road R Avenue over Interstate 80 in rural Iowa County, Iowa. This four span, steel girder, no skew bridge constructed in 1963 consists of two main continuously welded steel plate girders with rolled floor beam sections. The bridge is symmetrical about Pier #2 with end spans of 46 ft – 6 in. and interior spans of 61 ft – 6 in for a total bridge length of 216 ft, as shown in Fig. 2.5. The

Figure 2.1. Photograph of the south abutment and superstructure of Bridge #1.

Figure 2.2. Photograph of the bridge railing on Bridge #1.

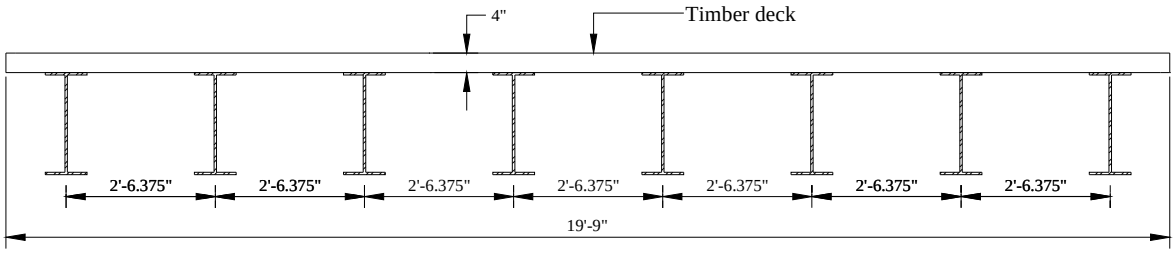

a. Cross-section of Bridge #1

Figure 2.3. Cross-section and plan view showing gage locations and load truck paths for Bridge #1.

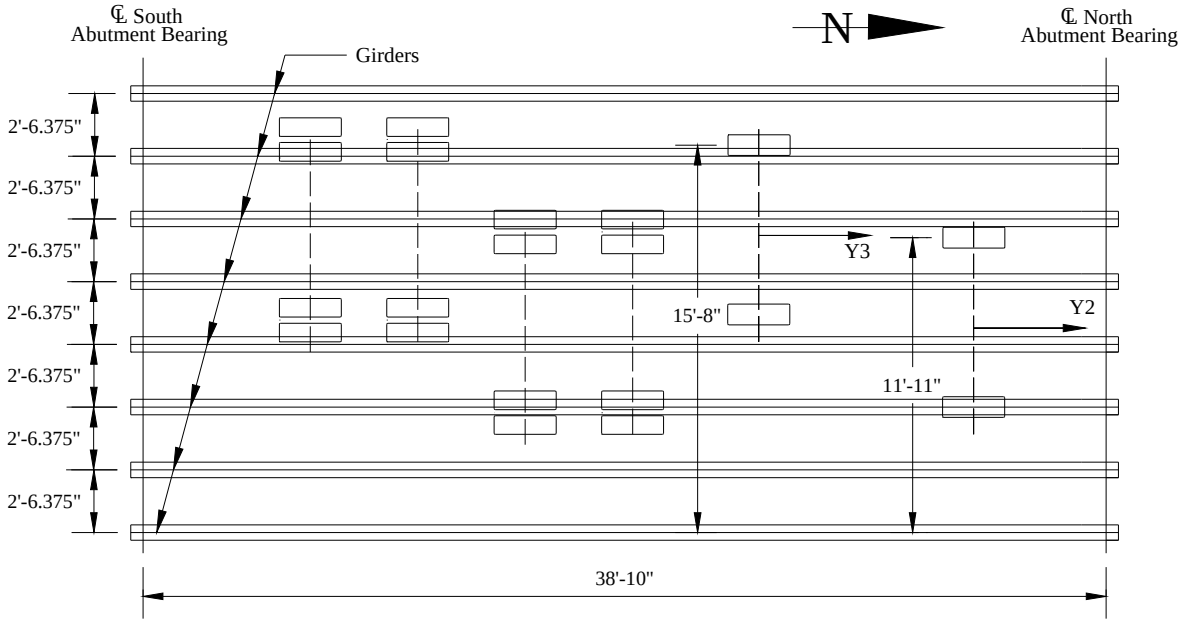

b. Plan view of bridge dimensions, girder spacing, and truck paths for Bridge #1.

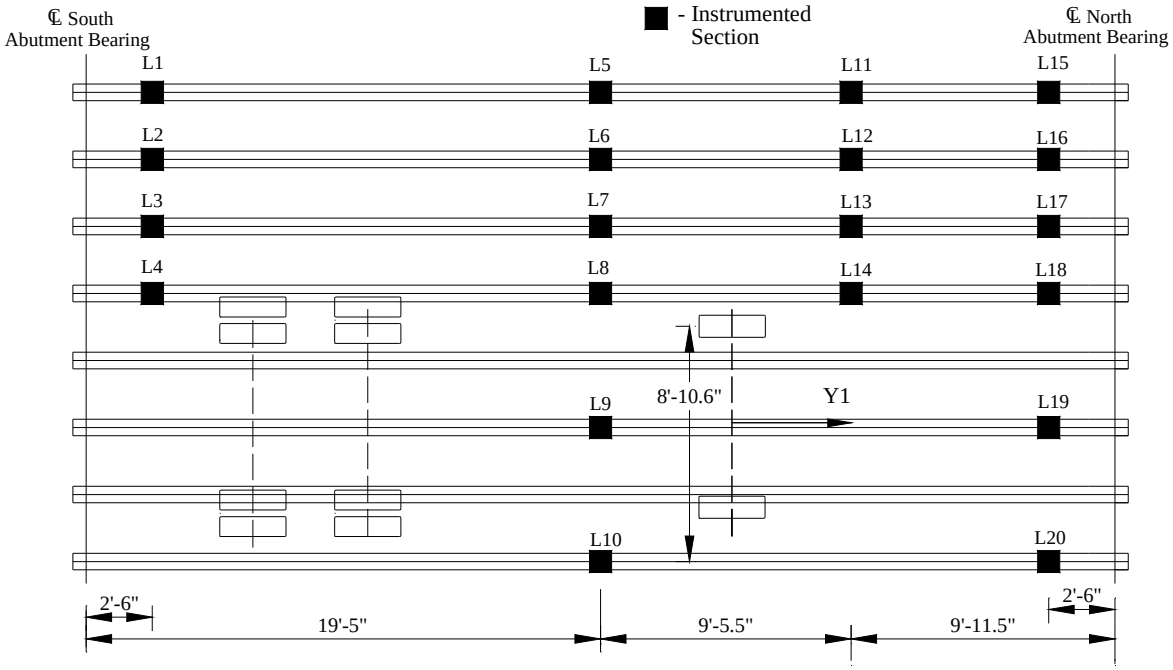

c. Plan view of gage locations, truck paths, and bridge dimensions or Bridge #1.

Figure 2.3. Continued

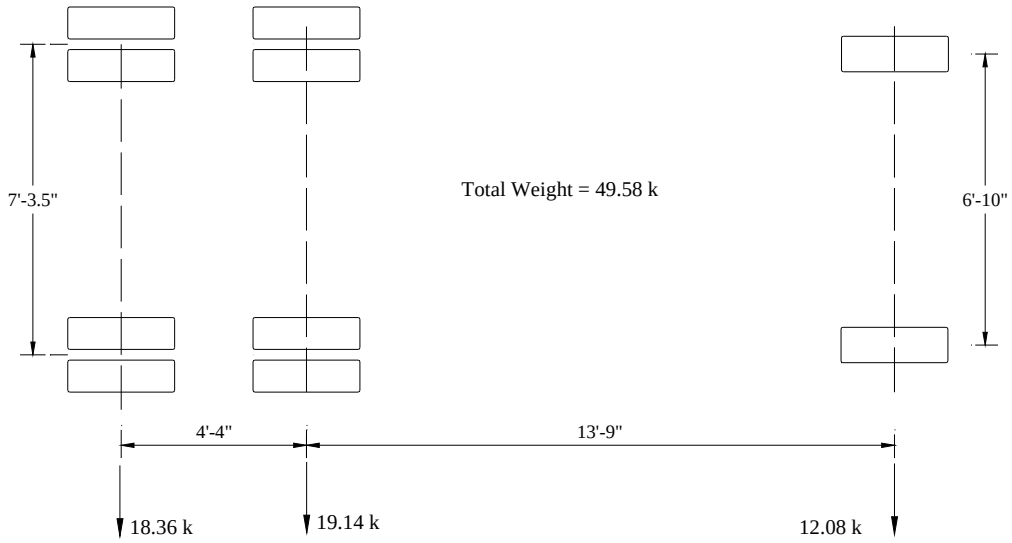

Figure 2.4. Load truck details for Bridge #1.

bridge has a 24 ft roadway and an out to out composite concrete deck measuring 28 ft – 4 in. with a steel handrail. The reinforced concrete deck is variable thickness with a thickness of 6 in. at the curb and 9 in. at centerline. The abutments are fixed type (stub) with rocker bearings at Piers 1 and 3, and a fixed bearing at Pier #2. The expansion devices at the pier are compression seals. The welded girders consist of three different cross-sections, one from the abutment to mid span in the end spans as well as the positive moment region of spans #2 and #3, one in the negative moment region about Piers #1 and #3, and another in the negative moment region about Pier #2.

Bridge #2 appears to be in good visual condition with only light rust on all bearings and no visible spalls or hallow areas on the deck. The reinforced concrete substructure units also appear to be in good visual condition. Rating calculations show that the floor beams are the controlling factor in the bridge load rating.

Given the symmetry of the bridge about Pier #2, it was decided that only half of the bridge needed to be instrumented with strain transducers. Spans #1 and #2 were instrumented with a total of 32 strain transducers at 16 different locations with two transducers at each location, one on the top flange and one on the bottom flange, as shown in Fig. 2.6. Each main girder was instrumented near the abutment, at mid-span of Span #1, each side of Pier #1 in the negative moment region, mid-span of Span #2, and in the negative moment region near Pier #2. A floor beam with the largest tributary deck area was selected and instrumented as verification of the load rating calculations. The floor

beam was instrumented a beam depth from each connection to the main girders, at mid-span of the floor beam, and 3 ft from center of the floor beam.

Load test data were collected from a total of four different load paths, as shown in Fig. 2.6. Paths Y1 and Y4 were symmetrical paths with a load truck wheel line directly over a main girder. Path Y2 placed a wheel line directly on the centerline of the bridge and path Y3 positioned the truck in the middle of the bridge roadway straddling the centerline. Data were collected twice for each load path to verify data collected. The BDI Autoclicker was used to record the load truck position; load truck details are given in Fig. 2.7.

a. Photograph showing profile of Bridge #2 over I-80 in Iowa County.

b. Photograph showing the roadway, deck, and railing of Bridge #2.

Figure 2.5. Photographs of Bridge #2.

2.4.3 Bridge #3

Bridge #3, designated by the Iowa Department of Transportation as bridge number 3150.7A 052, carries a local road over a drainage ditch north of the intersection of IA 386 and U.S. 52 in Dubuque County, Iowa. This 25 ft single span, zero degree skew, composite steel girder and reinforced concrete deck has integral abutments resting on timber piling as shown in Figs. 2.8 and 2.9. The five steel girders with steel channel section diaphragms support the original 8 in. reinforced concrete deck and a 1.75 in. P.C. overlay. The roadway width is 18 ft and the deck measures 19 ft – 8 in. out to out, and the barrier rails are reinforced concrete. The bridge, originally constructed with only four girders, was widened in 1984 and an additional girder was added. There was a visible construction joint between the original bridge deck and the deck added in 1984. Bridge #3 appeared to be in good visual condition with no rust present on the bridge girders and no serious concrete deterioration.

Bridge #3 was instrumented with 32 strain transducers at 15 different locations, as shown in Fig. 2.10. Each of the five girders were instrumented at the top and bottom flange 2 ft from each abutment face and at mid-span. Strain transducers were also installed at the top of the reinforced concrete barrier rail at two locations over one exterior girder 2 ft from the face of the abutment and at mid-span.

Only two load paths were used for the testing of Bridge #3, as shown in Fig. 2.10b. Path Y1 placed the driver's side wheel directly over the center of the middle girder. Path Y2 was symmetrical to path Y1 in that the passenger's side wheel was over the middle girder. Data were collected for each path twice to verify the collected data. Given the short span length of the bridge, the use of the Autoclicker was not feasible. (One wheel revolution was around 11 ft.) The data collected included vehicle position 'tick' marks every 5 ft. Load truck details are given in Fig. 2.11.

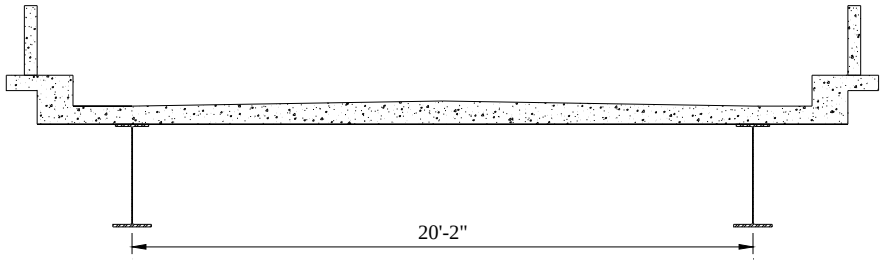

a. Cross-section of Bridge #2 near mid-span.

Figure 2.6. Load test details for Bridge #2.

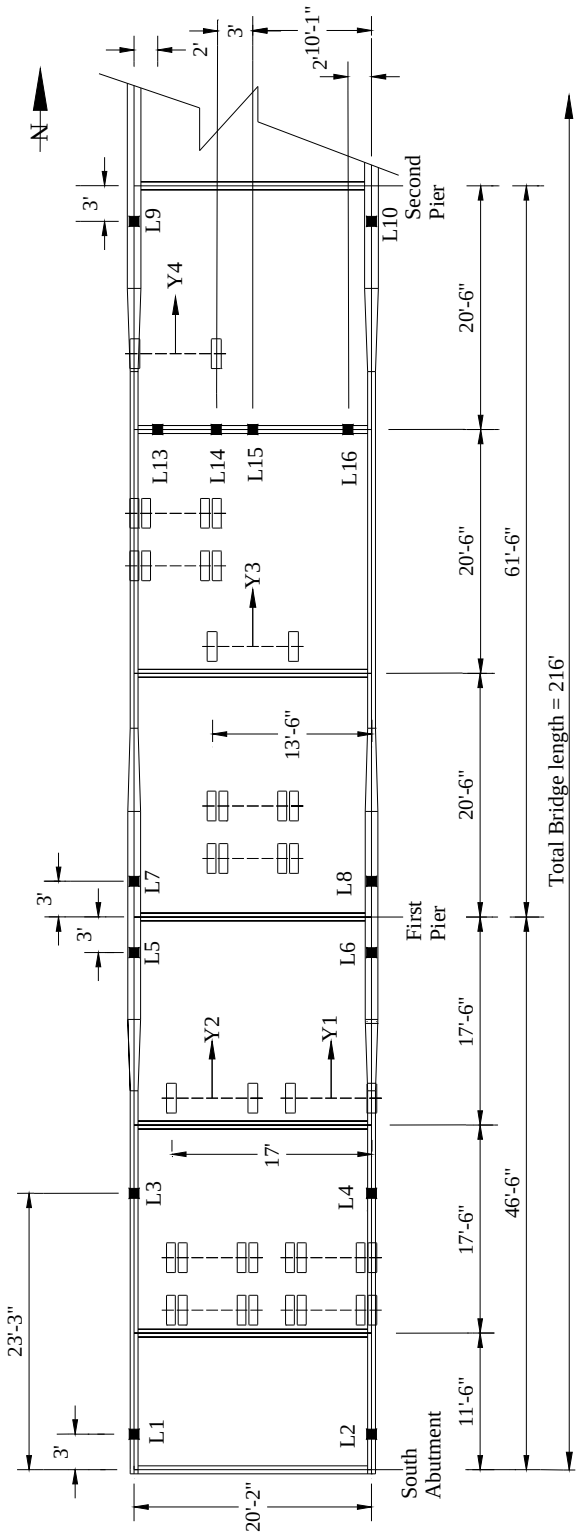

b. Test vehicle load paths, instrumentation layout, and geometry of Bridge #2.

Figure 2.6. Continued

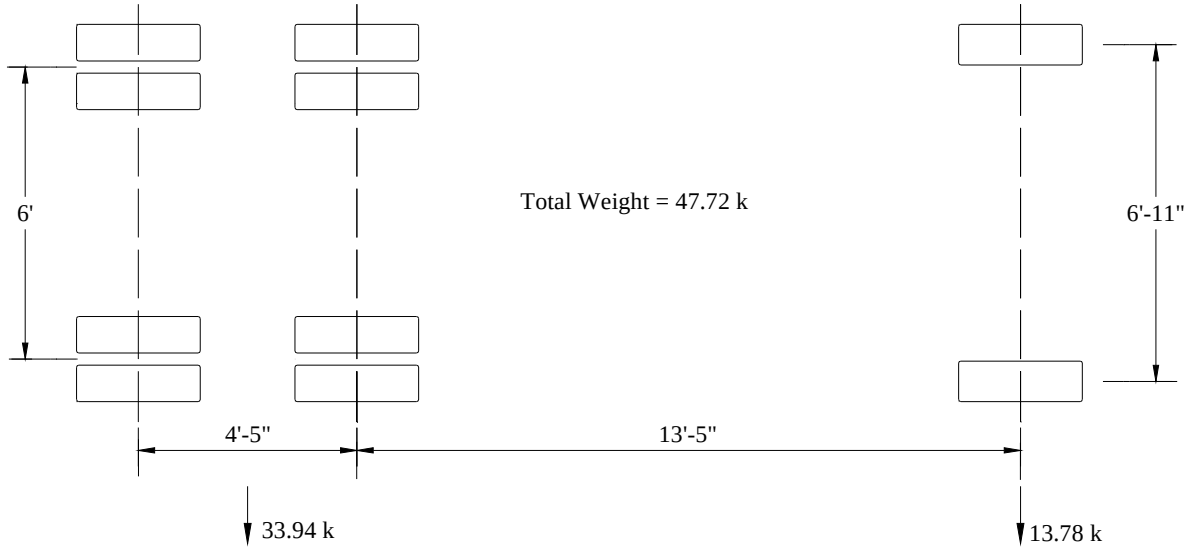

Figure 2.7. Load vehicle details for Bridge #2.

Figure 2.8. Roadway view of Bridge #3.

Figure 2.9. Profile of Bridge #3 showing barrier rail and exterior girder.

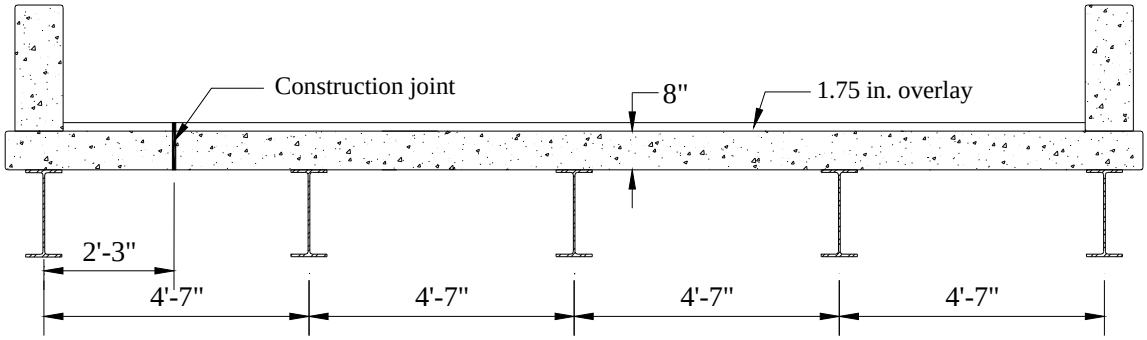

a. Cross-section of Bridge #3.

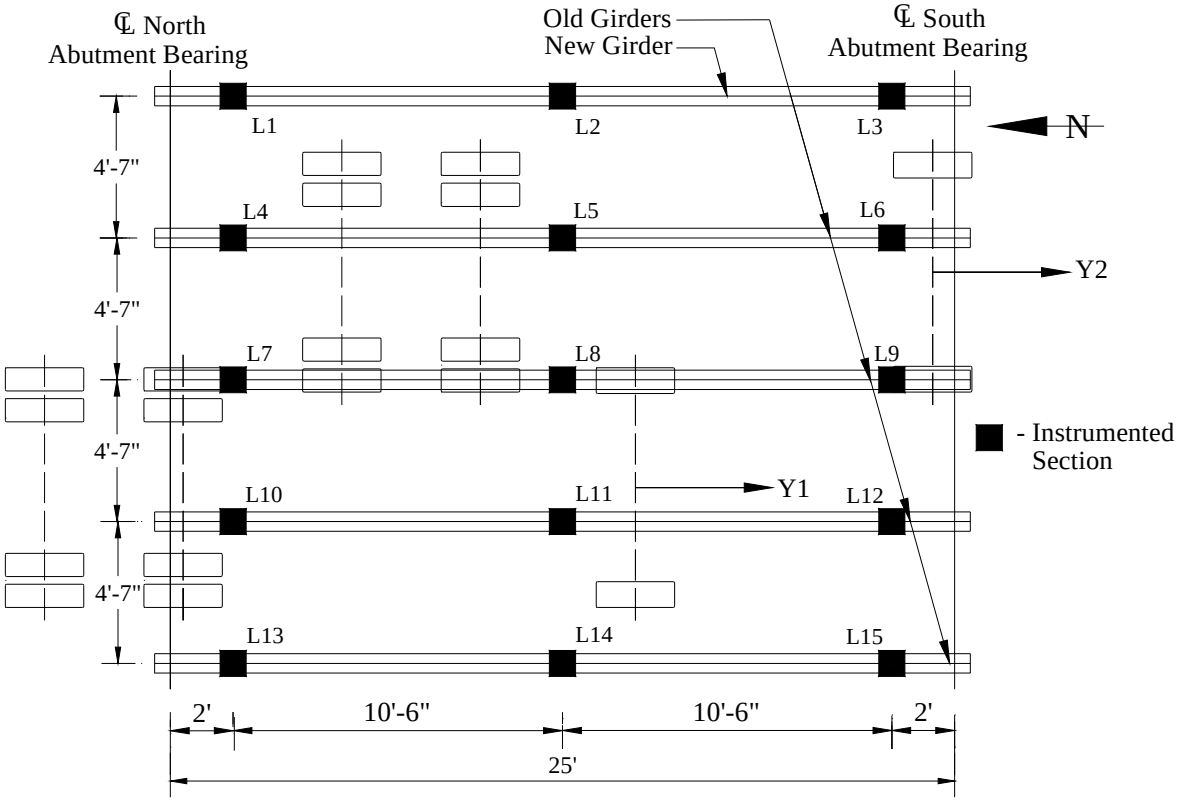

b. Plan view showing test vehicle paths and instrumentation layout for Bridge #3.

Figure 2.10. Load test details for Bridge #3.

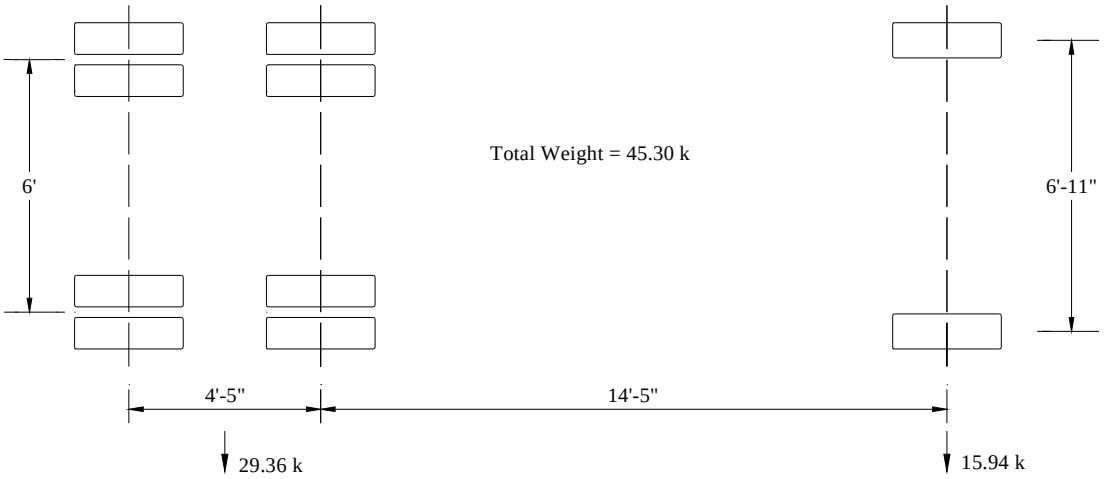

Figure 2.11. Load test vehicle for Bridge #3.

2.5 MODELING AND RATING RESULTS

Upon completion of data plotting and visual analysis of the field test results, preliminary finite element models of each bridge were created using WinGEN. Each preliminary model was created using the plan geometry, which had been verified in the field during load testing, and the assumed design structural properties for each structural member of the bridges. Once each preliminary model was assembled, an initial analysis was completed by subjecting the model to the same load and load paths as were examined in the field on the actual bridges. The resulting model strains were then plotted along with the field measured strains so that an assessment of the preliminary model could be completed. From this analysis, element group structural property limits and other model input variables were adjusted for final calibration of the model to the field measured data. The WinSAC program was used to calibrate the finite element model to the field measured strain data. This resulted in a final optimized model of each bridge that included the optimized model structural properties that were allowed as variables in the modeling process. Each optimized model was then load rated using features in the WinGEN and WinSAC programs. In each load rating model, the optimized structural properties were used to determine how dead and live loads were distributed to the load carrying members of the bridge. Structural capacities were computed by traditional methods and input into WinGEN for each structural member of each bridge. The final optimized models were then subjected to standard load rating vehicles and bridge load ratings were calculated using WinSAC.

In addition to the modeling completed for the calibration and rating of each bridge, additional models were created for each bridge with different end results in mind. Each calibrated model was copied and the limits established for optimization properties were increased by an order of magnitude for the upper bound and reduced to zero for the lower bound. This created a "limitless model" that was not limited by physical property limits and a true statistical optimization could be performed. This new "limitless model" was optimized using all strain transducer data and the resulting optimized properties recorded. Load ratings were then calculated for these additional models of each bridge by using previously calculated load capacities for each bridge member and utilizing the structural properties output from the additional models for determining the load distribution for each bridge.

In an effort to investigate what effect the number of transducers used on a diagnostic load test had, further modeling was completed by beginning with the 'limitless models' and full transducer layout for each bridge. Transducers were removed four at a time, two pairs of two transducers with one at the top flange and one at the bottom flange, to create these additional models. Ten new and unique models were created for each reduction of four transducers. For instance, if a bridge was instrumented and modeled with 40 strain transducers, one additional model was created with the expanded limits on optimized properties, ten new models were created with 36 strain transducers, ten new models with 32 strain transducers, and so on until the lower bound for transducers was reached. The lower bound was defined as the minimum number of strain transducers required to meet the requirements of the optimized parameters. This was determined by examining the number and type of structural properties being optimized and defining a minimum transducer layout that would provide sufficient data to optimize each structural property. Each new model was approached with the mindset that if only X number of transducer locations could be instrumented, what would the layout look like. As stated earlier, ten new transducer layouts were created resulting in ten additional models. Numerical results and transducer layouts used in the additional modeling are presented in Appendix A. A non-random approach to the reduction in strain transducers used in modeling is presented in Appendix B.

2.5.1 Bridge #1

All strain data were plotted against load vehicle position. A visual inspection of the data confirmed that transverse symmetry was present and that very little to no end restraint was present. The visual inspection of the strain data also confirmed that the timber deck provided no composite action. Further review of the strain data indicated that the steel rail on the exterior of the bridge did not contribute any additional stiffness to the exterior girders.

Three element groups were defined for the finite element model of Bridge #1: one for the moment of inertia (I_y) of the steel I-girders, one for the elasticity (E) of the timber deck, and one for the rotational restraint (K_y) of the girders at the abutments. These elements comprise the structural members present and behaviors expected from this type of bridge. Despite little to no end restraint visible in the examination of the field data, the abutments were modeled as rotational springs. Each girder was modeled with beam elements and the deck was modeled using shell elements. The rotational restraint was modeled using rotational spring elements.

The original calibrated model was optimized with all 40 strain transducers and placed limits on the acceptable values of girder I_y, deck E, and spring K_y. The optimized properties of the calibrated model are presented in Table 2.1. Placing limits on the acceptable values of the finite element properties guarantees that the optimized model properties are realistic. As part of this research, these limits were expanded in the additional modeling.

Given that the original model was created using 40 strain transducers at 20 different locations, each successive model group of ten reduced the number of strain transducers by four and locations by two. The lower bound for Bridge #1 was defined as eight strain transducers, four transducer locations. This minimum transducer arrangement met the requirements to measure the strain response of the girders for optimization of girder I_y, quantify girder end restraint for spring K_y, and measure the transverse load distribution of the bridge in order to quantify deck E. The initial model was modified by deleting transducer locations. Each model was optimized with the reduced number of strain data points. The results of the various models are presented in Fig. 2.12. As expected, in models where the I_y of the girders increased, the K_y value of the abutment spring decreased; the inverse is also true. Also, in most cases a lower I_y value resulted in a lower deck E value; the inverse of this is also true. No apparent link between deck E and spring K_y was found.

Given the simplicity of Bridge #1, a single simple span with steel girders and non-composite timber deck, the values for the additional model parameters did not vary greatly from the original optimized model parameters. The low variability of the additional model parameters verifies that the original optimized model parameters accurately represent Bridge #1. It should be noted that data outliers do exist in models utilizing 12 or less strain transducers in girder I_y values, the main structural value for Bridge #1. For instance, the highest girder I_y value (1478 in^4) corresponds to the lowest value of spring K_y (0 k-in/rad). The presence of these outliers represents the lower bound of strain transducers needed for an accurate finite element model of Bridge #1.

Load ratings for each additional reduced gage model were calculated using WinSAC. The output of each additional rating model was flexural load ratings for the interior and exterior girders

for HS-20 loading. The results of the additional ratings are presented in Fig. 2.13. Traditional codified load rating calculations, LFD method, for HS-20 loading yielded inventory ratings of 0.92 and 1.00 for interior and exterior girders, respectively. The optimized BDI model yielded HS-20

Table 2.1. Bridge #1: Initial and optimized properties for finite element model of Bridge #1.

Section	Property	Units	Initial	Optimized
Girder	I_y	in^4	1,230	1,255
Timber deck	E	ksi	1,000	845
Spring (rotational)	K_y	in-k/rad	0	29,210

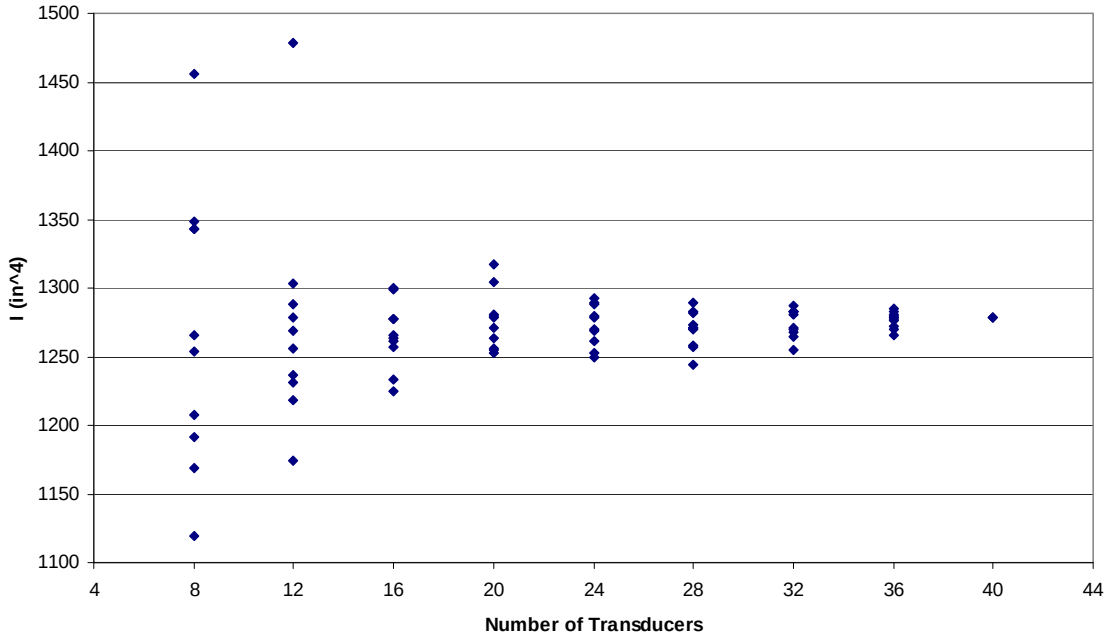

a. Optimized girder I_y values versus total number of strain transducers for Bridge #1.

Figure 2.12. Data plots showing optimized model properties versus number of strain transducers per model for Bridge #1.

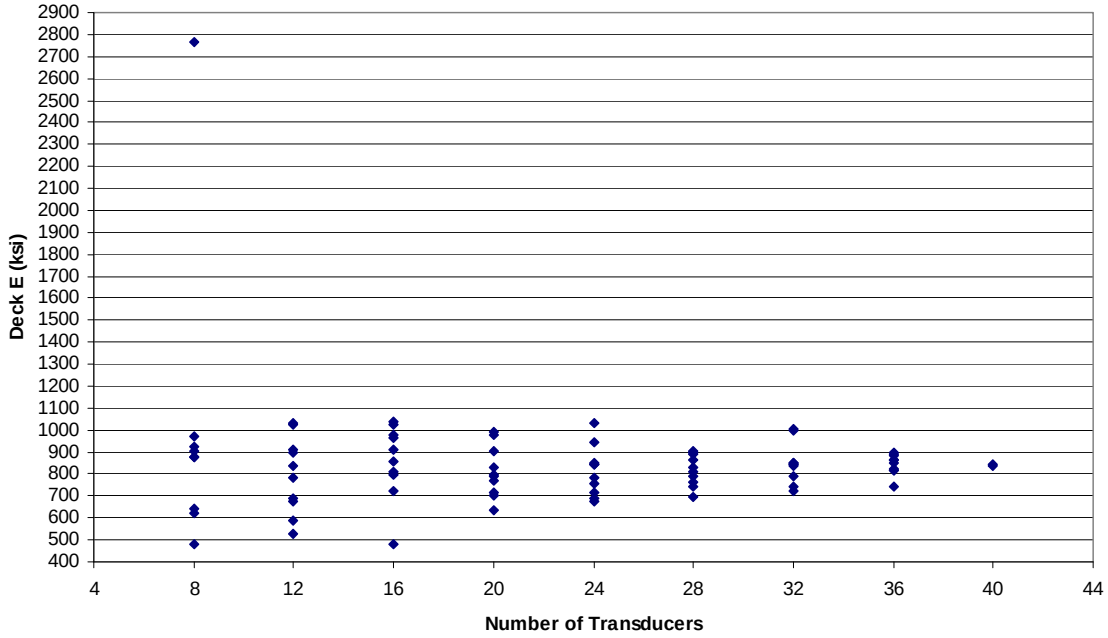

b. Optimized deck E values versus number of strain transducers for Bridge #1.

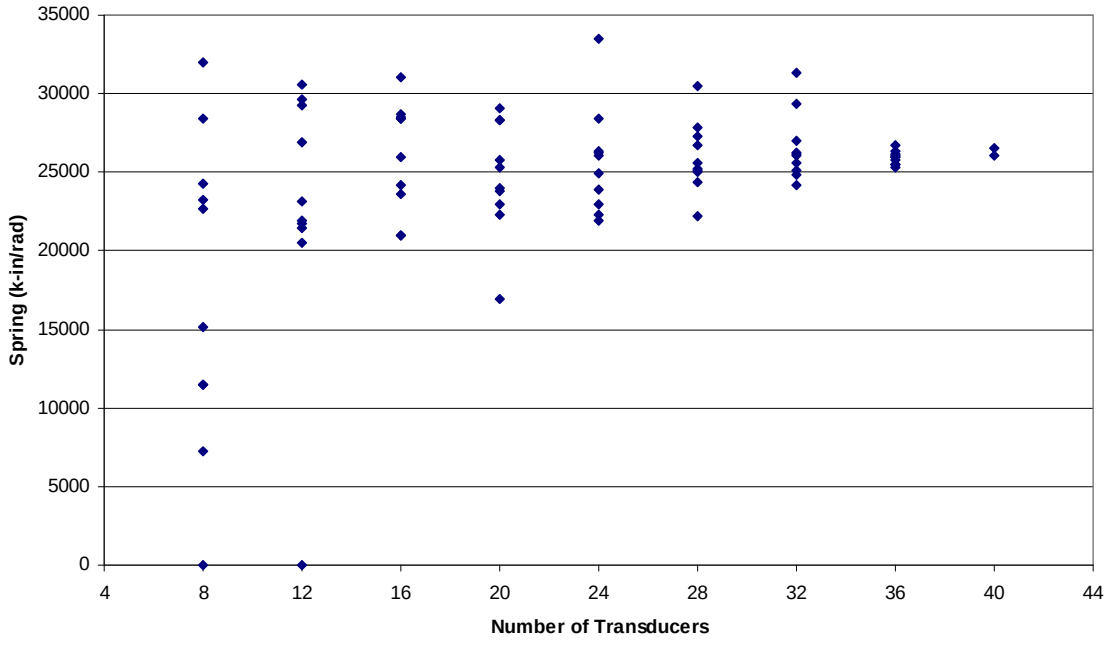

c. Optimized spring K_y values versus number of strain transducers for Bridge #1.

Figure 2.12. Continued.

inventory load ratings of 1.31 and 1.54 for interior and exterior girders, respectively. This represents increases in the HS-20 load ratings for the interior and exterior girders of 42% and 54%, respectively. The additional ratings created using optimized properties from the reduced transducer models had consistent rating values to the optimized ratings. The interior girder ratings were within 5% of the optimized rating, 1.31, for models using 16 or more transducers. The maximum variation from the optimized value for the exterior girder was 13.7% below the original BDI rating, or a rating of 1.13, in a 12 gage model. This low rating was the result of the spring K_y value of the model being zero, thus no end restraint in the bridge girder. Ratings for the interior girder were more consistent throughout the additional rating models. All but one additional rating was within 5% of the original BDI rating value of 1.54, and that rating was the result of an 8-gage model. As expected, optimized models with extreme property values, those not similar to others, produced ratings outside of the typical envelope presented in the plots.

While the additional rating models were consistent with the optimized model, given the small investment in time a full transducer layout required, the extra gage placement is warranted to ensure a more accurate picture of the bridge's behavior and an improved load rating.

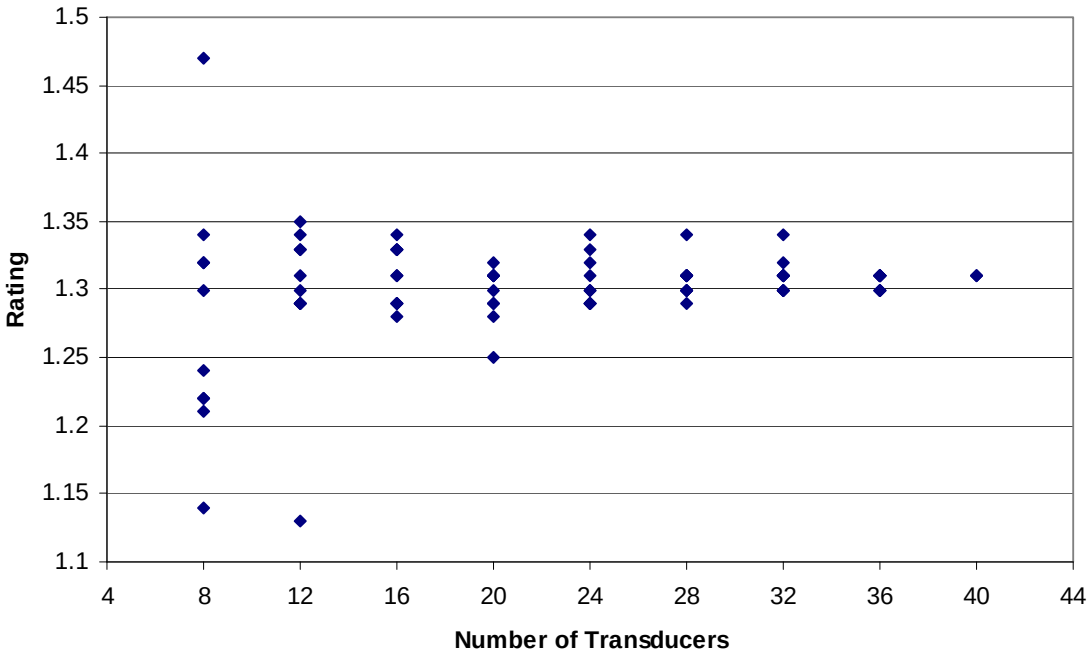

a. Interior girder load ratings for Bridge #1.

Figure 2.13. Additional HS-20 flexural load ratings for Bridge #1.

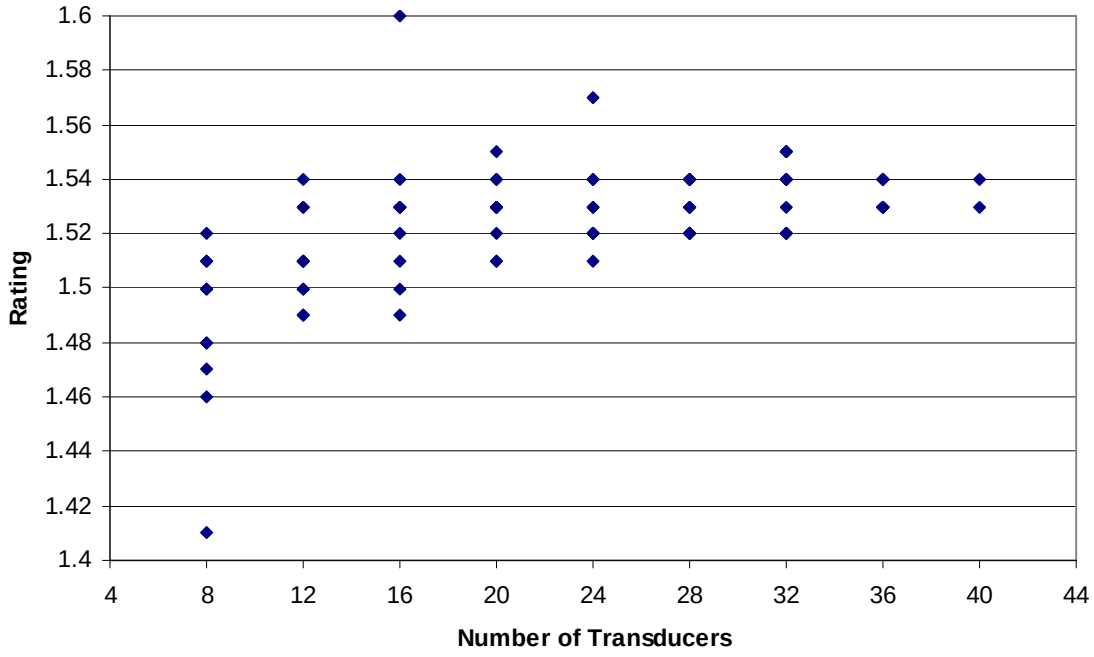

b. Exterior girder load ratings for Bridge #1.

Figure 2.13. Continued.

2.5.2 Bridge #2

Strain data for all load paths and test vehicle passes were plotted against load vehicle position. All transducer locations exhibited composite deck action with the steel girders and floor beams with the neutral axis being at or near the top flange, even in the negative moment region over the piers. The transducer locations near the abutment also showed composite deck action as well as indicating some end rotational restraint. Transverse symmetry was also exhibited.

Seven different element groups were defined for the finite element model of Bridge #2. Five of those elements were for the moment of inertia (I_y) for: the main girder from the abutment to the moment inflection point near Pier #1, the main girder in the positive moment region of Span #2, the main girder in the negative moment region about Pier #1, the main girder in the negative moment region about Pier #2, and the floor beams. Additional model elements included the concrete deck elasticity (E) and rotational restraint (K_y) at the abutments. The model was assembled using beam elements for the girders and floor beams, shell elements for the concrete deck, and rotational springs for the rotational restraint at the abutments.

The original model was calibrated with all 32 strain transducers at 16 different locations on Bridge #2. The optimized properties of the calibrated model are presented in Table 2.2. The original calibrated model placed limits on the values of I_y, E, and K_y for their respective elements. The limits for the girder and beam elements were established by evaluating the physical properties of just the steel and by calculating the composite section as described by code. The deck limits were established through traditional methods. These limits were expanded for the additional models. A second optimized model was created with all 32 strain transducers and expanded model parameter limits to verify that the change in limits had a minimal impact on the optimized values.

Table 2.2. Bridge #2: Initial and optimized properties for finite element model of Bridge #2.

Section	Property	Units	Non-Composite	Composite	Initial	Optimized
Girder at first span	I_y	in^4	5,155	21,630	21,630	25,030
Girder at second span	I_y	in^4	5,155	21,630	21,630	24,190
Girder near first pier	I_y	in^4	11,300	35,770	35,770	37,260
Girder near second pier	I_y	in^4	12,410	37,330	37,330	44,770
Floor beam	I_y	in^4	1,085	3,905	3,905	4,755
Concrete Deck	E	ksi	N/A	N/A	3,600	2,885
Spring (rotational)	K_y	in-k/rad	N/A	N/A	0	3,455,000

Given that 32 strain transducers at 16 different locations were used to optimize the initial model, each additional model group of ten reduced the number of strain transducers by four and locations by two. Each of the ten additional models was developed with the thought of creating the most complete instrumentation plans with a limited number of transducers. This approach was used to create ten additional models of 8, 12, 16, 20, 24, and 28 transducers. This created an additional 60 models. The results of the additional modeling are presented in Fig. 2.14.

Analysis of the results from the additional models indicate that values of the girder in Span #1, the girder in Span #2, and floor beam are consistent down to instrumentation plans of 20 transducers. It should be noted that in the modeling of the floor beam when location L15, center span of the floor beam, data were removed the moment of inertia for the beam dropped to nearly zero. As one would expect, when the value of I for the floor beam approached zero, the deck elasticity increased. The values in both negative moment regions, over Piers #1 and #2, are consistent in that the data spread does not increase greatly with a drop in the number of transducers used. The deck E and spring K_y are highly variable. The conclusion to be drawn from the consistency of the girder I_y

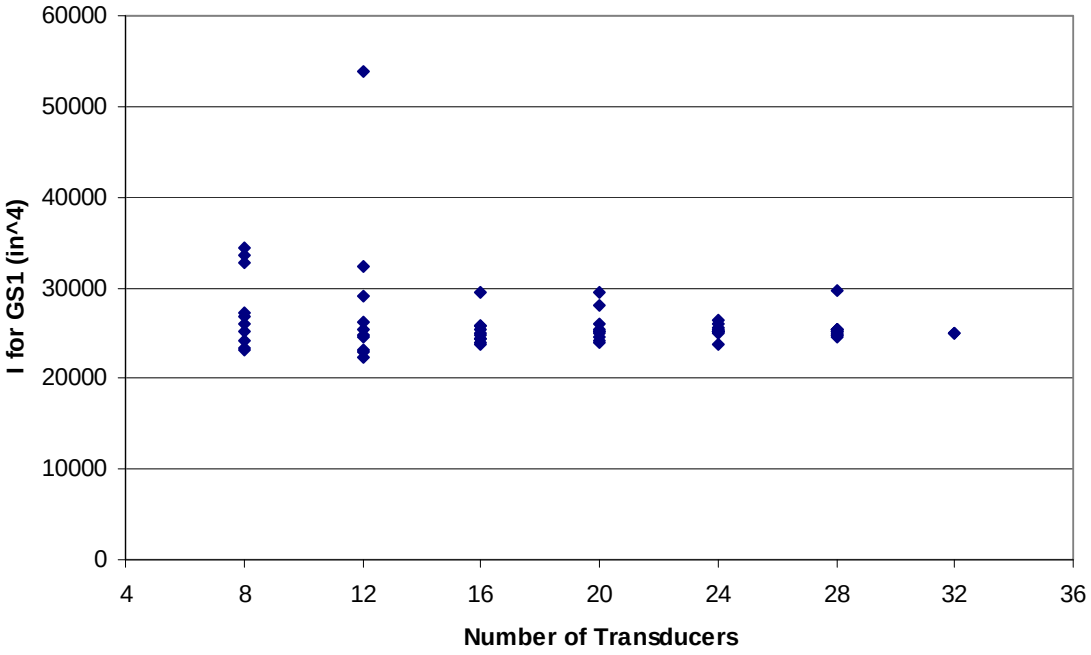

a. Optimized girder in Span #1 I_y values versus number of strain transducers.

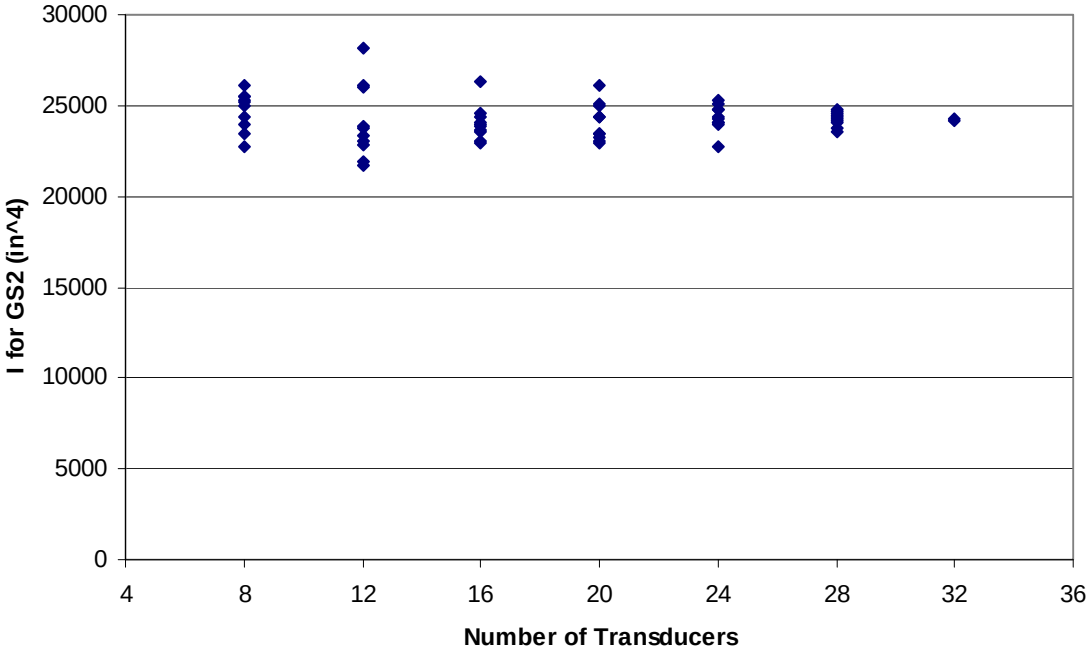

b. Optimized girder in Span #2 I_y values versus number of strain transducers.

Figure 2.14 Optimized model properties plotted against the number of strain transducers used for Bridge #2.

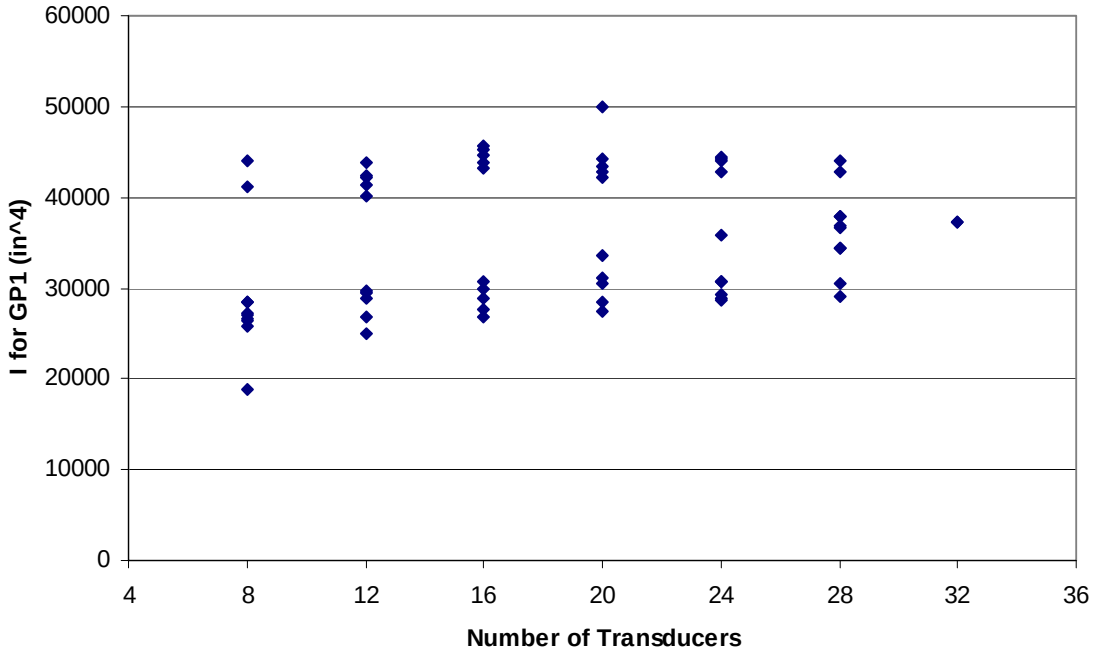

c. Optimized girder in negative moment region about Pier #1 I_y values versus number of strain transducers.

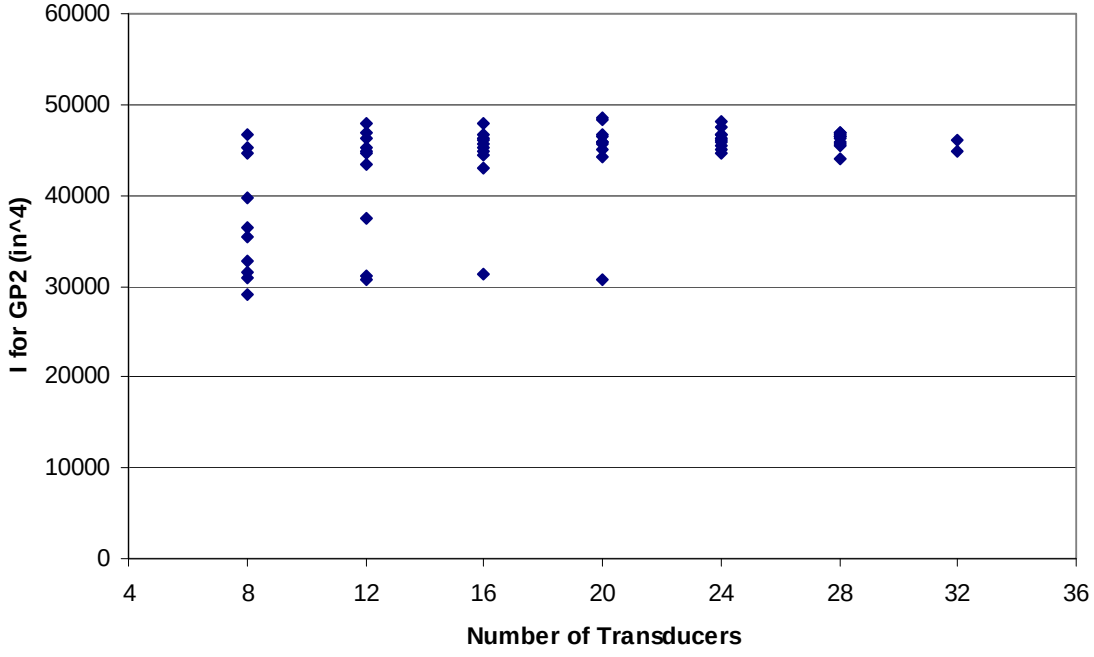

d. Optimized girder in negative moment region about Pier #2 I_y values versus number of strain transducers.

Figure 2.14 Continued.

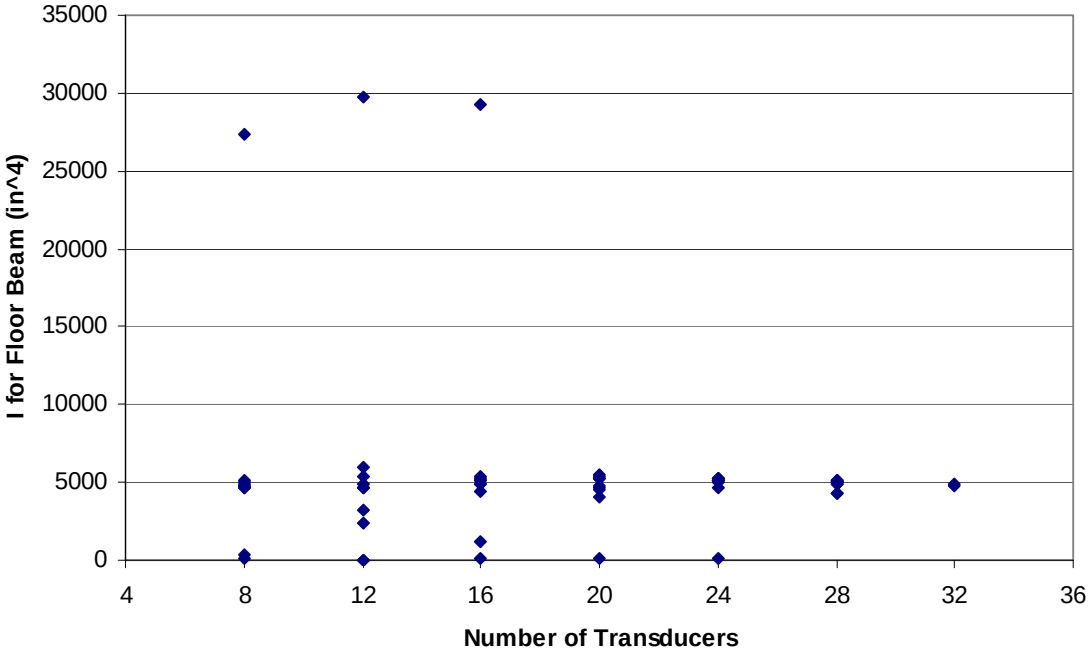

e. Optimized floor beam I_y values versus number of strain transducers.

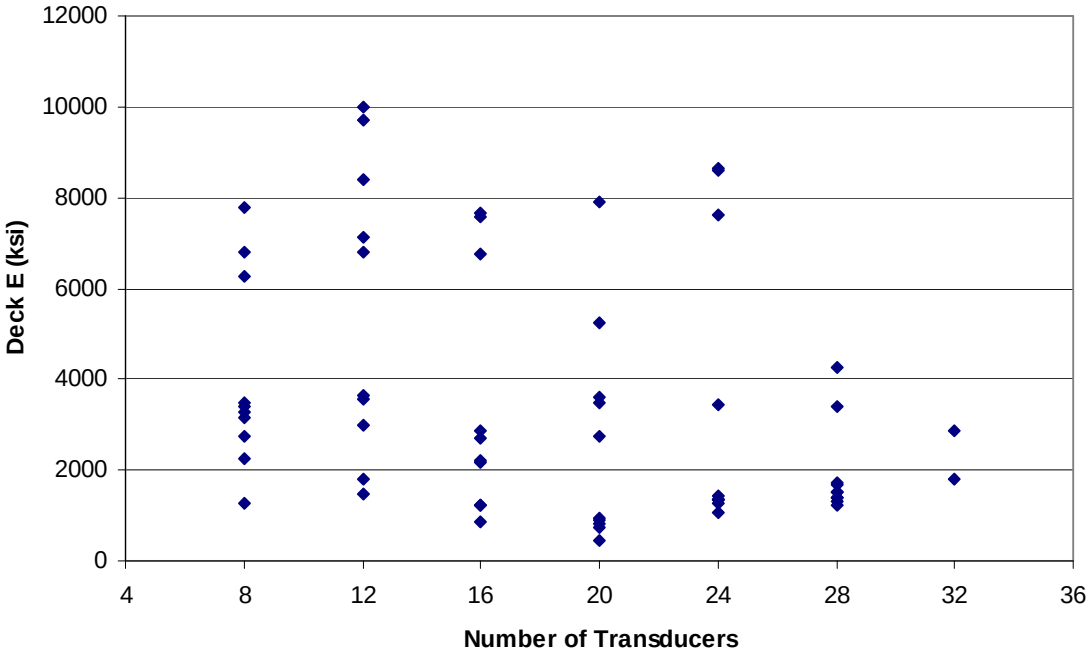

f. Optimized deck E versus number of strain transducers.

Figure 2.14 Continued.

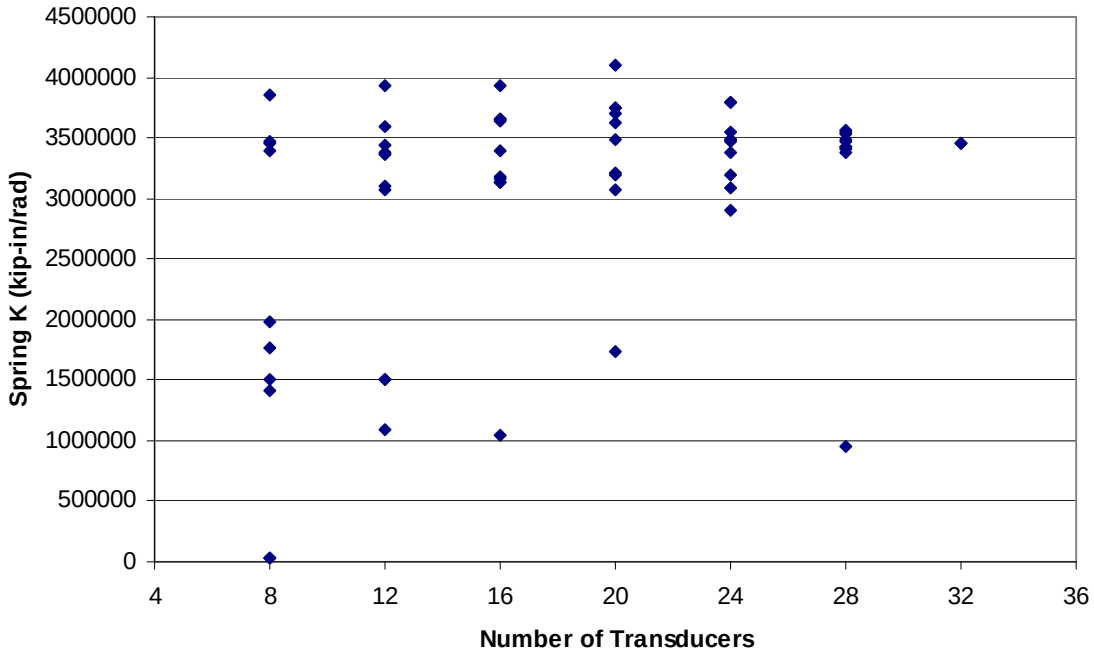

g. Optimized spring K_y values versus number of strain transducers

Figure 2.14. Continued.

values indicates that no matter what the instrumentation plan selected and number of transducers, the final results will be near the optimized solution. In models where 16 or less transducers were used, the optimized values become more variable, leading to the conclusion that 20 transducers is the bottom threshold for number of transducers needed to properly instrument the structure.

Additional BDI load ratings for a HS-20(14) load vehicle were calculated using the optimized parameters from the additional modeling of Bridge #2. The results of the additional load ratings are presented in Fig. 2.15. It should be noted that a reported rating from an earlier analysis of Bridge #2 is graphed along side the additional load rating data. The HS-20(14) flexural inventory ratings were significantly different from the earlier reported ratings. Simply by removing the limits on the model optimization parameters, the physical properties changed enough to cause a drastic shift in the load ratings. However, it should be noted that the graphical representation of the ratings shows little variation in the reduced gage load rating models occurred as compared to the expanded limit full gage load ratings. As earlier modeling showed, the floor beams are the limiting members in Bridge #2. This fact holds true on nearly all additional ratings calculated. As there was low variance in

additional model's properties, there was also low variability in their ratings. The rating outliers that did occur resulted from outliers in the optimized model parameters.

Field application of the transducers for Bridge #2 was complicated by the fact that the bridge is over I-80 in eastern Iowa. This heavily traveled interstate made traffic control on the roadway below the bridge vital to the testing process. This required an Iowa Department of Transportation crew to setup, teardown, and maintain the traffic control. One lane of the interstate had to be closed so that the transducers at mid-span of Span #2 and on the floor beam instrumented could be installed. All locations could be reached by ladder although the ladder had to reach heights of nearly 20 ft at most locations. The average time to install each transducer location was higher than Bridge #1, around 15 minutes per installation. This leads to an overall setup time of around 8 hours. Again, a crew of 2-3 reduced the installation approximately 4 hours. As stated in the previous paragraph, as few as 20 strain transducers could have produced similar results to the 32 strain transducer optimized model. An instrumentation plan with 20 transducers would have reduced the installation time by approximately 3 hours. However, with a multi-person crew completing the installation work, the actual result in time reduced is minimized. Despite the difficult site conditions and high traffic volume of the roadway below the bridge, the additional time needed to install a complete instrumentation plan with a higher number of strain transducers is worth the extra time and effort. The benefits are best shown in the minimization of unanswered questions after a diagnostic load test.

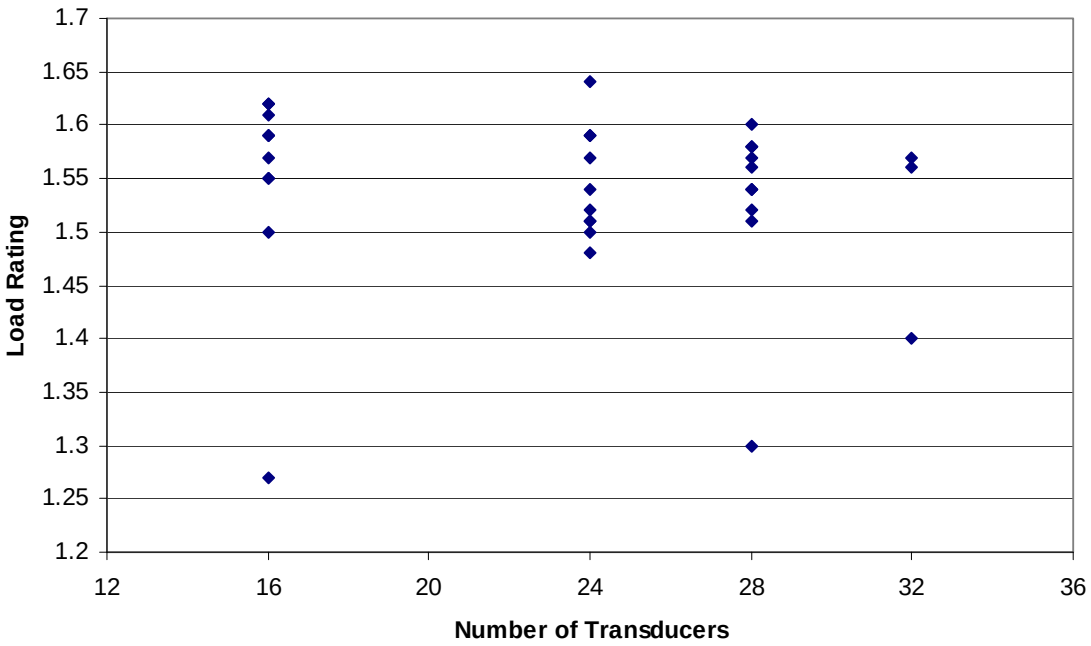

a. HS-20(14) flexural inventory load rating for girder in Span #1, Bridge #2.

Figure 2.15 Additional BDI ratings for Bridge #2.

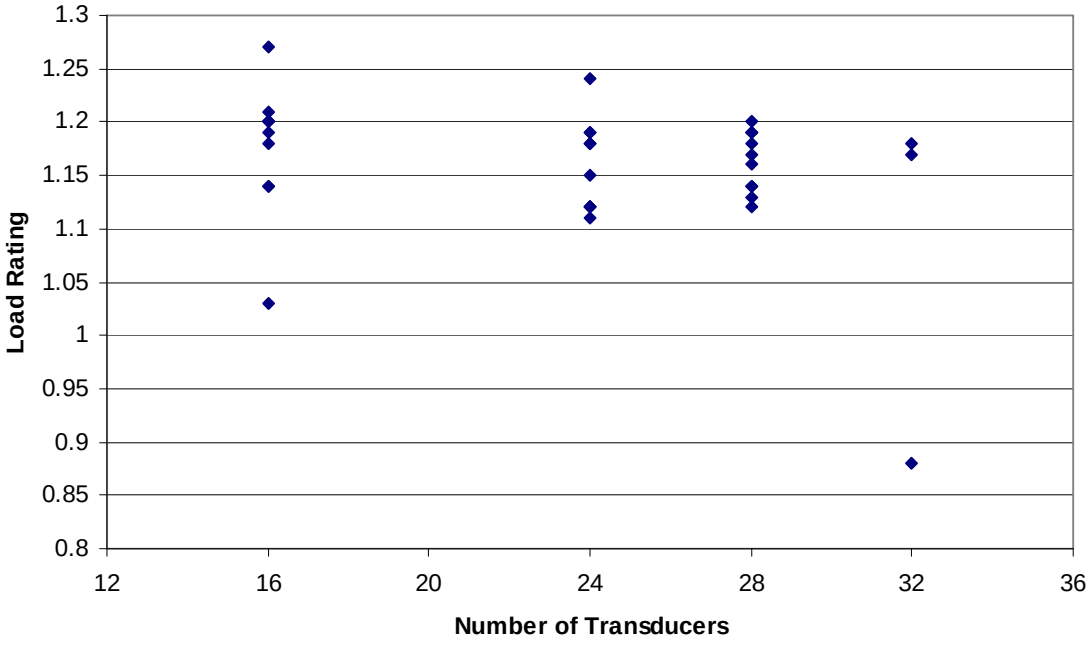

b. HS-20(14) flexural inventory load rating for girder in Span #2, Bridge #2.

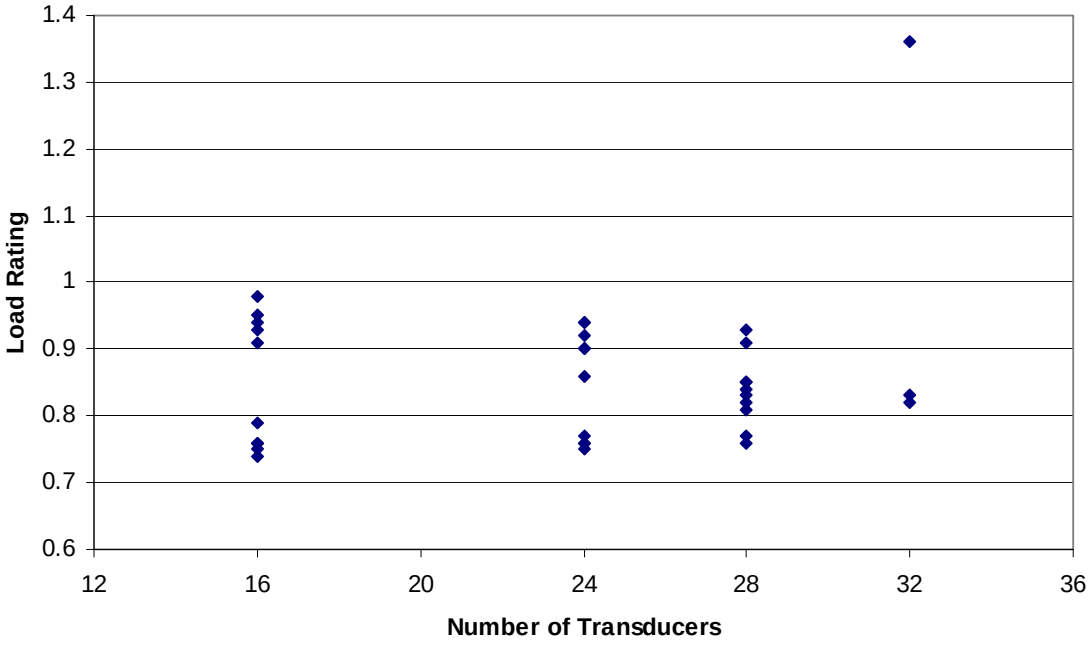

c. HS-20(14) flexural inventory load rating for girder at Pier #1, Bridge #2.

Figure 2.15 Continued.

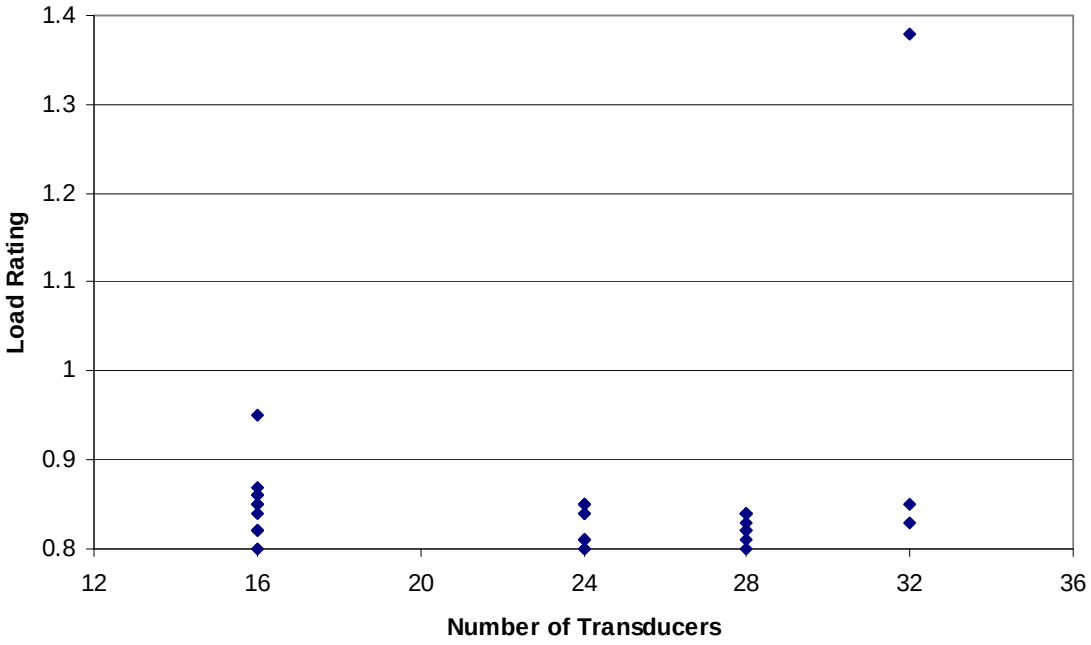

d. HS-20(14) flexural inventory load rating for girder at Pier #2, Bridge #2.

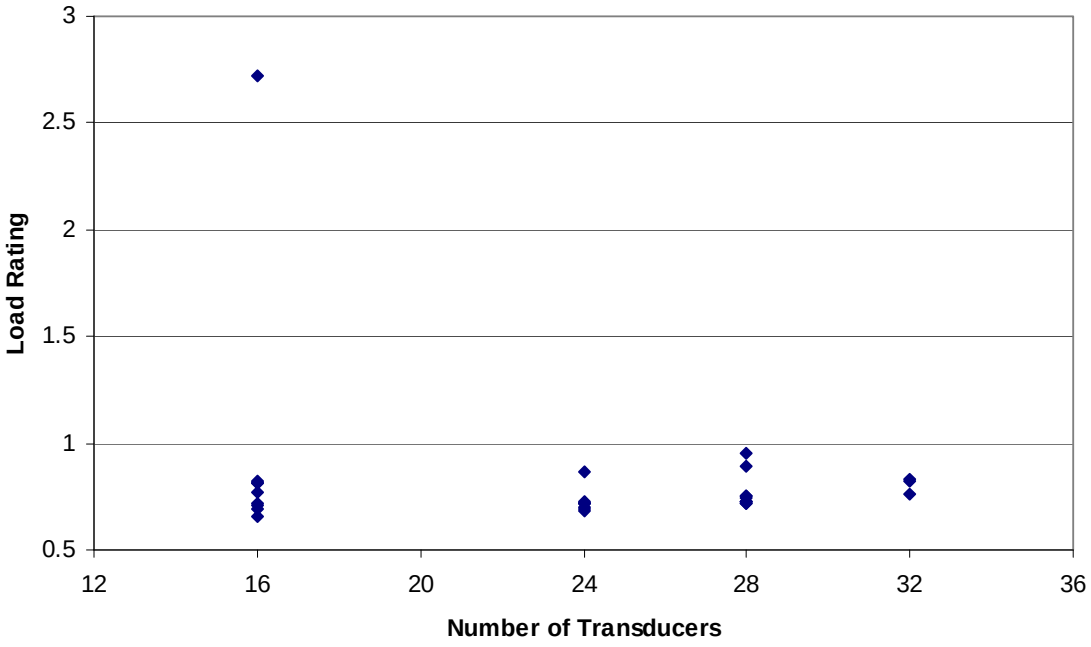

e. HS-20(14) flexural inventory load rating for floor beam in Bridge #2.

Figure 2.15. Continued.

2.5.3 Bridge #3

Strain data for both load vehicle paths were plotted versus load vehicle position. Analysis of the data revealed transverse symmetry was present and the neutral axis of the all mid-span locations was near the top flange of the girder, which confirmed composite action. Significant end restraint was observed at the abutments by the presence of negative strains on the bottom flanges of the instrumentation locations near the abutment. This was not unexpected given the integral abutment condition.

A model of Bridge #3 was created using eight different element groups. Eight groups were needed to account for differing conditions, end restraint at the abutments and composite action at mid-span, for each of the two different girder types. The new exterior girder was modeled with beam elements and consisted of two types, one for the section near the abutments and another for the girder at mid-span. The limits were set based on the physical properties of the new girder with and without the parapet weight included. The old exterior girder was modeled in the same manner with two different groups, one for the girder at the abutments and another at mid-span. The interior girders were treated the same as each exterior girder with the exception that the curb section was not included in the properties. The deck was modeled using plate elements and springs were placed at the abutments to account for the end restraint that appeared in the test data.

The initial model was optimized using property limits established through analysis of the material properties of each individual element group and by conditions observed during the field test and reflected in the test data. The deck calibration was removed from the original optimized analysis which allowed for the girder and spring elements to be optimized separately from the deck. Once the girder and spring elements were optimized, the deck was then optimized and a final model was assembled with the optimized properties of each element, as shown in Table 2.3. It should also be noted that the top flange data for all transducer locations near the abutments were removed from the analysis.

The optimized model used strain data from 20 different transducers at 15 different locations with a total of eight different element groups being optimized. As stated earlier, the deck was optimized separately from the girder and spring elements for the final rating model. For the purposes of the analysis documented here, the deck was included in the optimization process. This created an additional model with data from all 20 transducers. Yet another model with all data was created with the limits of optimization set to zero on the low end and ten times the original high end limit for each element group. This extended limits model served as the base for the further modeling completed with reduced transducer arrangements.

Table 2.3. Bridge #3: Initial and optimized properties for finite element model of Bridge #3.

Section	Property	Units	Non-Composite	Composite	Initial	Optimized
New ext. girder near abut.	I_y	in^4	800	14,415	800	1,160
New ext. girder at midspan	I_y	in^4	800	14,415	14,415	11,720
Old ext. girder near abut.	I_y	in^4	736	13,835	736	1,160
Old ext. girder at midspan	I_y	in^4	736	13,835	13,835	11,500
Int. girder near abut.	I_y	in^4	736	3,005	736	1,255
Int. girder at midspan	I_y	in^4	736	3,005	3,005	3,595
Deck	E	ksi	N/A	N/A	3,600	4,990
Spring (rotational)	K_y	in-k/rad	N/A	N/A	0	944,000

An additional 24 models were created for further analysis of the testing process. Ten models consisted of 16 transducers, ten of 12 transducers, and four of 8 transducers were optimized for all eight element groups. The optimized property results of the further modeling are shown in Fig. 2.16.

Analysis of the additional modeling reveals that the initial limits were instrumental in the optimized model. This is evident in the fact that the both exterior girder's value of I_y tended to increase in the no limits models independent from the number of transducers used. The inverse is true of the interior girders. The value of I in the interior girders tended to decrease in the no limit models. The deck E tended to increase while the spring values fluctuated as much below the optimized as they did above. While the optimized values from the additional modeling of Bridge #3 were consistent for some element groups, others were vastly different. Given the outcome of the analysis, any reduction in field data would have decreased the accuracy of the model and brought undesired confusion to the modeling process.

Load ratings for each additional reduced gage model were calculated using WinSAC. The additional ratings were only for HS-20 inventory flexural loading. The results of the reduced gage rating models are presented in Fig. 2.17. The traditional LFD rating calculations yielded a rating for the bridge of 0.87; the limiting member in the LFD rating was the interior girder. The optimized BDI model yielded at rating of 1.23 and the limiting member was the new exterior girder. It should be noted that the additional models utilizing the full gage layouts had significantly lower ratings than the optimized model. The reduced model ratings were generally lower, ranging from 1% to 66%, than the optimized BDI model. In every additional rating calculation, the new exterior girder was the limiting member. Given the short simple span arrangement and narrow width of Bridge #3, the load ratings are not greatly affected by the optimized parameters. The ratings were generally

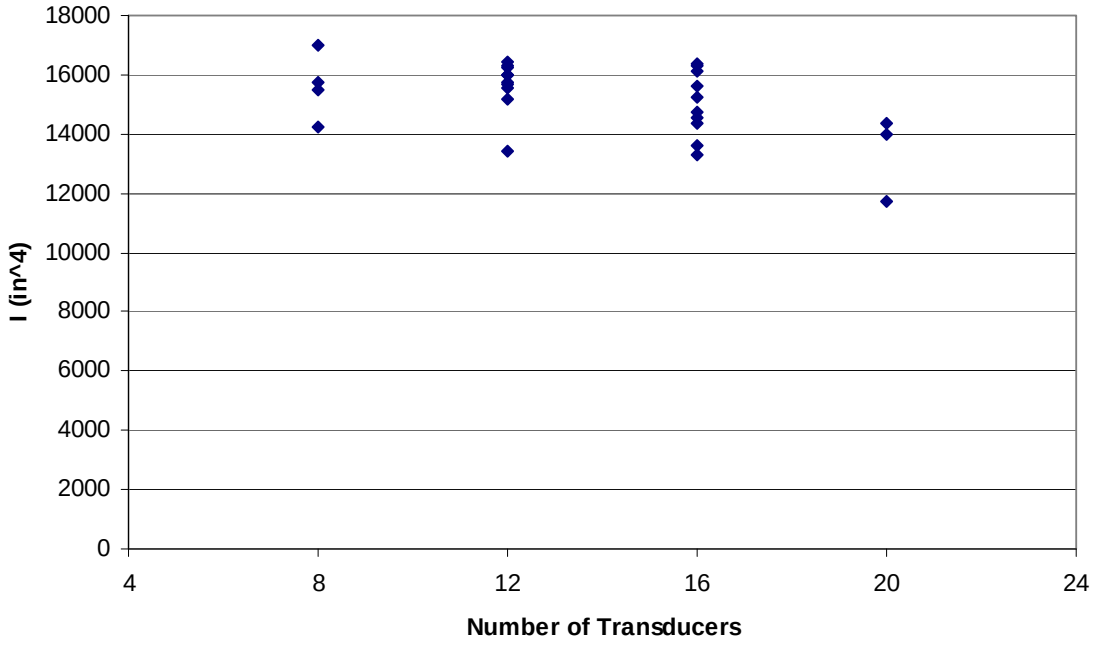

a. Optimized New Exterior girder at mid-span versus number of transducers used.

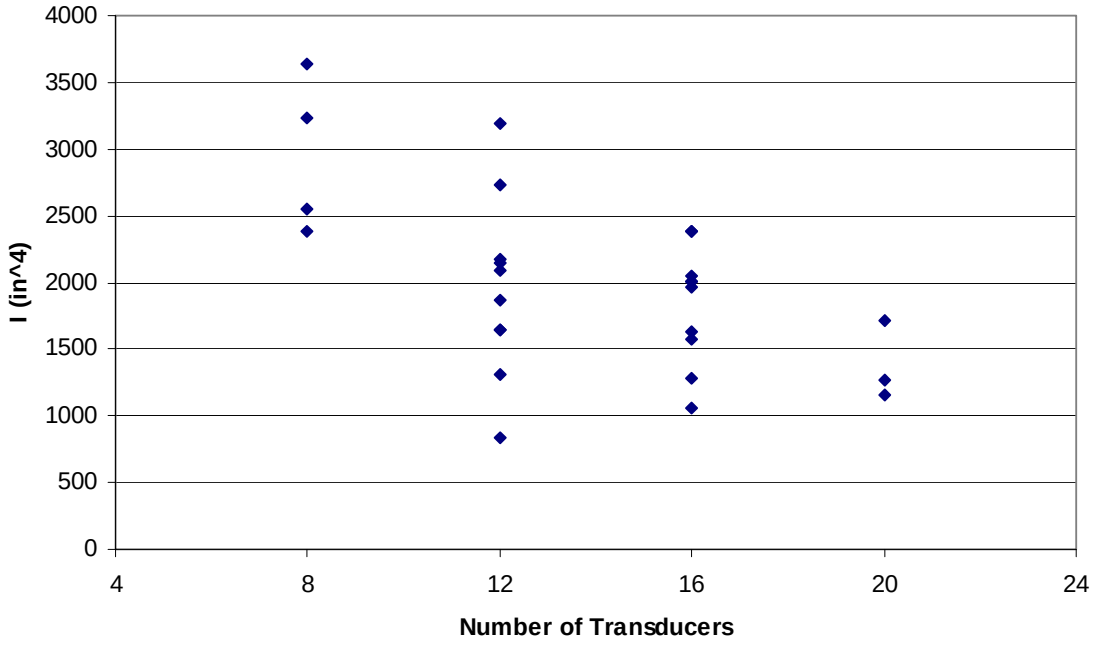

b. Optimized New Exterior girder at abutment versus number of transducers used.

Figure 2.16 Optimized model properties plotted against the number of strain transducers used for Bridge #3.

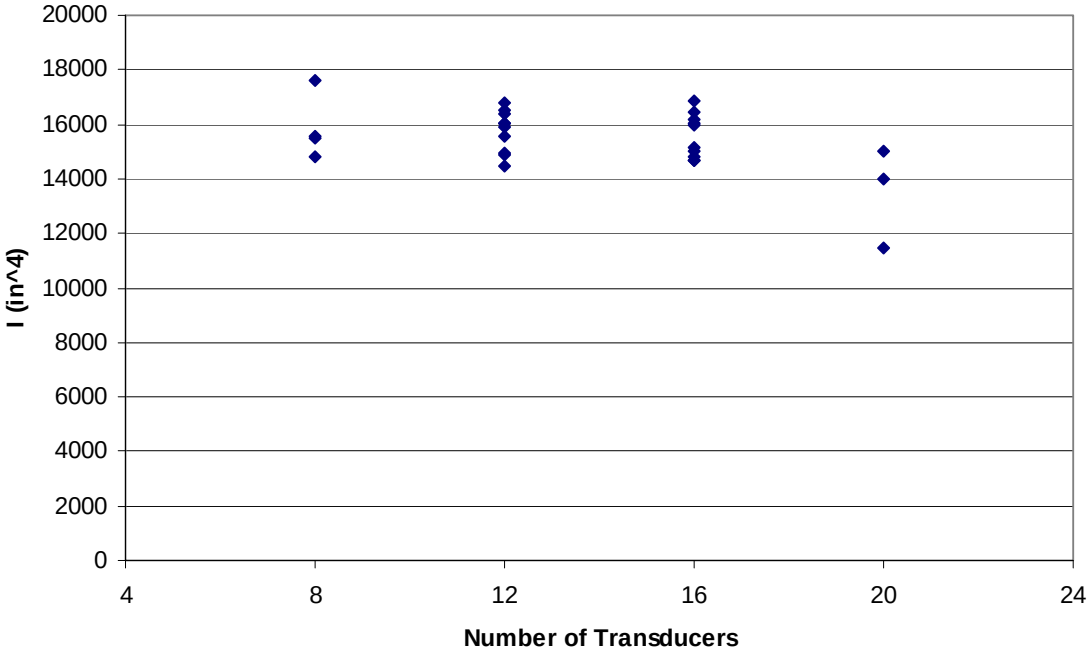

c. Optimized Old Exterior girder at mid-span versus number of transducers used.

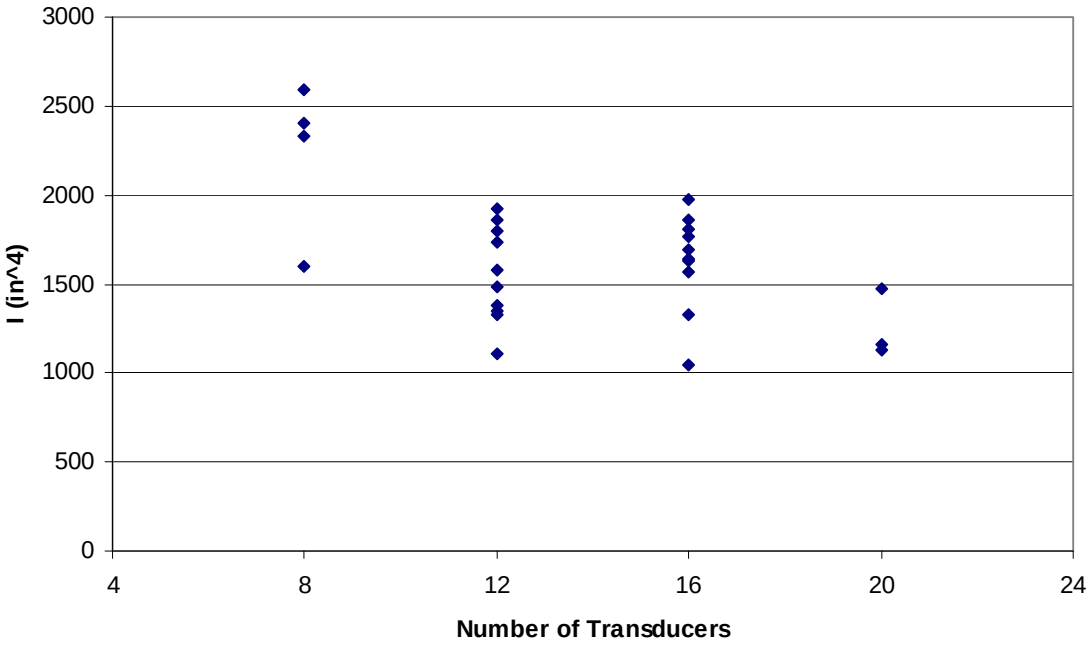

d. Optimized Old Exterior girder at abutment versus number of transducers used.

Figure 2.16 Continued.

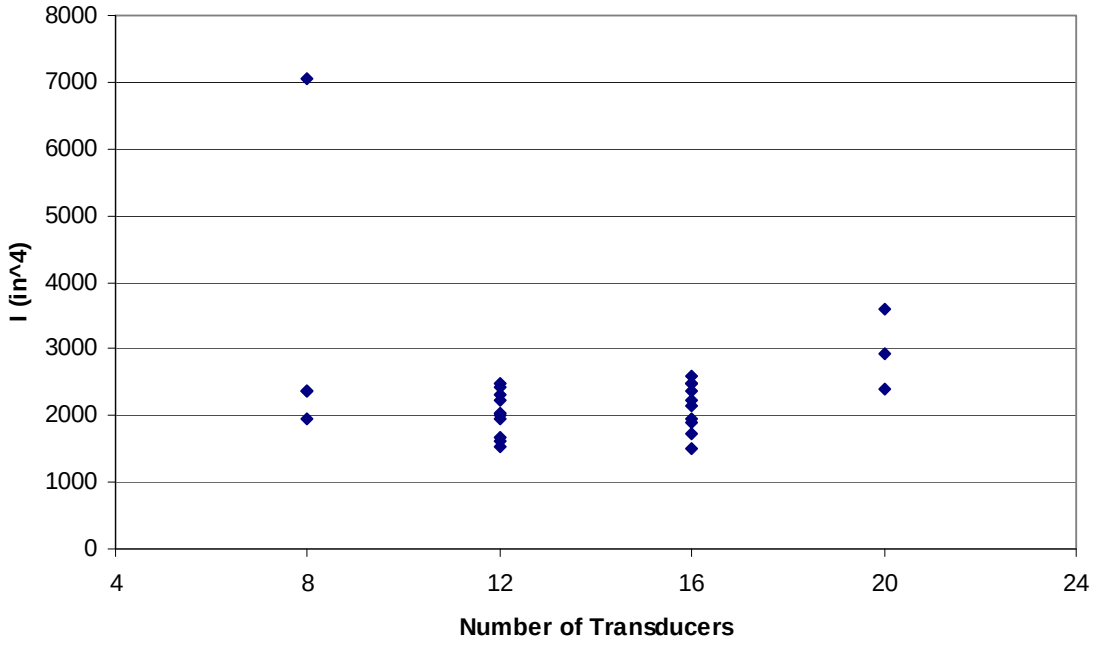

e. Optimized Interior girder at mid-span versus number of transducers used.

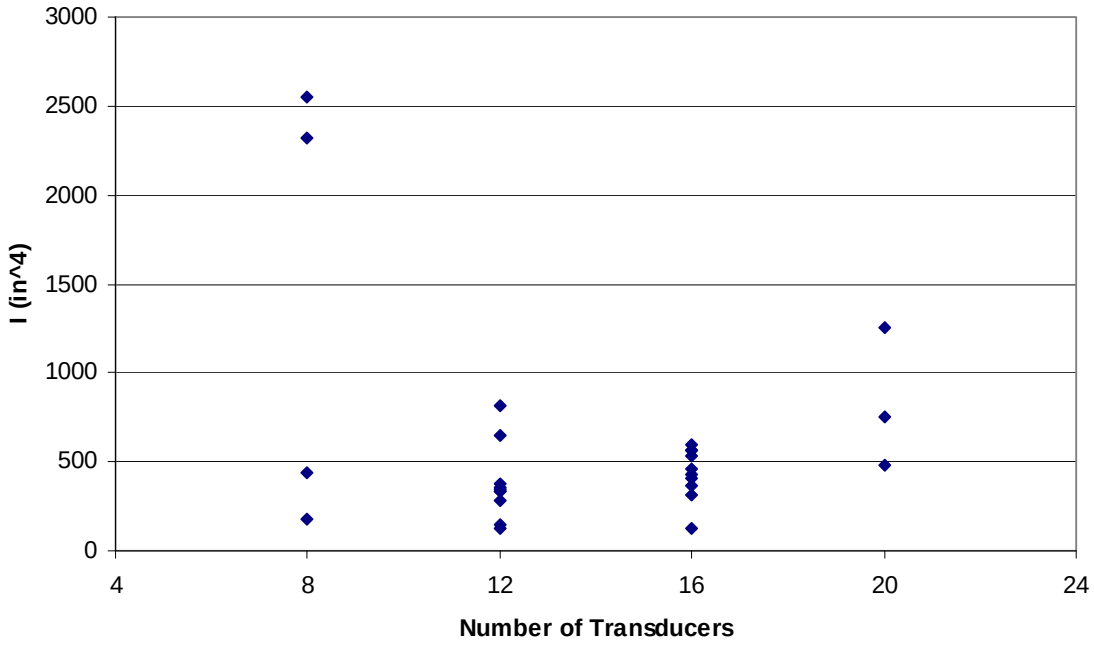

f. Optimized Interior girder at abutment versus number of transducers used.

Figure 2.16 Continued.

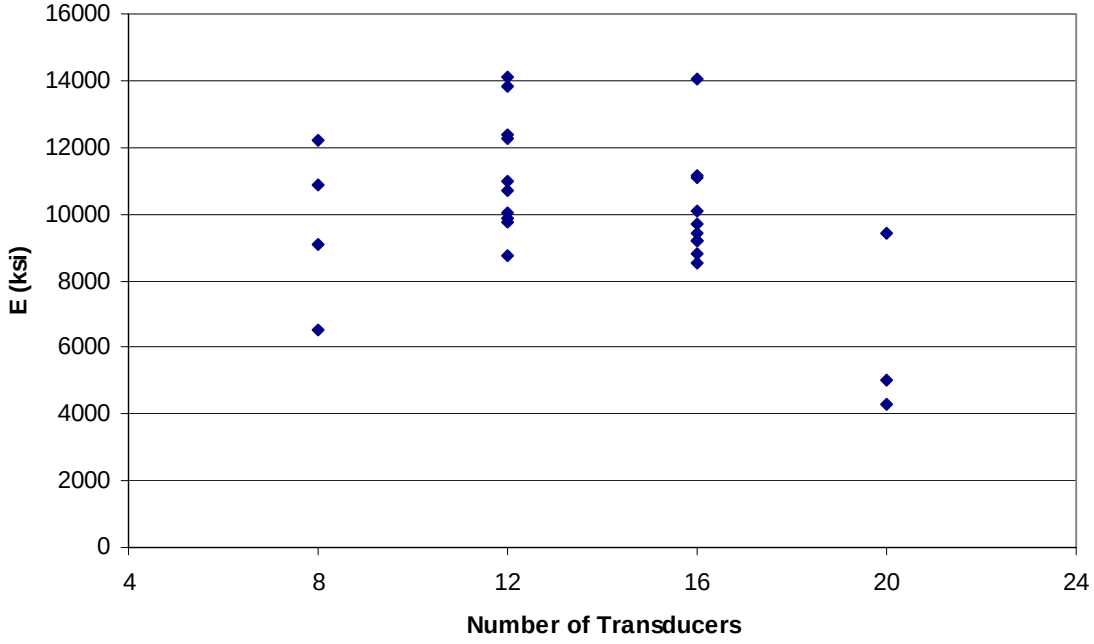

g. Optimized Deck E versus number of transducers used.

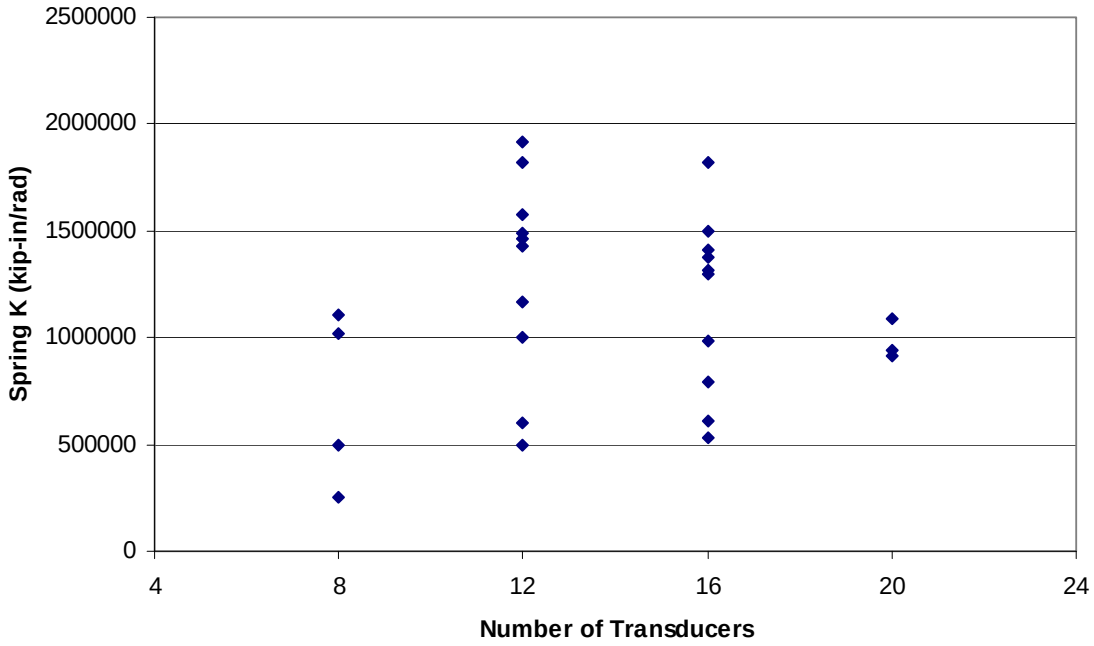

h. Optimized Spring K versus number of transducers used.

Figure 2.16. Continued.

grouped for additional models using 12 and 16 gages. The 8 gage models produced ratings that were more random, similar to the optimized parameters.

Field application of the transducers used for the testing of Bridge #3 were easily accessible. With the low vertical clearance, the top flange of the girders were reachable without the need of a ladder or any other device. The shallow abutment depth and muddy conditions did complicate transducer application, but not significantly enough to impact the transducer layout. Each transducer took approximately 5 minutes to install including surface preparation of the steel by grinding. The original bridge instrumentation used 32 strain transducers for a total installation time of nearly three hours. A crew of 2-3 reduced this to an actual field installation of around 1.5 hours. Given that the modeling process was complicated and that access to the bridge for instrumentation was easy, there would not be any reason to reduce the number of transducers used on Bridge #3.

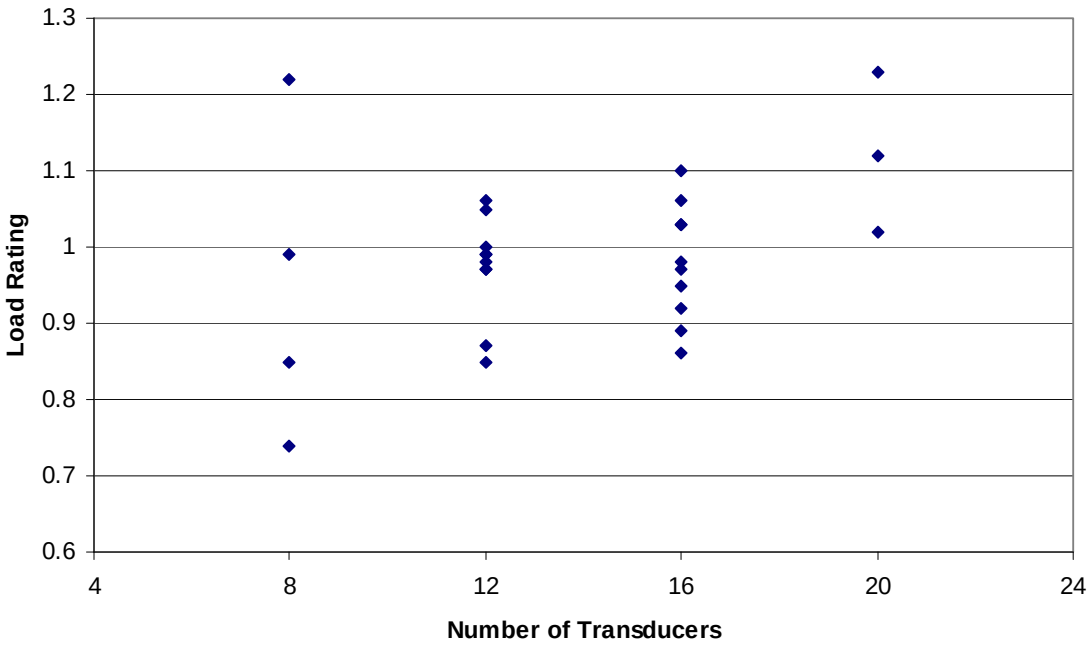

Figure 2.17. HS-20 flexural load ratings for Bridge #3.

2.6 CONCLUSION

Commercially available testing systems like the BDI system make diagnostic load testing easy and efficient. While traditional systems comprising of foil strain transducers and an individual wire for each transducer take typically a full day to install and an additional day for the actual testing and removal of the instrumentation for most bridges, the BDI system reduces the entire operation to one day. Additional benefits of the BDI system over traditional testing methods include reduced

long-term expenses in that all components of the BDI system are reusable whereas foil strain gages are not, ability to automatically track load vehicle distance on the tested structure, and ease of transition from field data to modeling and rating software programs. The entire BDI system is designed to be an all encompassing and simplified approach to diagnostic load testing.

Given the simplicity and efficiency of the BDI system, the additional time required to properly instrument a bridge for diagnostic load test versus a minimalist approach is not warranted. Any additional time spent in the field installing additional transducers to the bridge only increases the knowledge learned from the load test and answers more questions. The result of additional data works towards a more accurate finite element model and a more confident assessment of the load carrying capacity of the structure.

2.7 REFERENCES

1. National Bridge Inventory, NBI Report, 2004. http://www.nationalbridgeinventory.com/nbi_report_200414.htm

2. Wipf, T. J., Phares, B.M., Klaiber, F.W., Wood, D.L., Mellingen, E., Samuelson, A., "Development of Bridge Load Testing for Load Evaluation," Research Report, 2003.

3. Bridge Diagnostics, Inc. 'BDI Structural Testing System Operation Manual.' (1999)

4. Bridge Diagnostics, Inc. ' BDI Software Package Bridge Modeling and Analysis Program Manuals.' (2002)

3. EVALUATION OF AN INTEGERATED BRIDGE LOAD TESTING/RATING SYSTEM

A paper accepted to the First International Workshop on
Structural Health Monitoring of Innovative Civil Engineering Structures

Anthony J. Samuelson, Brent M Phares, Terry J. Wipf,
F. Wayne Klaiber, Espen Mellingen, Doug L. Wood

3.1 ABSTRACT

The problem of an aging and rapidly decaying infrastructure is an issue facing many agencies charged with maintaining a fully functioning traffic system. Numerous bridges of marginal condition must frequently be posted resulting in increased travel time and distances. However, when tested, these bridges often exhibit strength beyond traditional codified parameters. The use of diagnostic load testing for the purpose of load rating has become an accepted practice for addressing these bridges for many public agencies. Easy to use commercial tools, like the Bridge Diagnostics, Inc. (BDI) system, have simplified the process of testing, modeling, and rating bridges.

This paper documents efforts underway at Iowa State University to evaluate and document the applicability, ease-of-use, and accuracy of such an integrated bridge testing system. For this work, typical bridge was instrumented with 36 strain transducers and tested with known loads using the BDI system. A finite element model of the bridge was then developed and calibrated based on the observed behavior and the field measured strain. Results from the calibrated model were then used to carry out load rating calculations and then compared to traditional rating calculations. The resulting ratings showed a general increase over the traditional codified ratings.

3.2 INTRODUCTION

Diagnostic load testing of bridges is an important tool used by bridge engineers to understand global and local behavior of bridges. It has long been recognized that load tested bridges often exhibit strength and serviceability attributes that exceed the levels predicted by accepted codified parameters.[1] This means that many bridges have reserve strength/stiffness beyond that predicted by traditional calculations. Knowledge of these reserves is especially important for bridges of marginal condition which frequently must be posted at load levels below legal limits. This is important when the postings result in increased travel time and distances.

Although the use of load testing for the purpose of load rating is not a new technique, only recently have easy-to-use, integrated tools been developed to facilitate the rational integration of field test results into rating calculations. Bridge Diagnostics, Inc. (BDI) has developed a suite of software which, when used in combination with specially developed hardware, provide the needed tools for collecting field performance data, calibrating a finite element model with the field collected data, and performing load rating calculations based on the calibrated finite element model.

Commercial tools, like the BDI system, are being adopted by public agencies to better manage their existing bridge inventory. This form of asset management can be used to address structurally complex bridges, load ratings, and overload issues.

3.3 SYSTEM DESCRIPTION

The system developed by BDI is a systematic approach to the testing, modeling, and rating of bridges. The system is used in phases each with their own tools and individual processes. Initially existing data on the bridge being evaluated is examined. Often, previous load rating calculations or visual inspection reports reveal the limiting or critical elements and sections of a bridge. This survey of existing data can then be used to develop an instrumentation plan for the bridge.

Generally, the instrumentation plan is designed to address the issues and concerns identified from the evaluation of the existing condition data. The plan should include the collection of data that may impact the attributes of the finite element model. Common issues include girder end conditions and the presence of composite action.

3.3.1 Structural Testing System

Implementing the instrumentation plan in the field is simplified by the BDI Structural Testing System (STS). Installation of the strain transducers simply involves the cleaning of the surface at the gage location and placement of the transducer using an adhesive and accelerant.[2] Each transducer is referred to as an “Intelliducer” due to its ability to identify itself to the system control unit. This attribute allows for automatic calibration and balancing of the gages. Each Intelliducer connects to a small box, called an STS Unit, in groups of four. Individual STS Units are connected to one another (typically in series) and finally to the Power Unit. This allows for a minimum number of wires to relay data for up to 64 Intelliducers. The Power Unit is connected to a PC that controls the functions of the system. Data can be collected at rates from 0.01 to 100 Hz.

The system also has a remote load position indicator called the “Autoclicker.” The Autoclicker uses a reflective strip on the load vehicle wheel, a photo sensor, and a handheld radio to transmit the truck position (in terms of wheel revolution) to the Power Unit.

3.3.2 Software Suite

The BDI Software Suite is used for the analysis, modeling, and rating of the bridge. Included in the package are software for graphing field and analytical data, model generation, and model analysis and calibration.

WinGRF is the first of the analysis tools used in the analysis. WinGRF uses transducer output and load position data to plot results verses truck position. When the user inputs information related to gage location (e.g., gage pairs, vertical distance between gages, etc.) more advanced plots can be created.[3] Results such as strain, neutral axis, and curvature may all be plotted with respect to vehicle position. Options, such as data filtering and offset correction may also be completed in WinGRF. This information can be used to gain a preliminary understanding of the bridge behavior.

WinGEN is used to create a finite element model of the bridge. The software is limited to beam and shell elements. The initial model is created using the overall bridge geometry and the section properties from the as-built plans. Also, neutral axis location information identified from the field test data can be incorporated. Other significant differences discovered during the investigation of the field results can also be included in the model. The inclusion of rotational and/or translational springs at the supports is a typical model modification. Transducer locations are also input in the model for calibration with the field data.

WinSAC analyzes and calibrates the analytical model. Limits of properties, such as modulus of elasticity, moment of inertia, and spring constants, are input into WinGEN and then analyzed using WinSAC. Within these prescribed limits, the model is calibrated to the field results. WinSAC performs a statistical analysis of the model and analytical results to arrive at a final calibrated model from which load ratings can be calculated.

Final model results may be plotted using the WinGRF program. This will visually verify the analysis results generated from WinSAC.

3.4 FIELD TESTING OF BRIDGE #1

Bridge one, shown in Fig. 3.1, was one of five bridges tested in the field verification of the BDI system conducted by the Iowa State University in conjunction with the Iowa DOT. It was the

most structurally complex of the bridges tested, having two girders with four different cross sections, numerous floor beams, and various stringers.

3.4.1 Overview of the Structure

Bridge one is a single span, two girder bridge carrying US Highway 6 over a small natural stream in Iowa County. The roadway width is 8.99 m accommodating two traffic lanes and two shoulders, as shown in Fig. 3.2. The span length is 21.34 m and is supported on each end by curved bearing plates; the bridge has no skew. The superstructure consists of 1.09 m deep welded girders with various plates welded to the bottom flange. Angles have been bolted to the girders for additional strength as shown in Fig. 3.2b. The bridge deck is a variable thickness (i.e., 18 cm at the curb and 23 cm at the centerline) cast-in-place reinforced concrete slab with a 7.6-cm wearing surface; shear connectors are present for composite action. The deck is supported by various floor beams spaced approximately 5.33 m, with 25.4 cm and 38.1 cm deep stringer beams spaced at 1.22 m.

Based on a cursory visual inspection of the bridge, all structural elements appear to be in good condition with the exception of light rust on the ends of the girders and floor beams. Load rating calculations from 1999 revealed that the yielding of the top flange of the girders at mid-span were the critical section. The rating calculations gave an HS 21.7 Operating Rating and an HS 15.0 Inventory Rating.

The Iowa DOT expressed concern with certain elements of the bridge. Particularly, the top flange stresses and the effectiveness of the strengthening angles. Numerous steel girder bridges in Iowa have been strengthened by using angles bolted to the web; however, the overall ability of the angles to carry load has had little investigation.

Figure 3.1. Photograph of the main girders of bridge one.

3.4.2 Instrumentation

The instrumentation used to evaluate Bridge one focused on monitoring critical areas of the structure that may impact the load rating.[3] Each transition from section to section of the girders was instrumented with transducers on the top and bottom flange, as well as on the strengthening angle on the north girder, as shown in Fig. 3.2b. A typical floor beam was instrumented at the top and bottom flange 61 cm from each girder and at midspan. A stringer was instrumented in a similar fashion with gages at the top and bottom flanges 30.5 cm from the stringer to floor beam connection and at the stringer mid-span. A total of 36 strain transducers were used in the load test at 17 different cross sections, as shown in Fig. 3.2a.

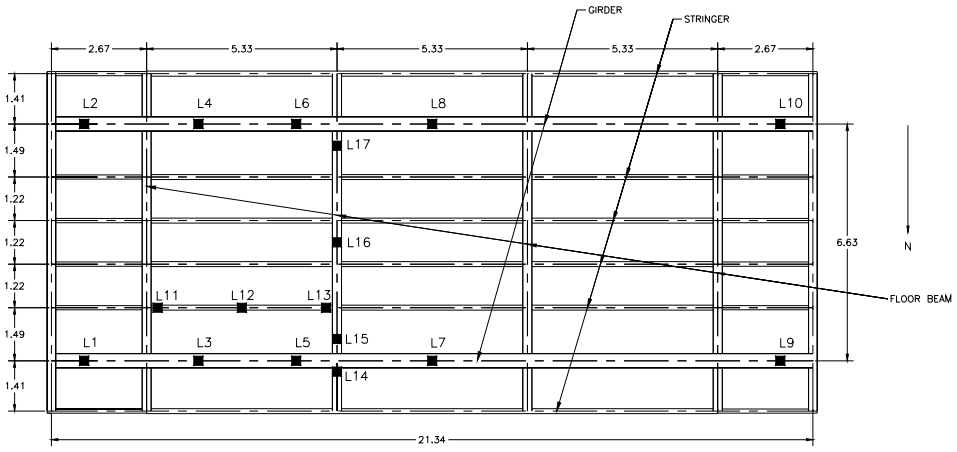

a) Plan view of Bridge one with transducer locations.

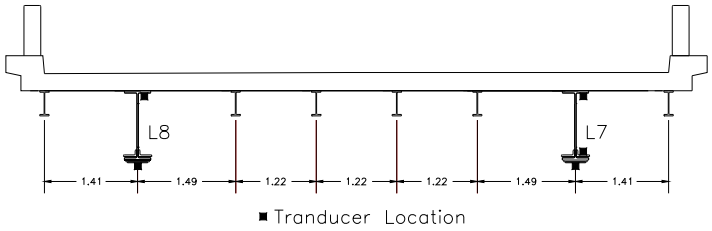

b) Cross section at mid-span with instrumentation.

Figure 3.2. Illustrations of bridge one.

3.4.3 Load Test Details

Data were collected for five different load paths at a frequency of 20 Hz. Two runs were conducted for each load path to verify data consistency. The Iowa DOT provided a standard maintenance truck as the load vehicle. Details of the load vehicle are given in Fig. 3.3. In all load cases, Y1 through Y5, the test vehicle was driven along the bridge from east to west at a crawl speed of approximately 8 km/h. The first load path, Y1, placed the vehicle passenger side wheels over the north girder. Load path Y5 was symmetric to the Y1 path in that the driver's side wheel line was directly over the south girder. The Y2 load path placed the passenger wheel line 61 cm from the face of the north curb. Load position Y3 placed the passenger wheel line over the instrumented stringer beam while Y4 centered the load vehicle on the longitudinal centerline of the bridge. The longitudinal load position was recorded using the Autoclicker. The load paths are illustrated in Fig. 3.4.

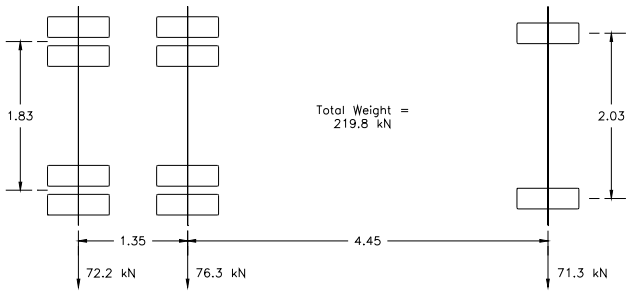

Figure 3.3. Description of load vehicle used in the testing of bridge one.

3.4.4 Field Test Results

The effectiveness of the strengthening angle was apparent in all truck paths. The Y1 and Y3 paths, both having the passenger wheel line in close proximity to the girders, yield the best illustration of the angle's contribution, as shown in Fig. 3.5. Strains in Fig. 3.6 indicate some rotational end restraint in the girder. The floor beams and stringers exhibited composite behavior.

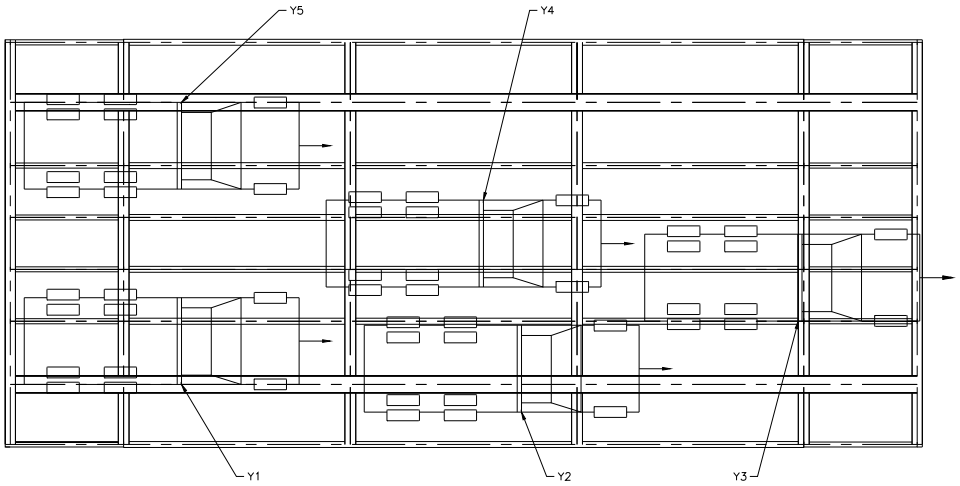

Figure 3.4. Load paths used for the testing of bridge one.

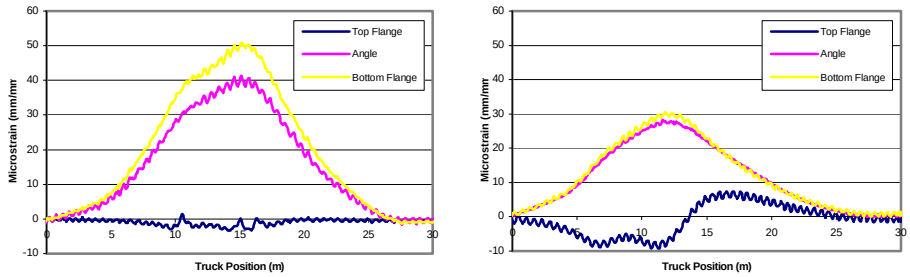

Figure 3.5. Plots of L7 for path Y1 and L5 for path Y3.

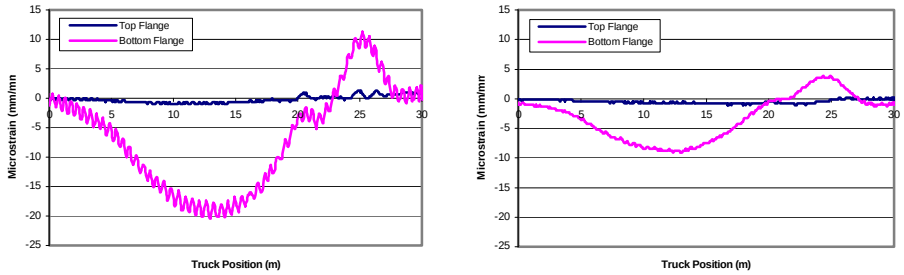

Figure 3.6. Plots of L9 for path Y2 and L10 for path Y3.

3.4.5 Modeling

The finite element model was created using WinGEN. The initial step in the modeling process was to generate the model geometry. Once the geometry of the bridge was input into WinGEN, the various sections were constructed. A total of eleven different cross-sections were defined for the model. The main girders consisted of four different cross-sections while three

different floor beams were present along with two types of stringers and two exterior beam cross-sections. The girders, floor beams, and stringers were modeled using beam elements. The slab was modeled using shell/plate elements.

The initial section properties input into the model were based on the composite section properties according to AASHTO provisions. Rotational springs were placed at each of the four girder ends to simulate the restraint observed in the field data. A modulus of elasticity of the slab and spring constant were assumed for the initial model. Based on the initial properties, the WinSAC software calculated the overall strain error to be 16.3 % with a correlation coefficient of 0.95.

The model was optimized using the WinSAC program. Before optimization, upper and lower end boundaries for the optimized properties were set as 1.2 times the composite section properties and 0.8 times the non-composite section properties to ensure the results were geometrically reasonable. The final optimized model had a total strain error of 9.1 % and a correlation coefficient of 0.96. Fig. 3.7 illustrates the accuracy of the model data to the field data. Table 3.1 illustrates the non-composite, composite, initial, and final optimized member properties.

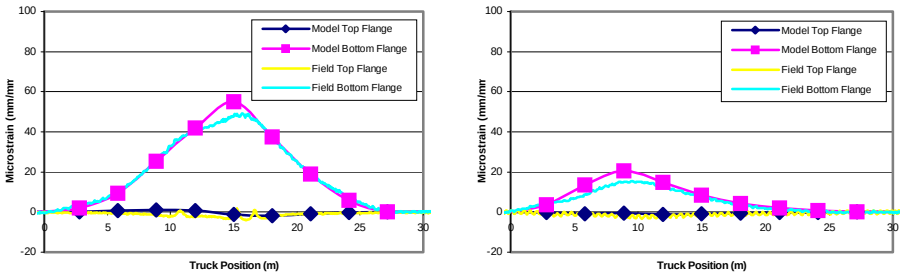

Figure 3.7. Plots of field and model data for L8 path Y5 and L4 path Y4.

3.4.6 Rating

Traditional hand rating calculations were preformed according to the AASHTO LFD code for the many locations of the bridge. In the initial rating calculation preformed by the Iowa DOT, the strengthening angles were not taken into account. With the field data illustrating the effectiveness of the angles, they were included in the final hand calculations. The limiting member in the traditional load rating for an HS-20 truck was found to be the girder with two cover plates and the strengthening angle with an inventory rating of 1.43 and an operating rating of 2.39 for flexure. The limiting member in shear was the smaller of the two stringer beams with an inventory rating of 1.46 and an operating rating of 2.44.

WinSAC performed load rating calculations based on the loads calculated through the optimized model. The limiting member in shear remained similar to the hand calculations, in that the small stringer beam had an inventory rating of 1.07 and an operating rating of 1.79. The limiting flexural member from the BDI analysis was one of the floor beams with an inventory rating of 2.20 and an operating rating of 3.67 for an HS-20 truck.

3.4.7 Discussion of Test Results

The field testing of bridge one answered many questions surrounding the structure. The effectiveness of the strengthening angles was confirmed with field data and with this knowledge, the hand calculated flexural rating of the girders increased. Girder restraint was also discovered in the field. This information led to a bridge model that distributed the vehicle loads in similar fashion to the actual structure. This optimized model was then used to distribute the standard AASHTO load to calculate rating factors.

Table 3.1. Section properties used in the modeling of bridge one.

Member	Non-Composite	Composite	Initial Model	Optimized Model
Floor Beam #1 I_y[a]	1,082	3,142	3,142	3,615
Floor Beam #2 I_y[a]	1,550	4,279	4,279	4,928
Floor Beam #3 I_y[a]	1,784	4,763	4,763	5,477
Stringer #1 I_y[a]	50.78	291.8	291.8	335.5
Stringer #2 I_y[a]	175.6	810.4	810.4	931.9
Girder w/ No Angle I_y[a]	8,889	19,310	19,310	17,700
Girder w/ Angle I_y[a]	11,080	26,840	26,840	30,360
Girder w/ 1 Cover I_y[a]	12,610	31,900	31,900	36,150
Girder w/ 2 Cover I_y[a]	13,350	34,460	34,460	38,680
Ext. Beam - End I_y[a]	672.6	4,668	672.6	672.6
Ext. Beam - Int. I_y[a]	805.8	5,772	805.8	805.8
Deck E[b]	22,750	22,750	22,750	25,050
Spring Stiffness[c]	564,900	564,900	564,900	669,630

[a] Units = mm^4 (10^6)
[b] Units = MPa
[c] Units = kN-m/rad.

3.5 CONCLUSION

Commercial systems, such as the BDI system, are commonly being used as the tools to implement the testing, modeling, and rating of existing structures. With an aging and rapidly decaying bridge inventory, the effective management of marginal condition structures is becoming a

pressing issue. Diagnostic load testing for the purpose of load rating is the only currently available technique for determining accurate load carrying characteristics. Most bridges exhibit strength that exceeds that which traditional calculations predict and results in a more accurate and increased load rating. Identification of this "reserve" strength often delays when bridges must be rehabilitated or replaced which results in significant long-term cost savings. While it is recognized that developing load ratings through diagnostic testing costs more than load ratings by traditional hand calculations, the long-terms saving resulting from extending a bridge's useful life minimizes these costs.

3.6 REFERENCES

1. Chajes, M.J., Mertz, D.R., and Commander, B. 'Experimental Load Rating of a Posted Bridge.' *Journal of Bridge Engineering* 2(1)(1997) 1-10.
2. Bridge Diagnostics, Inc. 'BDI Structural Testing System Operation Manual.' (1999)
3. Bridge Diagnostics, Inc. 'BDI Software Package Bridge Modeling and Analysis Program Manuals.' (2002)
4. Bridge Diagnostics, Inc. 'Load Testing and Load Rating Eight State Highway Bridges in Iowa.' *Final Rep. Iowa DOT*. (1999)

4. SYSTEMATIC APPROACH TO DIAGNOSTIC LOAD TESTING AND RATING OF BRIDGES.

A paper written for the Midwest Transportation Consortium student paper contest.

4.1 ABSTRACT

The condition evaluation and rating of bridges is most commonly done through visual inspection and review of the bridge plans. Often this approach does not account for additional strength the bridge exhibits. This results in many bridges being posted with load limits below their actual capacity. Diagnostic load testing and rating is an approach being developed around the nation and at Iowa State University (ISU). The approach taken by the ISU team was developed by Bridge Diagnostics, Inc. (BDI).

BDI has developed a system that includes the actual collection of field testing data to the modeling and rating process. The system includes a field testing system for recording data and a software suite for modeling and analysis. The field data are used to calibrate the finite element model of the structure and in turn used to load rate the bridge.

This paper highlights the system from the investigation of the structure, to field-testing, and through modeling and analysis.

4.2 INTRODUCTION

Many Iowa bridges are in poor visual condition. This poor visual condition often leads to rating calculations that do not truly reflect the strength of the structure thus causing the bridge to be posted at load limits below the legal limits. With an aging inventory of structures and money for replacement of these structures limited, an alternative to traditional visual inspection and load rating calculations is being developed. The diagnostic load testing approach is in the experimental phase throughout the United States and here in Iowa. An effort is underway at Iowa State University to develop procedures and protocols for the diagnostic testing of bridges. At present, numerous structures have been tested using a systematic approach developed by Bridge Diagnostics, Inc. (BDI) of Boulder, CO. The system has three basic phases each with their own tools and individual processes; each phase and its components are highlighted in Fig. 4.1.

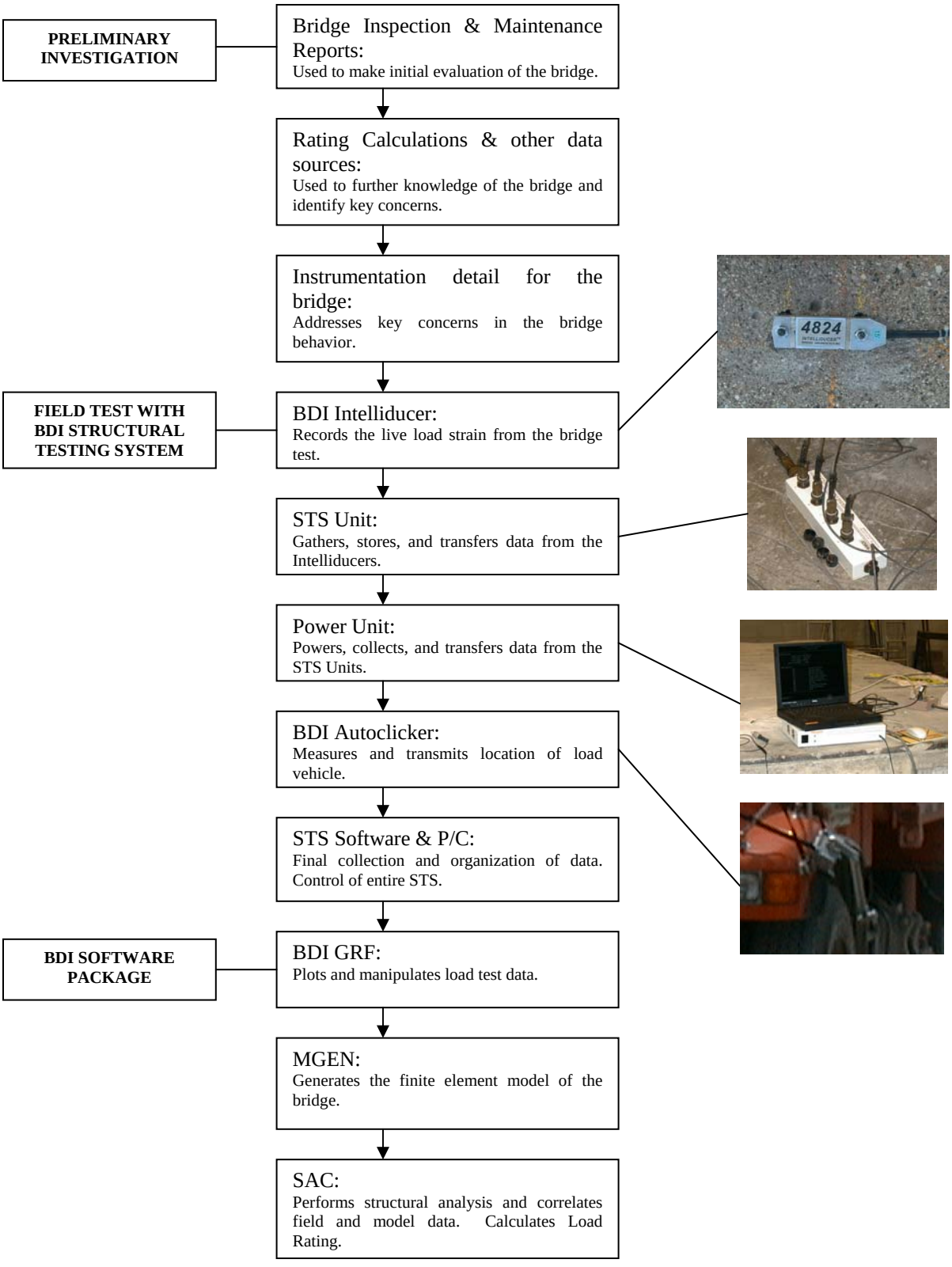

Figure 4.1. Systematic approach followed by the BDI STS.

4.3 PRELIMINARY INVESTIGATION

The preliminary investigation of the bridge is the first step in the bridge testing process. The purpose of such an investigation is to assess the structural issues that need to be addressed in the instrumentation plan used for testing and any other details involved in the testing process. The preliminary investigation involves the review and analysis of all data relating to the structure in question. This may include, but is not limited to, visual inspection reports, structure as-built plans, and previous rating calculations. Most of these items can be found in the bridge inspection and maintenance reports. Other sources of data can be the local maintenance shop, the rating engineer, or a reconnaissance visit to the bridge.

4.3.1 Bridge Inspection and Maintenance Reports

The information contained in the bridge inspection and maintenance reports is often the greatest source of information on a particular structure. The reports include many useful items related to the design and condition of the structure. Basic geometric data are given in the bridge condition report while the as-built plans often provide plan, elevation, and cross-section views of the bridge in detail.

Each report also contains a detailed visual inspection report. This report provides information on the condition of all parts of the structure, substructure to roadway. Any structural deficiencies as well as other concerns in the superstructure will be noted in the visual report. Load ratings are a part of the visual report. Other information such as photographs, legal documents, and miscellaneous notes are also part of the inspection and maintenance report.

4.3.2 Other Sources of Data

Quite often, the bridge inspection and maintenance report does not adequately describe the structure and its surroundings in the detail that may be required by the instrumentation designer. For this reason, a reconnaissance trip to the structure may be required. During such a trip, accurate measurements may be completed along with a visual inspection to confirm or expand the knowledge given in the visual report. Issues such as accessibility to the superstructure and traffic control could play a large part in the development of an instrumentation plan. For instance, the distance from the superstructure to the ground may require that a “Snooper” truck be used rather than ladders, and this may also alter the instrumentation plan.

Another source of data can be the actual rating calculations kept by the bridge owner. Rating calculations often bring specific issues to light such as concerns with certain members or questions in effectiveness of composite action. These concerns may then be addressed in the instrumentation plan.

4.3.3 Development of an Instrumentation Plan

The layout of the transducers is heavily dependent on the issues that arise in the review of all available data. All efforts should be made to instrument any specific concerns resulting from the data review. For instance, if a floor beam is found to be deficient through load rating calculations, the beam should be heavily instrumented. The instrumentation in question measures strain; the transducers themselves are to be addressed later in this paper. A typical bridge test will use 20 to 40 strain transducers, usually in pairs on a cross-section so that the neutral axis of the section may be calculated. Other common areas that should be addressed, in addition to the concern from data review, should be member end restraint and locations of maximum strains.

Once an instrumentation plan is set, the details of the test, including load truck, traffic control, etc., should be coordinated with the proper authorities.

4.4 BDI STRUCTURAL TESTING SYSTEM (STS)

The Structural Testing System (STS) is the field component of the testing and rating system designed by BDI. The STS is comprised of four main components: BDI Intelliducers, BDI STS Units, the BDI Autoclicker, and the BDI Power Unit. Each component of the system is involved in the data collection process.

4.4.1 BDI Intelliducer

The BDI Intelliducer, shown in Fig. 4.2, is the actual instrumentation used in the system. Each Intelliducer measures 4.4 in. x 1.2 in. x 0.4 in. with either a 15 ft or 25 ft transducer wire attached. The Intelliducer is nothing more than a strain transducer with extra features. The first feature is the ability of the transducer to identify itself to the rest of the system. A number, for instance 4696, 4788, etc., identify each Intelliducer. This is possible by the addition of an identification chip in each transducer. The chip allows for each transducer to be identified and recognized by the STS. The STS then has the ability to calibrate and zero the transducer using a pre-stored transducer calibration factor.

The second feature of the Intelliducer is its versatility so it can be used on many different surfaces, including but not limited to steel, concrete (reinforced and pre-stressed), and timber. This

versatility stems from the design and another feature, the ease of application of the transducers. Two holes are located 3 in. on center in the transducer to accommodate two tabs. The two tabs are the portions of the gage that actually come in contact with the surface being tested. This limited area of contact enables the placement of an Intelliducer in a few minutes.

Figure 4.2. A BDI Intelliducer in use on a steel girder.

The placement of an Intelliducer on steel requires that any paint or other material covering the steel be removed. This will usually require the use of a grinder and a rag. For concrete structures, either reinforced or pre-stressed, the surface needs only to be free of foreign debris and smooth to the touch. Once the surface is prepared, the transducer may be applied.

To apply a transducer to steel or pre-stressed concrete, a healthy amount of adhesive (Loctite 410 Black Toughened Adhesive) must be applied to the tabs. The transducer is then pressed against the prepared surface in the proper alignment and then removed. At this time, an adhesive accelerator (Loctite Tak Pak 7452) is be sprayed onto the glue that remains on the prepared surface. The transducer should now be placed in its proper position with as little time passing between the accelerator application and transducer placement as possible.

For transducer placement on reinforced concrete structures, the use of transducer extensions should be implemented, as shown in Fig. 4.3. The extension of the gage length from three inches to longer lengths enables surface strain to be averaged over a greater distance, thus reducing the effects of cracks in the concrete. BDI has prescribed a set of standards for the use and length of gage

extension. A gage length of 1.0 x d, where d is the member depth, and L/20, where L is the span length, are given as lower and upper bounds, respectively, for reinforced concrete slabs and rectangular beams. For T-beams, the lower and upper bounds are given as 1.5 x d and L/20, respectively. The gage extensions allow for lengths from six inches to 24 in. in 3 in. intervals.

Once a gage length has been selected, the extensions can be fitted with a tab at the proper distance. The wired end of the Intelliducer can also be fitted with a tab, but the non-wired end should remain open. When the gage is needed in the field, the extension should be attached to the Intelliducer. Extensions attach to the non-wired end of the Intelliducer through the tab hole. Special bolts are included with the STS for this purpose. It is important to align the bolt and extension properly such that the extension and transducer are straight. Once the extension is secured to the transducer, the Intelliducer can be installed. The procedure remains the same for the actual application of the transducer to the structural surface. Once all transducers in a given setup have been placed, the transducer wires should be connected to the BDI STS Units.

Figure 4.3. An Intelliducer with gage extension in use.

4.4.2 STS Unit

The BDI STS Unit, shown in Fig. 4.4, is the heart of the system. The STS Unit records and stores the data collected from the Intelliducers during the test. Each STS Unit, Iowa-1 through Iowa – 10, is capable of collecting data from four Intelliducers. An STS Unit has the capability of storing

50,000 data points during a single test. Once the testing is complete, the data are transferred to the STS Power Unit.

Figure 4.4. BDI STS Units in use during a load test.

Each STS Unit measures 2.3 in. x 3.0 in. x 11.0 in. and weighs approximately 1.8 lbs. The unit is equipped with six connection points: four transducer connections, “a line out”, and “a line in.” All of the connections are quick-lock military-style for fast and easy assemblage. When connections are locked properly, there is no chance that a transducer wire may become loose and cease functioning. The units are connected via heavy cables to one another and eventually to the Power Unit. The cable varies in length from 15 ft to 100 ft. The “line out” or P/C end of the unit carries to data toward the Power Unit and to the P/C. The “line in” connection is designed to attach to other STS Units in use. The STS Units are designed to run in series or parallel. All ten boxes may be directly linked in a chain or they may branch out through the use of Y-cables. When all of the units are connected, only one cable is connected to the Power Unit. This is a great advantage over traditional transducer wiring where each instrument must have its own wire connection to the data acquisition system.

4.4.3 Power Unit

The Power Unit, shown in Fig. 4.5, collects the final data and transmits commands to the system during the test. Each transducer requires a 5-volt excitation voltage that is provided by the

Power Unit. The unit has the ability to operate under two different energy sources, DC current from an automobile battery or AC current from a small portable generator.

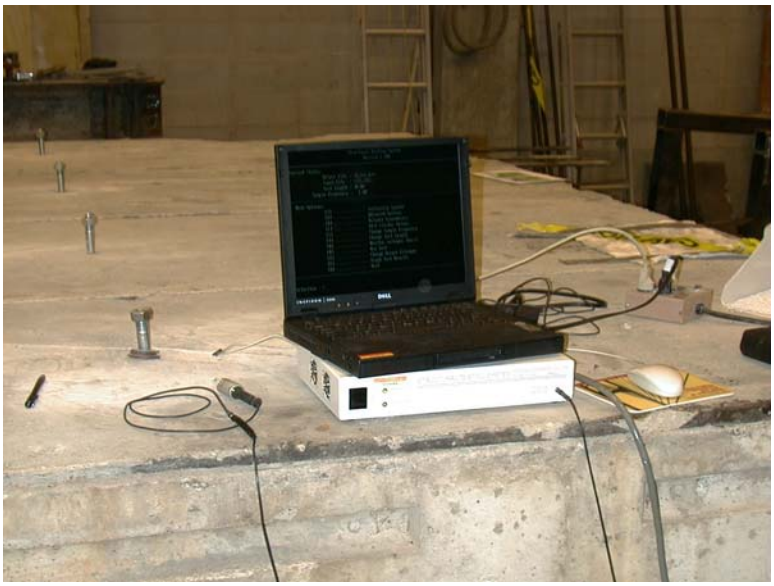

Figure 4.5. BDI Power Unit connected and ready for use.

4.4.4 BDI Autoclicker

The BDI Autoclicker, shown in Fig. 4.6, measures and transmits the load vehicle position to the STS system through the use an electronic eye and hand-held radio transmitters. A reflective strip placed on the load vehicle's wheel triggers the electronic eye, located at the end of the "arm". Thus, every wheel revolution creates a "click." A click is nothing more than a tap of the transmission button on the radio resulting in an audible click. The click is transmitted to the STS through a hand-held radio attached to the Autoclicker and received by a radio attached to the Power Unit. This will yield the exact truck position every 10 to 12 ft, a typical wheel revolution. For bridges that have a very short span as compared to a wheel revolution, the clicks may be recorded by hand by simply removing the Autoclicker radio and tapping the transmit button at regularly spaced intervals.

It should be noted that the use of the Autoclicker could cause EM interference that will affect the Intelliducers in the immediate area. The usual result will be large spikes in the strain data at regular intervals. Twisting the Intelliducer wires into a spiral can relieve this problem.

4.4.5 STS Software and Personal Computer

The brain functions of the system are performed by the STS software. The software is run in a Microsoft Windows environment on a laptop computer that is attached via parallel port to the Power Unit. The system is relatively easy to use via mouse with pull down menus and large command buttons. The initial setup of the software should be completed after all connections between Intelliducers, STS Units, and the Power Unit have been completed. The initial setup verifies that all Intelliducers are recognized by the rest of the system and that all connections are tight. This information will appear on the computer screen.

Figure 4.6. BDI Autoclicker in use during a load test.

The main software menu window contains most of the information that is critical to the load test. Items such as sample frequency, test length, and file output name are easily accessible in the main window. Other options specifically related to Intelliducers such as channel gain, initial offset, and filtering are located in the advanced options menu. Channel gains default to 1000, but can be set at 1, 250, or 500. Gain becomes an issue where very large strains are measured. If a high gain is used, the sensitivity of the Intelliducers is increased while its range is decreased. Careful attention should be given to this if high strains are expected.

Once all test parameters have been set, the running of the test requires a few taps of the mouse. All transducers should be balanced just prior to the test to minimize offset. When all

transducers are balanced, the testing may proceed. The Windows version of the software allows for four different channels to be viewed during a test. This “real time” data can visually verify that the system is working properly and that the Intelliducers are recording.

4.5 BDI SOFTWARE PACKAGE

The analysis and modeling portion of the load test in completed with the BDI Software Package. Included in the package are software for graphing field and model data, model generation, and model analysis and correlation. When all of these tools are used correctly, an accurate bridge model will be developed.

4.5.1 BDI Graph Data Viewer (BDIGRF)

BDIGRF is the first of the analysis software to be used in the modeling process. An initial investigation of the field data is required to develop the proper bridge model. The BDIGRF program takes a field data file with transducer output and clicker values and plots the strain versus truck position for the desired gage locations and truck paths, shown in Fig. 4.7. In all cases, the clicker distance, a wheel revolution or other interval, needs to be input into the program. Other items, such as gage factors and distance between transducers, may also need to be input. Besides the strain versus truck position plot, other plots such as neutral axis location versus truck position may be constructed. Options such as data filtering and offset correction may also be completed in BDIGRF.

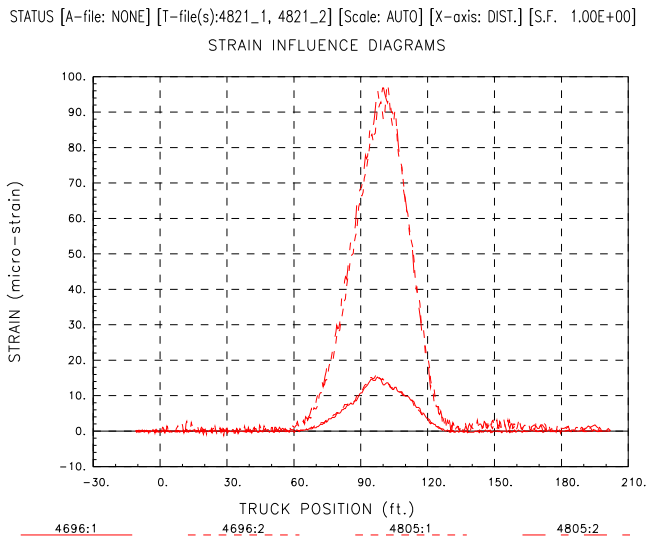

Figure 4.7. Typical BDIGRF plot of field strain versus truck position.

When all field data has been plotted, an initial evaluation of the structure response may be made. Items such as neutral axis depth and maximum strain values can yield insight into the initial material properties to be input into the model. Other issues, such as direction of curvature at connections, expose the actual support conditions at that location. After all issues in the field data have been resolved and general behavior has been established, all information required for an initial model is available.

4.5.2 Model Generator (MGEN)

The actual bridge model is created in the MGEN software. The finite element model is comprised of beam and shell elements only. Most structures can be modeled using these elements. The first input data are the structure geometry from the as-built plans and any notes from the field. All dimensions and structural elements are described in the geometry portion of the model development. Once the geometry has been set, the material and section properties may be input. Data from the field results becomes useful in this portion of modeling. Neutral axis depth can be assumed using a linear strain profile. This will generate various section properties such as effective slab width in composite bridge structures. The addition of springs throughout the structure, especially at supports, can be justified through the field data.

Once the model is defined and all parameters have been set, the transducer locations may be defined. The model is now ready for calibration.

4.5.3 Structural Analysis and Correlation (SAC)

The calibration of the finite element model is done through the use of the SAC program. The SAC program takes the model and the field data and relates the strain values. The model is optimized through the use of multiple variables, such as E (elasticity of the bridge deck), spring constants, and I (moment of inertia of structural elements) . The modeler sets the optimization boundaries. Appropriate boundaries should be set such that the final results are realistic.

Multiple iterations are usually required to arrive at a satisfactory model. SAC runs a statistical analysis of the model strains as compared to the field strains. The results are given in percent error, total error, scale error, and correlation confinement. BDIGRF may be used to plot field and model results for an illustration of the model accuracy. When all parties involved are satisfied with the model, ratings may be calculated using the SAC software.

4.6 CONCLUSION

The diagnostic load testing process often reveals additional strength and redundancy in the bridge that is not taken into account in traditional load rating calculations. Through a detailed analysis of the field data and engineering judgment, it is possible that load ratings of many bridges could be raised or in some cases an existing posting could be removed. This would in turn lengthen the lifespan of many structures and better manage a large inventory of structures. The usefulness of diagnostic load testing and rating is yet to be determined, but promises to be an influence in how structural inventories are managed in the future.

4.7 REFERENCES

Bridge Diagnostics, Inc. (2002). "BDI Structural Testing System Operational Manual."

Bridge Diagnostics, Inc. (2000). "BDI Software Package Bridge Modeling and Analysis Program Manuals."

Chajes, M.J., Shenton, H. W., O'Shea, D. (2000). "Use of Field Testing in Delaware's Bridge Management Program." Eighth International Bridge Management Conference.

5. GENERAL CONCLUSION

5.1 SUMMARY

The common thread within all three of the papers presented is that the BDI STS gives one the ability to plan, implement, and execute a diagnostic load test of a bridge in the field in a single day with the simplest of efforts. As a companion to the STS, the BDI Software Suite allows for a simple transition from the field to the realm of finite element modeling and advanced computer analysis.

Chapter 2 explored the efficiency and ease of the field implementation of the BDI STS while Chapter 3 documented the process from field testing through final rating for a particular bridge. Chapter 4 reviewed and detailed the general processes and systems within the BDI diagnostic testing approach.

5.2 CONCLUSION

- **The limits placed on an element group can greatly influence the optimized parameters of a finite element model using BDI WinGEN and WinSAC.** The further analysis of Bridge #3 in Chapter 2 showed that the limits can impact the final optimized parameters. The initial model optimized parameters were bound by the limits established based on the physical properties of the structure. When those limits were widened, the optimization process pushed the optimized properties past the initial limits.
- **Given the simplicity of the BDI STS setup and installation, there is not a great savings in reducing the number of transducers used for a typical load test.** As shown in all three case studies in Chapter 2, the time savings that would occur on a typical diagnostic load test by reducing the transducers installed by half, is minimal when compared to the data collected by those transducers. Bridge #3 in Chapter 2 is an example of where having as much data as possible can greatly aid the modeling process.
- **The BDI STS simplifies the diagnostic load testing process to single day for a typical bridge.** In all cases presented, the instrumentation, testing, and dismantling of the STS system took less than one day. This cuts by more than half the typical bridge testing procedures for foil gage based testing.
- **The BDI STS and Software Suite combine to simplify the transition of field data into data used for the modeling process.** The raw STS field data can easily be imported into the BDI Software Suite for inclusion in the model optimization process. A seamless transition can be made without the need for hours of post-test data processing.

- **The BDI STS can be used to determine if additional strengthening of bridges by structural modification is useful and increases the load rating of the bridge in question.** The case study presented in Chapter 3 illustrates a case where a bridge had been strengthened by modification to the existing condition. The diagnostic load test proved that the modification had the intended end result.
- **The STS and Software Suite are useful in determining the structural behavior in a structure.** The system was used in multiple cases to study the true behavior of structures. This true behavior often differs from the assumptions that rating engineers are forced to make during the traditional hand calculation rating methods.

5.3 RECOMMENDATIONS

- **The Iowa Department of Transportation should develop a formal policy for guidance on the use of diagnostic load testing.** A document that outlines when and where a diagnostic load test should be considered should be prepared by the Iowa DOT. This document could serve as the basis of a diagnostic load testing program in which bridges with questionable load rating by traditional methods could further be examined and more accurate load ratings derived through testing.
- **The Iowa Department of Transportation should adopt a policy for use of diagnostic load testing for monitoring the behavior of bridge subject to loads higher than the legal load limits.** More and more often larger loads are making their way across bridges. Analyses of the route and the structures on that route are compiled by computer programs. As an additional measure of safety, occasional testing of bridges during a higher load event could determine if structural damage occurred during that event. A policy should be adopted for loads that exceed a given limit and those events should be observed and tested.
- **Further diagnostic load test should be completed for integral abutment bridges.** Integral abutment bridges complicate the modeling process by exhibiting significant end restraint. Only one integral abutment bridge was tested as a part of this effort. Further testing of integral abutments and generalized behavior of a larger test set could aid in establishing testing procedures for integral abutments and aid in rating of integral abutment bridges.
- **A program should be developed to aid Iowa's Counties in the use of diagnostic load testing.** Iowa's counties own most of the state's deficient structures. Development of a program to financially aid the counties, or make the STS available to counties to use, would assist the counties in their management of a rapidly aging system.

- **Standardized procedures and outlines for conducting a diagnostic load test should be developed.** A formal document should be prepared to guide someone new to the STS and BDI software package so they could, with a bit of oversight and input from experienced users, test, create and optimize a model, and rate a bridge using the BDI package.
- **Further testing of prestressed concrete beam bridges should conducted.** A vast majority of Iowa's bridge are prestressed concrete beam with reinforced concrete deck systems. A large body of data should be collected on these types of bridges so in the future simplified generalizations about prestressed beam bridge behavior can be made. A large library of data on any one bridge type could reduce the need for specific testing of bridges in the future.

ACKNOWLEDGEMENTS

The work described in this report was conducted at the Bridge Engineering Center at the Center for Transportation Research and Education at Iowa State University and sponsored by the Iowa Highway Research Board through the Iowa Department of Transportation.

I would like to thank Dr. Terry J. Wipf, Dr. F. Wayne Klaiber, and Dr. Brent Phares for their patience and support through this research process as well as their guidance and encouragement. I would also like to thank Dr. Les Schmerr for serving on my Program of Study Committee.

I owe a great debt to Espen Mellingen for his work on this project. Espen was responsible for a great deal of the modeling associated with this project and delivered the Iowa Highway Research Board report when I was unable to.

Thanks are also due to many of the civil engineering graduate students that were at ISU at the same time. Many assisted in the research documented here including Brian Kempers, Justin Vander Werff, David Tarries, J. Scott Ingersoll, Travis Konda, and Justin Doornick. The 'Bulpen' crew pulled many late night study sessions for anything from steel design to mechanics of materials.

Special thanks are due for the Iowa Department of Transportation Office of Bridge and Structures for their patience throughout this process. Particular special thanks are due to Ahmad Abu-Hawash, Gary Novey, Scott Neubauer, Ronald Meyer, and Norm McDonald.

This work is dedicated to the memory of those who achieved much at a young age only to be taken at a young age, Adam Sundall and Melissa Peterson. They both accomplished a great deal in their short lives and led their lives without fear and took chances, "burn the boats."

This work could not have been completed without the spiritual guidance and prayerful support of Pastor Phil Dicks. Pastor Phil came into my life at the exact moment that he was needed and has provided plenty of 'God moments' over the past year.

More than thanks are due to my wife, Barbara, for her patience, understanding, and encouragement during this process. This thesis was at times a great struggle in our marriage and an obstacle to overcome. When the work seemed overwhelming and the results disappointing, Barb was there as a steady head and constant support. God could not have given me a better companion to share this life with.

All of the credit for this work is to go to Christ Jesus who suffered that I may have a chance at life everlasting. "For it is by grace you have been saved, through faith – and this not from yourselves, it is the gift of God." – Ephesians 2:8

APPENDIX A

MODELING AND RATING RESULTS FROM CHAPTER 2

Table A.1. Bridge #1: Transducer locations used for additional modeling.

Model	Transducers	Transducer Locations Used (Marked with X)																			
Name	Used	L1	L2	L3	L4	L5	L6	L7	L8	L9	L10	L11	L12	L13	L14	L15	L16	L17	L18	L19	L20
AJ1A	40	X	X	X	X	X	X	X	X	X	X	X	X	X	X	X	X	X	X	X	X
AJ1B	40	X	X	X	X	X	X	X	X	X	X	X	X	X	X	X	X	X	X	X	X
AJ2A	36	X	X		X	X	X	X	X	X	X	X	X	X	X	X	X		X	X	X
AJ2B	36	X	X	X	X	X	X	X	X	X	X	X			X	X	X	X	X	X	X
AJ2C	36	X			X	X	X	X	X	X	X	X	X	X	X	X	X	X	X	X	X
AJ2D	36	X	X	X	X	X	X	X	X	X	X		X		X	X	X	X	X	X	X
AJ2E	36	X	X	X	X	X	X	X	X		X	X	X	X	X	X	X	X	X		X
AJ2F	36	X	X	X	X	X	X		X	X	X	X	X	X	X	X	X		X	X	X
AJ2G	36	X		X	X	X	X	X	X	X	X	X	X	X	X	X		X	X	X	X
AJ2H	36	X	X		X	X	X	X	X	X	X	X	X		X	X	X	X	X	X	X
AJ2I	36	X		X	X	X	X	X	X	X	X	X		X	X	X	X	X	X	X	X
AJ2J	36	X	X	X	X	X	X	X		X	X	X	X	X		X	X	X	X	X	X
		L1	L2	L3	L4	L5	L6	L7	L8	L9	L10	L11	L12	L13	L14	L15	L16	L17	L18	L19	L20
AJ3A	32					X	X	X	X	X	X	X	X	X	X	X	X	X	X	X	X
AJ3B	32	X	X	X	X	X	X	X	X	X	X					X	X	X	X	X	X
AJ3C	32	X	X	X	X	X	X	X	X			X	X	X	X	X	X	X	X		
AJ3D	32	X			X	X	X	X	X	X	X	X	X	X	X	X			X	X	X
AJ3E	32	X	X		X	X	X		X	X	X	X	X		X	X	X		X	X	X
AJ3F	32	X		X	X	X		X	X	X	X	X		X	X	X		X	X	X	X
AJ3G	32	X	X			X	X	X	X	X	X	X	X	X	X	X	X			X	X
AJ3H	32	X	X	X	X	X	X			X	X	X	X			X	X	X	X	X	X
AJ3I	32	X	X	X	X	X			X	X	X	X			X	X	X	X	X	X	X
AJ3J	32	X			X	X	X	X	X	X	X	X	X			X	X	X	X	X	X
		L1	L2	L3	L4	L5	L6	L7	L8	L9	L10	L11	L12	L13	L14	L15	L16	L17	L18	L19	L20
AJ4A	28	X			X	X	X	X	X	X	X					X	X	X	X	X	X
AJ4B	28					X	X	X	X	X	X	X			X	X	X	X	X	X	X
AJ4C	28	X	X	X	X	X	X	X	X			X			X	X	X	X	X		
AJ4D	28	X			X	X	X	X	X		X	X			X	X	X	X	X		X
AJ4E	28	X			X	X	X	X	X	X	X	X			X	X			X	X	X
AJ4F	28	X	X			X	X	X	X	X	X	X	X			X	X			X	X
AJ4G	28	X	X	X		X	X	X			X	X	X	X		X	X	X			X
AJ4H	28	X	X		X	X	X		X		X	X	X		X	X	X		X		X
AJ4I	28	X	X	X	X	X	X	X	X	X	X					X	X	X			X
AJ4J	28	X	X			X	X			X	X	X	X			X	X	X	X	X	X

Table A.1. Continued.

Model	Transducers	Transducer Locations Used (Marked with X)																			
Name	Used	L1	L2	L3	L4	L5	L6	L7	L8	L9	L10	L11	L12	L13	L14	L15	L16	L17	L18	L19	L20
AJ5A	24					X	X	X	X	X	X					X	X	X	X	X	X
AJ5B	24					X	X	X	X			X	X	X	X	X	X	X	X		
AJ5C	24	X	X	X	X	X	X	X	X							X	X	X	X		
AJ5D	24	X	X		X	X	X		X			X	X		X	X	X		X		
AJ5E	24	X			X	X			X	X	X	X			X	X			X	X	X
AJ5F	24	X			X	X	X	X	X	X	X					X			X	X	X
AJ5G	24	X	X		X	X	X		X	X	X					X	X		X		X
AJ5H	24	X		X		X		X		X	X	X		X		X		X		X	X
AJ5I	24		X		X		X		X	X	X		X		X		X		X	X	X
AJ5J	24	X	X		X	X	X	X	X		X					X	X		X		X
		L1	L2	L3	L4	L5	L6	L7	L8	L9	L10	L11	L12	L13	L14	L15	L16	L17	L18	L19	L20
AJ6A	20					X	X	X	X	X	X					X	X	X	X		
AJ6B	20	X			X	X			X	X	X	X			X	X			X		
AJ6C	20	X			X	X			X	X	X					X			X	X	X
AJ6D	20					X	X	X	X	X	X					X			X	X	X
AJ6E	20	X		X		X		X		X	X	X		X		X		X			
AJ6F	20	X	X			X	X			X	X	X	X			X	X				
AJ6G	20	X	X			X	X			X	X					X	X			X	X
AJ6H	20	X	X	X	X	X	X	X	X							X			X		
AJ6I	20	X			X	X	X	X	X							X	X	X	X		
AJ6J	20	X	X	X	X	X	X	X	X	X	X										
		L1	L2	L3	L4	L5	L6	L7	L8	L9	L10	L11	L12	L13	L14	L15	L16	L17	L18	L19	L20
AJ7A	16					X	X			X	X					X	X			X	X
AJ7B	16					X		X		X	X					X		X		X	X
AJ7C	16	X			X	X			X		X					X			X		X
AJ7D	16	X		X		X		X			X					X		X			X
AJ7E	16					X			X	X	X					X			X	X	X
AJ7F	16	X				X	X	X	X		X					X					X
AJ7G	16	X				X		X		X	X					X				X	X
AJ7H	16					X	X	X			X					X	X	X			X
AJ7I	16	X			X	X			X	X						X			X	X	
AJ7J	16		X				X	X	X	X							X		X	X	
		L1	L2	L3	L4	L5	L6	L7	L8	L9	L10	L11	L12	L13	L14	L15	L16	L17	L18	L19	L20
AJ8A	12	X				X				X	X					X					X
AJ8B	12					X				X	X					X				X	X
AJ8C	12	X				X					X	X				X					X
AJ8D	12	X			X	X			X		X					X			X		
AJ8E	12					X			X		X					X			X		X
AJ8F	12					X	X				X					X	X				X
AJ8G	12	X				X		X			X					X					X
AJ8H	12		X				X				X		X				X				X
AJ8I	12	X			X	X					X					X					X
AJ8J	12					X	X	X	X	X	X										

Table A.1. Continued.

Model	Transducers	Transducer Locations Used (Marked with X)																			
Name	Used	L1	L2	L3	L4	L5	L6	L7	L8	L9	L10	L11	L12	L13	L14	L15	L16	L17	L18	L19	L20
AJ9A	8	X				X					X					X					
AJ9B	8	X				X			X		X										
AJ9C	8					X					X					X					X
AJ9D	8				X	X					X								X		
AJ9E	8	X			X	X			X												
AJ9F	8				X				X		X								X		
AJ9G	8	X			X	X			X												
AJ9H	8					X			X	X	X										
AJ9I	8	X	X			X	X														
AJ9J	8	X									X					X					X

Table A.2. Bridge #1: Additional modeling results.

									Flexural Rating	
Model	Gages	I (in^4)	E (ksi)	k (k-in/rad)	Total Error	% Error	Scale Error	Corr. Coef.	Interior	Exterior
aj1a	40	1279	838	26500	3330	2.1	1.8	0.989	1.31	1.54
aj1bc	40	1279	841	26036	3335	2.1	1.8	0.9893	1.31	1.53
aj2a	36	1279	820	26138	3093	2.1	1.7	0.9895	1.31	1.54
aj2b	36	1280	889	25330	3005	2.2	1.8	0.9888	1.31	1.53
aj2c	36	1277	861	26740	3098	2.1	1.8	0.9896	1.31	1.54
aj2d	36	1283	884	25809	3095	2.3	1.9	0.9884	1.3	1.53
aj2e	36	1270	818	25521	2889	2.1	1.8	0.9892	1.31	1.53
aj2f	36	1276	826	26322	3043	2.3	1.9	0.9882	1.31	1.54
aj2g	36	1281	867	26044	3127	2.1	2	0.9896	1.31	1.53
aj2h	36	1285	853	26003	3087	2.2	1.8	0.9887	1.3	1.54
aj2i	36	1272	896	25940	3011	2	1.9	0.9897	1.31	1.53
aj2j	36	1266	745	25487	2899	2.2	1.7	0.9889	1.3	1.53
aj3a	32	1255	848	31360	2685	1.9	1.7	0.9906	1.34	1.55
aj3b	32	1271	839	24175	2697	2.1	1.8	0.9894	1.3	1.52
aj3c	32	1283	720	26075	2550	2.1	1.7	0.9893	1.3	1.55
aj3d	32	1281	848	26175	2886	2	1.8	0.9898	1.31	1.54
aj3e	32	1283	841	26295	2791	2.5	1.8	0.9874	1.31	1.54
aj3f	32	1283	1000	24881	2686	2	2.1	0.9899	1.31	1.52
aj3g	32	1268	846	29365	2646	1.7	1.6	0.9913	1.32	1.55
aj3h	32	1265	744	25615	2615	2.8	1.8	0.9858	1.3	1.53
aj3i	32	1287	1007	25104	2598	2.6	2	0.9869	1.31	1.52
aj3j	32	1270	789	27002	2633	1.9	1.6	0.9903	1.31	1.54

Table A.2. Continued.

									Flexural Rating	
Model	Gages	I (in^4)	E (ksi)	k (k-in/rad)	Total Error	% Error	Scale Error	Corr. Coef.	Interior	Exterior
aj4a	28	1271	865	24399	2458	2	1.7	0.9898	1.3	1.52
aj4b	28	1258	902	30499	2361	1.9	1.7	0.9903	1.34	1.54
aj4c	28	1282	765	25191	2226	2.3	1.7	0.9885	1.3	1.54
aj4d	28	1270	889	25057	2332	2.2	1.8	0.989	1.31	1.52
aj4e	28	1283	900	25089	2555	2.1	1.8	0.9894	1.3	1.53
aj4f	28	1271	789	27817	2301	1.6	1.5	0.9918	1.31	1.54
aj4g	28	1244	698	26713	2025	1.7	1.7	0.9914	1.31	1.53
aj4h	28	1273	808	25579	2369	2.6	1.8	0.9868	1.31	1.53
aj4i	28	1289	829	22227	2302	1.7	1.8	0.9914	1.29	1.52
aj4j	28	1257	746	27281	2257	2.6	1.7	0.9869	1.31	1.54
aj5a	24	1253	847	28444	2062	1.8	1.5	0.991	1.33	1.53
aj5b	24	1249	719	33495	1902	1.8	1.6	0.9911	1.34	1.57
aj5c	24	1269	676	23936	1923	2.1	1.6	0.9895	1.29	1.53
aj5d	24	1289	691	26315	1999	2.7	1.7	0.9865	1.32	1.54
aj5e	24	1293	1031	24900	2141	2.4	2.1	0.9877	1.3	1.52
aj5f	24	1279	845	22979	2239	2	1.7	0.9901	1.29	1.52
aj5g	24	1280	780	21950	2115	2.2	1.7	0.989	1.29	1.52
aj5h	24	1270	944	26059	1815	1.6	1.9	0.9922	1.31	1.52
aj5i	24	1288	842	26220	2280	2.6	1.9	0.9869	1.3	1.54
aj5i	24	1261	757	22293	2016	2	1.6	0.9899	1.29	1.51
AJ6A	20	1256	796	29031	1737	1.6	1.3	0.9921	1.32	1.54
AJ6B	20	1304	990	23778	1820	2.2	1.8	0.9892	1.29	1.53
AJ6C	20	1281	979	22930	1834	2.3	2	0.9884	1.3	1.51
AJ6D	20	1255	828	28349	1853	1.7	1.5	0.9913	1.31	1.54
AJ6E	20	1279	903	25272	1494	1.3	1.7	0.9937	1.31	1.53
AJ6F	20	1263	713	28332	1592	1.8	1.3	0.9907	1.31	1.55
AJ6G	20	1253	772	25815	1638	2.2	1.6	0.9888	1.31	1.52
AJ6H	20	1280	636	22268	1688	2	1.5	0.99	1.28	1.53
AJ6I	20	1271	703	24001	1687	2	1.5	0.99	1.29	1.53
AJ6J	20	1317	790	16974	1809	1.5	1.5	0.9927	1.25	1.51
AJ7A	16	1233	794	31067	1352	2	1.4	0.99	1.34	1.54
AJ7B	16	1266	1025	28501	1323	1.6	1.6	0.992	1.33	1.53
AJ7C	16	1263	910	21011	1378	2.4	2	0.9882	1.29	1.49
AJ7D	16	1261	981	24167	1116	1.6	2.1	0.9921	1.31	1.5
AJ7E	16	1257	964	28460	1452	2	1.8	0.9901	1.33	1.53
AJ7F	16	1277	807	20959	1342	1.4	1.7	0.9931	1.28	1.51
AJ7G	16	1277	1036	25932	1327	1.6	1.8	0.9918	1.31	1.52
AJ7H	16	1225	720	28424	1220	1.6	1.4	0.9921	1.33	1.53
AJ7I	16	1299	855	23604	1541	2.4	1.8	0.9881	1.29	1.53
AJ7J	16	1300	483	28692	1429	1.7	1.3	0.9913	1.29	1.6

Table A.2. Continued.

									Flexural Rating	
Model	Gages	I (in^4)	E (ksi)	k (k-in/rad)	Total Error	% Error	Scale Error	Corr. Coef.	Interior	Exterior
AJ8A	12	1303	1033	21891	967	1.8	2	0.9912	1.29	1.51
AJ8B	12	1256	1027	30547	1026	1.9	1.6	0.9913	1.34	1.53
AJ8C	12	1288	687	23187	838	1.9	1.9	0.9915	1.31	1.5
AJ8D	12	1279	838	21485	1069	2.5	1.8	0.9874	1.29	1.51
AJ8E	12	1237	897	26894	1019	1.9	1.7	0.9903	1.33	1.51
AJ8F	12	1174	530	29615	917	1.7	1.4	0.9913	1.35	1.53
AJ8G	12	1269	913	21694	867	1.4	1.8	0.9929	1.3	1.5
AJ8H	12	1218	590	29280	974	2.3	1.6	0.9885	1.33	1.54
AJ8I	12	1231	677	20520	938	1.6	2	0.9871	1.29	1.49
AJ8J	12	1478	781	0	1348	1.4	1.3	0.9943	1.13	1.49
AJ9A	8	1207	620	24259	588	1.6	1.5	0.9919	1.32	1.51
AJ9B	8	1348	904	7247	676	1.1	1.3	0.9946	1.21	1.46
AJ9C	8	1191	642	28392	598	1.7	1.5	0.9913	1.34	1.52
AJ9D	8	1169	484	23286	776	2.7	1.2	0.9866	1.32	1.5
AJ9E	8	1343	876	11517	715	1.5	1.5	0.9925	1.22	1.48
AJ9F	8	1266	969	22628	846	2.2	1.5	0.9892	1.3	1.5
AJ9G	8	1343	876	11517	715	1.5	1.5	0.9925	1.22	1.48
AJ9H	8	1456	923	0	858	1.2	1.2	0.9946	1.14	1.47
AJ9I	8	1254	363	15185	588	1.6	1.3	0.9922	1.24	1.51
AJ9J	8	1119	2763	31950	526	1.6	3	0.9921	1.47	1.41

Table A.3. Bridge #2: Transducer locations used for additional modeling.

Model	Transducers	Gage Locations Used (Marked with X)															
Name	Used	L1	L2	L3	L4	L5	L6	L7	L8	L9	L10	L11	L12	L13	L14	L15	L16
a1	32	X	X	X	X	X	X	X	X	X	X	X	X	X	X	X	X
b1	32	X	X	X	X	X	X	X	X	X	X	X	X	X	X	X	X
a2	28	X	X	X	X	X		X		X	X	X	X	X	X	X	X
b2	28	X	X	X	X		X		X	X	X	X	X	X	X	X	X
c2	28	X	X	X	X	X	X	X	X	X	X	X	X			X	X
d2	28	X	X	X	X			X	X	X	X	X	X	X	X	X	X
e2	28	X	X	X	X	X	X			X	X	X	X	X	X	X	X
f2	28			X	X	X	X	X	X	X	X	X	X	X	X	X	X
g2	28	X	X	X	X		X	X	X	X	X		X	X	X	X	X
h2	28	X	X	X	X	X		X	X	X	X	X		X	X	X	X
i2	28	X	X	X	X	X	X	X	X	X	X	X	X		X	X	
j2	28	X	X	X		X	X	X	X	X		X	X	X	X	X	X

Table A.3. Continued.

Model Name	Transducers Used	Gage Locations Used (Marked with X)															
		L1	L2	L3	L4	L5	L6	L7	L8	L9	L10	L11	L12	L13	L14	L15	L16
a3	24	X	X	X	X	X	X	X	X	X	X	X	X				
b3	24	X	X	X	X					X	X	X	X	X	X	X	X
c3	24	X	X	X	X			X	X	X	X	X	X			X	X
d3	24	X		X	X	X		X		X	X	X		X	X	X	X
e3	24		X	X	X		X		X	X	X		X	X	X	X	X
f3	24	X		X	X	X	X			X	X	X		X	X	X	X
g3	24		X	X	X			X	X	X	X		X	X	X	X	X
h3	24	X	X	X		X		X		X		X	X	X	X	X	X
i3	24	X	X		X		X		X		X	X	X	X	X	X	X
j3	24			X	X	X	X			X	X	X	X	X	X	X	X
		L1	L2	L3	L4	L5	L6	L7	L8	L9	L10	L11	L12	L13	L14	L15	L16
a4	20	X	X	X	X					X	X			X	X	X	X
b4	20	X	X	X	X	X	X			X	X	X	X				
c4	20	X		X		X		X		X		X		X	X	X	X
d4	20		X		X		X		X		X		X	X	X	X	X
e4	20	X	X					X	X			X	X	X	X	X	X
f4	20					X	X			X	X	X	X	X	X	X	X
g4	20	X		X	X	X		X		X	X	X				X	X
h4	20		X	X	X		X		X	X	X		X	X		X	
i4	20	X		X	X	X		X	X	X	X	X				X	
j4	20		X	X	X		X	X		X	X		X			X	X
		L1	L2	L3	L4	L5	L6	L7	L8	L9	L10	L11	L12	L13	L14	L15	L16
a5	16	X	X	X	X					X	X	X	X				
b5	16	X		X		X		X		X		X				X	X
c5	16		X		X		X		X		X		X			X	X
d5	16			X	X					X	X			X	X	X	X
e5	16	X		X				X	X	X		X				X	X
f5	16	X			X	X		X			X	X			X	X	
g5	16		X	X			X	X		X			X	X		X	
h5	16		X	X			X	X			X	X			X		X
i5	16	X		X	X			X	X	X	X	X					
j5	16		X	X	X	X	X			X	X		X				
		L1	L2	L3	L4	L5	L6	L7	L8	L9	L10	L11	L12	L13	L14	L15	L16
a6	12	X	X	X	X	X	X										
b6	12							X	X	X	X	X	X				
c6	12	X		X		X		X		X		X					
d6	12		X		X		X		X		X		X				
e6	12		X	X			X				X	X				X	
f6	12	X			X			X		X			X			X	
g6	12	X		X		X			X		X		X				
h6	12		X		X			X		X		X				X	
i6	12				X						X			X	X	X	X
j6	12			X	X					X	X			X		X	

Table A.3. Continued.

Model Name	Transducers Used	Gage Locations Used (Marked with X)															
		L1	L2	L3	L4	L5	L6	L7	L8	L9	L10	L11	L12	L13	L14	L15	L16
a7	8			X						X	X					X	
b7	8				X					X	X					X	
c7	8	X			X						X					X	
d7	8	X		X						X	X						
e7	8				X						X			X	X		
f7	8			X	X					X						X	
g7	8			X		X					X	X					
h7	8				X				X	X		X					
i7	8			X		X					X					X	
j7	8			X							X	X				X	

Table A.4. Bridge #2: Additional modeling optimized structural property results.

Model Name	Gages	GS1 (in^4)	GS2 (in^4)	GP1 (in^4)	GP2 (in^4)	FB (in^4)	Deck (ksi)	Spring (k-in/rad)
a1	32	25018	24178	37254	44773	4756	2883	3454400
b1	32	25085	24291	37303	46164	4891	1819	3461300
a2	28	25458	24166	42746	46451	5088	1322	3554900
b2	28	24996	24816	30568	46952	5017	1505	3427400
c2	28	24503	23536	36733	45610	4308	4272	3413200
d2	28	25450	24721	28992	46794	5054	1412	3527600
e2	28	25456	24059	44085	46498	5061	1388	3557800
f2	28	29649	24228	37842	46346	4923	1738	944800
g2	28	25211	24537	34308	45515	5018	1499	3479700
h2	28	25157	24512	34476	44088	4955	1663	3471800
i2	28	24700	23784	36928	45823	4332	3402	3428200
j2	28	24776	24353	37945	46592	5117	1249	3380600
a3	24	23744	22690	35839	44957	147	8587	3374100
b3	24	25175	25264	28893	47500	5198	1048	3478400
c3	24	24929	24039	28628	46318	4631	3453	3479100
d3	24	25173	24232	42725	44732	5106	1274	3788000
e3	24	25462	24821	30772	45982	5048	1425	3094700
f3	24	25175	24112	44097	45877	5080	1340	3794000
g3	24	25922	24739	29190	45442	5084	1334	3192200
h3	24	25199	24339	44325	46719	5310	7638	3483900
i3	24	25578	25122	30816	48179	5270	8632	3541800
j3	24	26367	24003	44397	46620	5080	1341	2898300

Table A.4. Continued.

Model Name	Gages	GS1 (in^4)	GS2 (in^4)	GP1 (in^4)	GP2 (in^4)	FB (in^4)	Deck (ksi)	Spring (k-in/rad)
a4	20	25211	26128	27411	30812	5248	919	3740600
b4	20	24238	22902	42857	45578	147	7895	3483900
c4	20	24900	24387	44334	44994	5322	730	3708400
d4	20	26054	25025	31099	48303	5290	813	3193700
e4	20	28018	25076	28506	48630	5442	436	4105300
f4	20	29436	23018	49964	46622	5236	944	1739500
g4	20	24592	23433	42192	44181	4558	3618	3742200
h4	20	25129	24358	30519	45789	4836	2724	3065700
i4	20	24035	23469	33575	46457	4004	5238	3630900
j4	20	25341	23281	43462	45944	4610	3484	3205900
a5	16	24005	23643	29829	46313	147	6742	3395300
b5	16	24351	23541	43892	44519	4922	2684	3649200
c5	16	25717	24524	30778	48003	5126	2174	3165000
d5	16	29390	26269	26824	31246	5272	873	1037000
e5	16	24435	23928	28777	44766	4864	2847	3653200
f5	16	25782	24374	44581	45715	5143	1227	3937700
g5	16	25447	23887	45762	46630	5424	1209	3177000
h5	16	25023	24027	45191	45269	4363	2221	3127400
i5	16	23668	22995	27658	42924	29278	7575	3646400
j5	16	24689	22913	43172	46075	1174	7659	3135300
a6	12	23139	28148	40078	30804	37	9706	3434900
b6	12	53797	21686	28782	44789	2348	6800	1500000
c6	12	22913	21947	42330	43442	18	9975	3587400
d6	12	24693	23310	29731	46913	29766	7113	3108800
e6	12	24520	23753	43844	45306	4614	3629	3077700
f6	12	25396	23824	41346	47947	4860	2982	3934200
g6	12	22293	22804	29482	46243	3207	8400	3383200
h6	12	26197	23025	42153	44669	4632	3571	3360500
i6	12	32328	26060	24950	37556	5964	1800	1500000
j6	12	29071	25972	26805	31133	5323	1467	1094000
a7	8	26910	25260	27151	30997	4671	3463	1406400
b7	8	34337	25479	25886	31502	4789	3152	23438
c7	8	25214	25480	27081	36457	5132	2254	3859400
d7	8	23054	24366	28504	32690	398	6285	3473600
e7	8	33684	26076	26640	35447	4976	1271	23438
f7	8	27275	25223	26423	29067	4747	3261	1760600
g7	8	23301	23406	41222	44680	147	7772	3392000
h7	8	32728	22776	18785	45172	27348	6800	1500000
i7	8	24103	23966	43974	39671	4694	3404	3453800
j7	8	26008	24981	28423	46690	4955	2740	1978800

Table A.5. Bridge #2: Additional model rating results.

Model Name	Transducers Used	GS1 (in^4)	GS2 (in^4)	GP1 (in^4)	GP2 (in^4)	FB (in^4)	OVERALL RATING
Espen's	32	1.4	0.88	1.36	1.38	0.82	0.82
a1	32	1.57	1.18	0.83	0.85	0.83	0.83
b1	32	1.56	1.17	0.82	0.83	0.76	0.76
a2	28	1.57	1.18	0.77	0.84	0.72	0.72
b2	28	1.52	1.13	0.91	0.81	0.74	0.74
c2	28	1.6	1.2	0.84	0.84	0.95	0.84
d2	28	1.51	1.12	0.93	0.8	0.73	0.73
e2	28	1.58	1.19	0.76	0.84	0.73	0.73
f2	28	1.3	1.17	0.81	0.83	0.75	0.75
g2	28	1.54	1.14	0.85	0.82	0.73	0.73
h2	28	1.54	1.14	0.85	0.84	0.75	0.75
i2	28	1.58	1.19	0.83	0.84	0.89	0.83
j2	28	1.56	1.16	0.82	0.82	0.72	0.72
a3	24	1.64	1.24	0.86	0.85	19.1	0.85
b3	24	1.51	1.11	0.94	0.8	0.7	0.7
c3	24	1.54	1.15	0.94	0.81	0.87	0.81
d3	24	1.59	1.18	0.77	0.85	0.72	0.72
e3	24	1.5	1.12	0.9	0.81	0.73	0.73
f3	24	1.59	1.19	0.76	0.85	0.72	0.72
g3	24	1.48	1.12	0.92	0.81	0.72	0.72
h3	24	1.57	1.18	0.76	0.84	0.68	0.68
i3	24	1.51	1.12	0.9	0.8	0.69	0.69
j3	24	1.52	1.19	0.75	0.84	0.72	0.72
a4	20						
b4	20						
c4	20						
d4	20						
e4	20						
f4	20						
g4	20						
h4	20						
i4	20						
j4	20						
a5	16	1.59	1.18	0.94	0.82	15.36	0.82
b5	16	1.62	1.21	0.76	0.86	0.81	0.76
c5	16	1.5	1.14	0.91	0.8	0.77	0.77
d5	16	1.27	1.03	0.95	0.95	0.69	0.69
e5	16	1.55	1.14	0.93	0.82	0.82	0.82
f5	16	1.59	1.19	0.75	0.85	0.72	0.72
g5	16	1.55	1.2	0.74	0.84	0.71	0.71
h5	16	1.57	1.2	0.76	0.86	0.81	0.76
i5	16	1.61	1.2	0.98	0.85	0.66	0.66
j5	16	1.62	1.27	0.79	0.87	2.72	0.79

Table A.6. Bridge #3: Transducer locations used for additional modeling.

Model Name	Transducers Used	Transducer Locations Used (Marked with X)														
		L1	L2	L3	L4	L5	L6	L7	L8	L9	L10	L11	L12	L13	L14	L15
opt	20	X	X	X	X	X	X	X	X	X	X	X	X	X	X	X
a1	20	X	X	X	X	X	X	X	X	X	X	X	X	X	X	X
b1	20	X	X	X	X	X	X	X	X	X	X	X	X	X	X	X
a2	16	X		X		X	X	X	X	X	X	X		X		X
b2	16	X	X	X	X	X	X		X		X	X	X	X	X	X
c2	16	X		X	X	X	X		X	X	X	X		X	X	X
d2	16	X	X	X		X	X	X	X		X	X	X	X		X
e2	16	X	X		X	X	X	X		X	X	X	X		X	X
f2	16	X	X	X	X	X	X	X			X	X	X	X	X	X
g2	16	X	X	X	X	X	X			X	X	X	X	X	X	X
h2	16	X	X	X	X	X	X	X	X	X	X			X		
i2	16			X			X	X	X	X	X	X	X	X	X	X
j2	16	X	X	X			X	X	X	X	X			X	X	X
		L1	L2	L3	L4	L5	L6	L7	L8	L9	L10	L11	L12	L13	L14	L15
a3	12	X		X		X	X		X		X	X		X		X
b3	12	X			X	X	X			X	X	X			X	X
c3	12	X	X			X	X	X			X	X	X			X
d3	12						X		X	X	X	X		X	X	X
e3	12	X		X	X	X	X		X		X			X		X
f3	12	X	X	X		X	X	X	X		X					
g3	12	X				X	X		X		X	X	X		X	X
h3	12	X	X		X	X	X		X		X	X				X
i3	12					X	X	X	X		X	X		X		X
j3	12	X		X	X	X	X	X			X	X	X			
		L1	L2	L3	L4	L5	L6	L7	L8	L9	L10	L11	L12	L13	L14	L15
a4	8						X		X		X	X				X
b4	8	X				X	X		X		X					
c4	8						X	X			X	X	X			
d4	8	X				X	X			X	X					

Table A.7. Bridge #3: Additional modeling results.

Model Name	Transducers Used	NE MS (in^4)	OE MS (in^4)	OI MS (in^4)	Deck (ksi)	Spring (k-in/rad)	NE Abut (in^4)	OE Abut (in^4)	OI Abut (in^4)
opt	20	11720	11500	3595	4990	944000	1160	1160	1255
a1	20	13969	14017	2921	4300	911230	1269	1134	749
b1	20	14387	15028	2403	9437	1092200	1708	1474	486
a2	16	14523	15017	2356	9716	531600	2008	1859	592
b2	16	16088	16474	1514	14054	1816300	1627	1331	128
c2	16	14736	16210	1957	11149	607670	1963	1646	370
d2	16	15613	14702	2227	11109	793930	1580	1566	412
e2	16	15239	15963	2133	8511	1501200	2053	1690	460
f2	16	16359	16011	1902	10090	1415500	2007	1770	312
g2	16	16304	16864	1738	8783	1313800	2382	1980	430
h2	16	14391	15122	2492	9206	1302000	1058	1046	532
i2	16	13312	14808	2579	9194	1380200	2383	1626	568
j2	16	13583	14686	2481	9435	984880	1276	1805	563
		NE MS (in^4)	OE MS (in^4)	OI MS (in^4)	Deck (ksi)	Spring (k-in/rad)	NE Abut (in^4)	OE Abut (in^4)	OI Abut (in^4)
a3	12	16015	16369	1612	13808	1821600	1650	1353	128
b3	12	16247	16765	1682	8730	1486900	2171	1794	350
c3	12	16412	16035	2005	9887	1460100	2143	1862	334
d3	12	15714	16011	2039	12379	601060	839	1580	339
e3	12	13433	14912	2419	10061	1163600	2735	1737	643
f3	12	15675	14931	2242	10990	1005900	1312	1375	378
g3	12	16023	16488	1540	14121	1912800	1648	1326	149
h3	12	15533	15560	2308	12263	499050	2085	1926	353
i3	12	15198	14478	2482	10729	1427600	3197	1482	819
j3	12	16288	15885	1963	9775	1573000	1871	1110	282
a4	8	15750	15483	7045	10895	1104200	3637	2407	182
b4	8	17020	17586	2358	12224	250000	2557	2594	2552
c4	8	14265	14798	2376	9087	1020500	3235	1603	444
d4	8	15500	15556	1950	6547	500000	2378	2329	2317

Table A.8. Bridge #3: Additional model rating results.

Model Name	Transducers Used	Rating Model Used	NE MS (in^4)	OE MS (in^4)	OI MS (in^4)	NE Abut (in^4)	OE Abut (in^4)	OI Abut (in^4)	Lowest Member Rat.	Lowest Rating
opt	20	rat1	1.23	1.3	1.67	3.2	3.42	3.92	1.23	
	20	rat3	1.24	1.3	1.68	3.75	4.07	3.97	1.24	
	20	rat5	1.4	1.45	2.03	4.21	4.49	5.17	1.4	1.23
a1	20	rat1	1.12	1.18	1.77	2.84	3.1	4.62	1.12	
	20	rat3	1.13	1.18	1.77	3.37	3.74	4.65	1.13	
	20	rat5	1.26	1.3	2.16	3.73	4.08	6.08	1.26	1.12
b1	20	rat1	1.02	1.03	2.56	2.87	3.12	9.05	1.02	
	20	rat3	1.03	1.05	2.58	3.35	3.72	9.05	1.03	
	20	rat5	1.15	1.14	3.24	3.72	4.04	12.27	1.14	1.02
a2	16	rat1	0.89	0.89	2.48	2.19	2.31	6.96	0.89	
	16	rat3	0.91	0.92	2.52	2.65	2.85	7.18	0.91	
	16	rat5	1	0.99	3.12	2.88	3.03	9.4	0.99	0.89
b2	16	rat1	0.98	0.99	4.34	3.41	3.83	41.16	0.98	
	16	rat3	0.99	1	4.37	3.91	4.47	41.16	0.99	
	16	rat5	1.1	1.09	5.68	4.36	4.82	59.77	1.09	0.98
c2	16	rat1	0.87	0.86	3	2.27	2.44	11.15	0.86	
	16	rat3	0.89	0.88	3.04	2.73	3	11.37	0.88	
	16	rat5	0.97	0.95	3.83	2.96	3.19	15.18	0.95	0.86
d2	16	rat1	0.92	0.95	2.8	2.64	2.8	10.63	0.92	
	16	rat3	0.94	0.97	2.83	3.15	3.39	10.73	0.94	
	16	rat5	1.04	1.05	3.56	3.44	3.64	14.37	1.04	0.92
e2	16	rat1	1.03	1.05	2.73	2.93	3.21	9.58	1.03	
	16	rat3	1.04	1.06	2.74	3.38	3.78	9.58	1.04	
	16	rat5	1.16	1.16	3.48	3.78	4.13	13.42	1.16	1.03
f2	16	rat1	0.97	1	3.14	2.84	3.12	13.44	0.97	
	16	rat3	0.99	1.01	3.15	3.3	3.67	13.44	0.99	
	16	rat5	1.09	1.1	4.04	3.66	3.99	18.91	1.09	0.97
g2	16	rat1	0.95	0.97	3.13	2.62	2.86	10.36	0.95	
	16	rat3	0.96	0.98	3.15	3.05	3.39	10.36	0.96	
	16	rat5	1.06	1.07	4.04	3.38	3.67	14.77	1.06	0.95
h2	16	rat1	1.06	1.08	2.51	3.54	3.72	8.64	1.06	
	16	rat3	1.08	1.09	2.52	4.13	4.42	8.64	1.08	
	16	rat5	1.2	1.2	3.16	4.57	4.77	11.81	1.2	1.06
i2	16	rat1	1.1	1.12	2.48	2.95	3.37	8.38	1.1	
	16	rat3	1.11	1.13	2.48	3.37	3.95	8.38	1.11	
	16	rat5	1.24	1.24	3.11	3.81	4.34	11.47	1.24	1.1
j2	16	rat1	1.03	1.03	2.48	3.1	2.87	8.05	1.03	
	16	rat3	1.05	1.04	2.5	3.65	3.43	8.05	1.04	
	16	rat5	1.16	1.13	3.13	4.03	3.72	10.84	1.13	1.03

Table A.8. Continued.

Model Name	Transducers Used	Rating Model Used	NE MS (in^4)	OE MS (in^4)	OI MS (in^4)	NE Abut (in^4)	OE Abut (in^4)	OI Abut (in^4)	Lowest Member Rat.	Lowest Rating
a3	12	rat1	0.99	1	4.11	3.4	3.81	40.26	0.99	
	12	rat3							0	
	12	rat5							0	0.99
b3	12	rat1	0.97	0.98	3.21	2.78	3.05	12.13	0.97	
	12	rat3							0	
	12	rat5							0	0.97
c3	12	rat1	0.98	1.01	3.02	2.82	3.11	13.11	0.98	
	12	rat3							0	
	12	rat5							0	0.98
d3	12	rat1	1.05	1.05	2.64	2.69	3.1	8.07	1.05	
	12	rat3							0	
	12	rat5							0	1.05
e3	12	rat1	0.88	0.87	3.03	3.23	2.54	12.48	0.87	
	12	rat3							0	
	12	rat5							0	0.87
f3	12	rat1	0.97	1	2.83	3.03	3.16	11.78	0.97	
	12	rat3							0	
	12	rat5							0	0.97
g3	12	rat1	1	1	4.32	3.47	3.91	36.42	1	
	12	rat3							0	
	12	rat5							0	1
h3	12	rat1	0.85	0.85	2.76	2.14	2.26	11.33	0.85	
	12	rat3							0	
	12	rat5							0	0.85
i3	12	rat1	1.06	1.1	2.73	2.75	3.58	7.62	1.06	
	12	rat3							0	
	12	rat5							0	1.06
j3	12	rat1	0.99	1.03	3.04	2.98	3.71	14.94	0.99	
	12	rat3							0	
	12	rat5							0	0.99
a4	8	rat1	1.22	1.28	1.58	2.5	2.92	15.7	1.22	
	8	rat3							0	
	8	rat5							0	1.22
b4	8	rat1	0.75	0.74	2.59	1.79	1.82	3.47	0.74	
	8	rat3							0	
	8	rat5							0	0.74
c4	8	rat1	0.99	1.02	2.54	2.39	2.96	9.29	0.99	
	8	rat3							0	
	8	rat5							0	0.99
d4	8	rat1	0.85	0.87	2.41	2	2.09	3.7	0.85	
	8	rat3							0	
	8	rat5							0	0.85

APPENDIX B

ADDITIONAL MODELING FROM CHAPTER 2 – BRIDGE #1

B.1 Introduction & Methods

At the request of the Program of Study Committee, an additional group of models were created for Bridge #1 from Chapter 2. The modeling was approached in a systematic manner rather than the more random approach presented in Chapter 2. In this new modeling, a series of models were developed that created a data set that would progress through the reduction in transducers resulting in a visible cause and effect relationship between model optimization parameters and the transducer locations employed in the modeling.

Each new model was developed from the original optimized model utilizing all 40 transducers. Four transducers, two locations, were then removed and the model optimized with the reduced transducer data. Ten different models were created with four transducers removed, each model with a unique transducer configuration. The series of models utilizing 36 transducers were named 2A through 2J. Each of those models was then used to create another series of models with further reductions in the number of transducers used. This was done until only eight transducers remained. The impact of specific transducer locations and data was visible due to the fact that the same transducers removed in model using 36 transducer were removed in the model using 32 transducers and so on. Figure B.1 illustrates the process for this new modeling while Fig. B.2 provides an illustration of the transducer locations used in the field testing and modeling of Bridge #1.

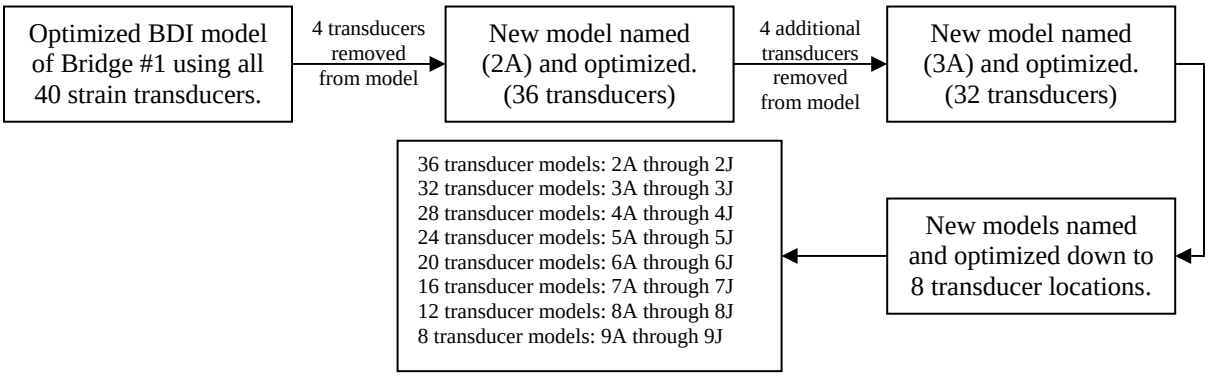

Figure B.1. Illustration of process for new modeling.

B.2 Results

Transducer locations used in the additional modeling are presented in Table B.1 while the results of the modeling are presented in Table B.2. Figure B.3 presents the modeling results in graphic form. Additional load ratings were not calculated for this additional modeling as the results from the additional modeling presented in this appendix closely resemble the results of the Chapter 2 work.

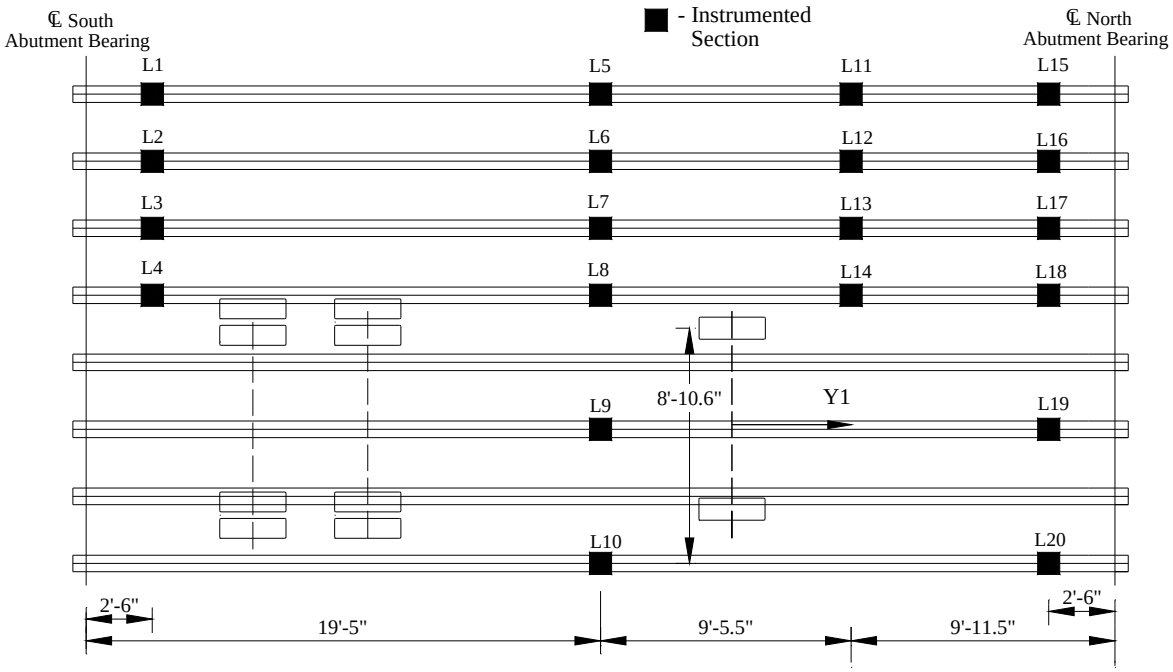

Figure B.2. Plan view of gage locations, truck paths, and bridge dimensions or Bridge #1.

Table B.1. Bridge #1: Transducer locations used for additional systematic modeling.

Model	Transducers	Transducer Locations Used (Marked with X)																			
Name	Used	L1	L2	L3	L4	L5	L6	L7	L8	L9	L10	L11	L12	L13	L14	L15	L16	L17	L18	L19	L20
1A	40	X	X	X	X	X	X	X	X	X	X	X	X	X	X	X	X	X	X	X	X
1B	40	X	X	X	X	X	X	X	X	X	X	X	X	X	X	X	X	X	X	X	X
2A	36	X	X		X	X	X	X	X	X	X	X	X	X	X	X	X		X	X	X
2B	36	X	X	X	X	X	X	X	X	X	X	X			X	X	X	X	X	X	X
2C	36	X			X	X	X	X	X	X	X	X	X	X	X	X	X	X	X	X	X
2D	36	X	X	X	X	X	X	X	X	X	X		X		X	X	X	X	X	X	X
2E	36	X	X	X	X	X	X	X	X		X	X	X	X	X	X	X	X	X		X
2F	36	X	X	X	X	X	X		X	X	X	X	X	X	X	X	X		X	X	X
2G	36	X		X	X	X	X	X	X	X	X	X	X	X	X	X		X	X	X	X
2H	36	X	X		X	X	X	X	X	X	X	X	X		X	X	X	X	X	X	X
2I	36	X		X	X	X	X	X	X	X	X	X		X	X	X	X	X	X	X	X
2J	36	X	X	X	X	X	X	X		X	X	X	X	X		X	X	X	X	X	X

Table B.1. Continued.

Model	Transducers	Transducer Locations Used (Marked with X)																			
Name	Used	L1	L2	L3	L4	L5	L6	L7	L8	L9	L10	L11	L12	L13	L14	L15	L16	L17	L18	L19	L20
3A	32	X	X		X	X	X	X	X	X	X	X			X	X	X		X	X	X
3B	32	X			X	X	X	X	X	X	X	X			X	X	X	X	X	X	X
3C	32	X			X	X	X	X	X	X	X	X		X	X	X		X	X	X	X
3D	32	X	X	X	X	X	X	X	X	X	X					X	X	X	X	X	X
3E	32	X	X	X	X	X	X	X	X		X	X	X			X	X	X	X		X
3F	32	X	X		X	X	X		X	X	X	X	X		X	X	X		X	X	X
3G	32	X		X	X	X	X	X	X	X	X	X	X	X	X	X				X	X
3H	32	X	X		X	X	X	X	X		X	X	X		X	X	X	X	X		X
3I	32	X		X	X	X	X	X	X	X	X			X		X	X	X	X	X	X
3J	32	X	X	X	X	X	X	X		X	X		X			X	X	X	X	X	X
		L1	L2	L3	L4	L5	L6	L7	L8	L9	L10	L11	L12	L13	L14	L15	L16	L17	L18	L19	L20
4A	28	X	X		X	X	X	X	X	X	X					X	X		X	X	X
4B	28					X	X	X	X	X	X	X			X	X	X	X	X	X	X
4C	28	X			X	X		X	X	X	X	X			X	X		X	X	X	X
4D	28	X	X	X	X	X	X	X	X		X					X	X	X	X		X
4E	28	X	X	X	X	X			X		X	X	X			X	X	X	X		X
4F	28	X			X	X	X		X	X	X	X			X	X	X		X	X	X
4G	28	X		X	X	X	X	X	X	X	X	X	X	X	X	X					
4H	28	X	X		X	X	X	X	X		X				X	X	X	X	X		X
4I	28	X		X	X	X	X	X	X		X					X	X	X	X	X	X
4J	28	X	X	X	X	X		X		X	X					X	X	X	X	X	X
		L1	L2	L3	L4	L5	L6	L7	L8	L9	L10	L11	L12	L13	L14	L15	L16	L17	L18	L19	L20
5A	24	X	X		X	X		X		X	X					X	X		X	X	X
5B	24					X			X	X	X	X			X	X	X	X	X	X	X
5C	24	X			X	X		X	X	X	X					X		X	X	X	X
5D	24	X		X	X	X		X	X		X					X	X	X	X		X
5E	24	X	X	X	X	X			X		X	X				X		X	X		X
5F	24	X			X	X	X		X	X	X					X	X		X	X	X
5G	24	X			X	X	X	X	X	X	X	X	X	X	X						
5H	24	X			X	X	X	X	X		X					X	X	X	X		X
5I	24	X		X	X	X			X		X					X	X	X	X	X	X
5J	24	X	X	X	X	X		X		X	X					X			X	X	X
		L1	L2	L3	L4	L5	L6	L7	L8	L9	L10	L11	L12	L13	L14	L15	L16	L17	L18	L19	L20
6A	20	X			X	X		X		X	X					X			X	X	X
6B	20					X			X	X	X					X	X	X	X	X	X
6C	20	X			X	X		X	X		X					X		X	X		X
6D	20	X		X	X	X		X	X		X					X		X	X		
6E	20	X			X	X			X		X	X				X		X	X		X
6F	20	X			X	X	X		X	X	X					X			X		X
6G	20	X			X	X	X	X	X	X	X	X			X						
6H	20	X			X	X	X	X	X		X					X			X		X
6I	20	X			X	X			X		X					X	X	X	X		X
6J	20	X	X	X	X	X				X	X					X				X	X

Table B.1. Continued.

Model	Transducers	Transducer Locations Used (Marked with X)																			
Name	Used	L1	L2	L3	L4	L5	L6	L7	L8	L9	L10	L11	L12	L13	L14	L15	L16	L17	L18	L19	L20
7A	16	X			X	X				X	X					X				X	X
7B	16					X			X	X	X					X			X	X	X
7C	16	X			X	X			X		X					X			X		X
7D	16	X			X	X		X	X		X					X			X		
7E	16				X	X			X		X	X				X			X		X
7F	16	X				X	X		X	X	X					X					X
7G	16	X			X	X			X	X	X	X			X						
7H	16					X	X	X	X		X					X			X		X
7I	16	X				X			X		X					X	X	X			X
7J	16	X			X	X				X	X					X				X	X
		L1	L2	L3	L4	L5	L6	L7	L8	L9	L10	L11	L12	L13	L14	L15	L16	L17	L18	L19	L20
8A	12	X			X	X					X					X					X
8B	12					X				X	X					X				X	X
8C	12	X			X	X			X							X			X		
8D	12	X			X				X		X					X			X		
8E	12				X	X			X		X					X					X
8F	12					X	X		X	X	X										X
8G	12	X			X	X			X	X	X										
8H	12					X	X	X			X					X					X
8I	12	X				X			X		X					X					X
8J	12	X			X	X					X					X					X
		L1	L2	L3	L4	L5	L6	L7	L8	L9	L10	L11	L12	L13	L14	L15	L16	L17	L18	L19	L20
9A	8					X					X					X					X
9B	8					X				X						X				X	
9C	8				X	X			X										X		
9D	8				X				X		X								X		
9E	8				X	X			X							X					
9F	8					X	X			X	X										
9G	8	X			X					X	X										
9H	8					X		X			X					X					
9I	8					X			X		X					X					
9J	8	X			X						X										X

Table B.2. Bridge #1: Additional systematic modeling results.

Model Name	Transducers Used	I (in^4)	E (ksi)	k (k-in/rad)	Total Error	% Error	Scale Error	Corr. Coef.
1A	40	1279	838	26500	3330	2.1	1.8	0.989
1B	40	1279	841	26036	3335	2.1	1.8	0.9893
2A	36	1279	820	26138	3093	2.1	1.7	0.9895
2B	36	1280	889	25330	3005	2.2	1.8	0.9888
2C	36	1277	861	26740	3098	2.1	1.8	0.9896
2D	36	1283	884	25809	3095	2.3	1.9	0.9884
2E	36	1270	818	25521	2889	2.1	1.8	0.9892
2F	36	1276	826	26322	3043	2.3	1.9	0.9882
2G	36	1281	867	26044	3127	2.1	2	0.9896
2H	36	1285	853	26003	3087	2.2	1.8	0.9887
2I	36	1272	896	25940	3011	2	1.9	0.9897
2J	36	1266	745	25487	2899	2.2	1.7	0.9889
3A	32	1280	867	25224	2766	2.2	1.7	0.989
3B	32	1278	914	25916	2768	2.2	1.8	0.9891
3C	32	1279	893	24890	2825	2	1.9	0.9898
3D	32	1271	839	24175	2697	2.1	1.8	0.9894
3E	32	1266	746	24626	2559	2.1	1.7	0.9895
3F	32	1283	841	26295	2792	2.5	1.8	0.9874
3G	32	1284	866	26390	2797	1.8	1.9	0.9909
3H	32	1277	831	25293	2657	2.3	1.8	0.9885
3I	32	1265	853	24717	2697	1.9	1.8	0.9904
3J	32	1271	781	25142	2664	2.5	1.8	0.9876
4A	28	1274	812	23653	2458	2	1.6	0.9897
4B	28	1258	902	30499	2361	1.9	1.7	0.9903
4C	28	1291	1029	24771	2439	2.1	2	0.9893
4D	28	1256	789	23327	2260	2.1	1.8	0.9896
4E	28	1267	835	24595	2168	2.5	1.9	0.9872
4F	28	1275	902	26241	2476	2.4	1.9	0.9878
4G	28	1291	829	25916	2468	1.6	1.7	0.9919
4H	28	1270	897	23829	2359	2.3	1.8	0.9884
4I	28	1246	844	25078	2314	2.2	1.9	0.9891
4J	28	1271	946	23996	2225	2.5	1.9	0.9874
5A	24	1273	913	23493	1988	2.4	1.7	0.9877
5B	24	1269	1033	30426	1951	2.2	1.9	0.989
5C	24	1282	994	23077	2125	2	1.9	0.99
5D	24	1261	967	23620	1869	2	2	0.9899
5E	24	1260	842	22711	1880	2.5	2	0.9877
5F	24	1266	838	24492	2175	2.3	1.8	0.9885
5G	24	1313	825	21541	2245	1.6	1.6	0.9922
5H	24	1259	816	23221	2021	2	1.8	0.99
5I	24	1237	961	25081	1895	2.7	2.1	0.9864
5J	24	1278	926	22863	2008	2.4	1.8	0.9878

Table B.2. Continued

Model Name	Transducers Used	I (in^4)	E (ksi)	k (k-in/rad)	Total Error	% Error	Scale Error	Corr. Coef.
6A	20	1282	971	22784	1766	2.3	1.8	0.9883
6B	20	1255	980	28430	1657	2.1	1.8	0.9897
6C	20	1272	960	21497	1674	2	1.9	0.9902
6D	20	1267	941	22922	1650	1.9	1.8	0.9907
6E	20	1265	877	22420	1640	2.3	2	0.9882
6F	20	1290	813	20450	1887	2.1	1.8	0.9894
6G	20	1328	875	18095	1900	1.6	1.5	0.9922
6H	20	1271	789	20817	1787	1.9	1.7	0.9904
6I	20	1251	938	23293	1608	2.5	2	0.9876
6J	20	1286	956	22352	1643	2.6	2	0.987
7A	16	1293	1018	22135	1398	2.4	2	0.9877
7B	16	1257	964	28460	1452	2	1.8	0.9901
7C	16	1263	910	21011	1379	2.4	2	0.9882
7D	16	1275	906	21265	1407	1.8	1.5	0.9911
7E	16	1257	825	23818	1378	2.2	1.7	0.9891
7F	16	1296	833	20804	1442	1.6	1.8	0.9922
7G	16	1344	1017	17342	1490	1.7	1.7	0.9916
7H	16	1245	773	26538	1424	1.6	1.3	0.9918
7I	16	1252	996	25618	1164	1.6	2	0.9919
7J	16	1293	1018	22135	1398	2.4	2	0.9877
8A	12	1231	677	20520	938	2.6	2	0.9871
8B	12	1256	1026	30547	1026	1.9	1.6	0.9903
8C	12	1279	838	21485	1069	2.5	1.8	0.9874
8D	12	1255	993	24830	1066	2.5	1.9	0.9877
8E	12	1273	907	21372	1056	1.7	1.9	0.9915
8F	12	1328	800	14330	1202	1.4	1.7	0.993
8G	12	1355	956	10585	1158	1.4	1.4	0.993
8H	12	1232	679	26574	1002	1.4	1.2	0.9928
8I	12	1269	959	22420	940	1.5	2.1	0.9927
8J	12	1231	677	20520	938	2.6	2	0.9871
9A	8	1191	942	28392	598	1.7	1.5	0.9913
9B	8	1264	893	35441	669	1.8	1.2	0.9911
9C	8	1287	803	20343	839	2.2	1.4	0.989
9D	8	1266	967	22628	846	2.2	1.5	0.9892
9E	8	1292	790	22564	734	1.6	1.3	0.9919
9F	8	1605	736	0	1162	3.3	2.2	0.9926
9G	8	1369	1128	9646	753	1.8	1.4	0.9908
9H	8	1192	875	39208	612	1	1.1	0.995
9I	8	1188	931	40856	684	1.1	1.6	0.9946
9J	8	1251	859	14963	617	3	2.1	0.9851

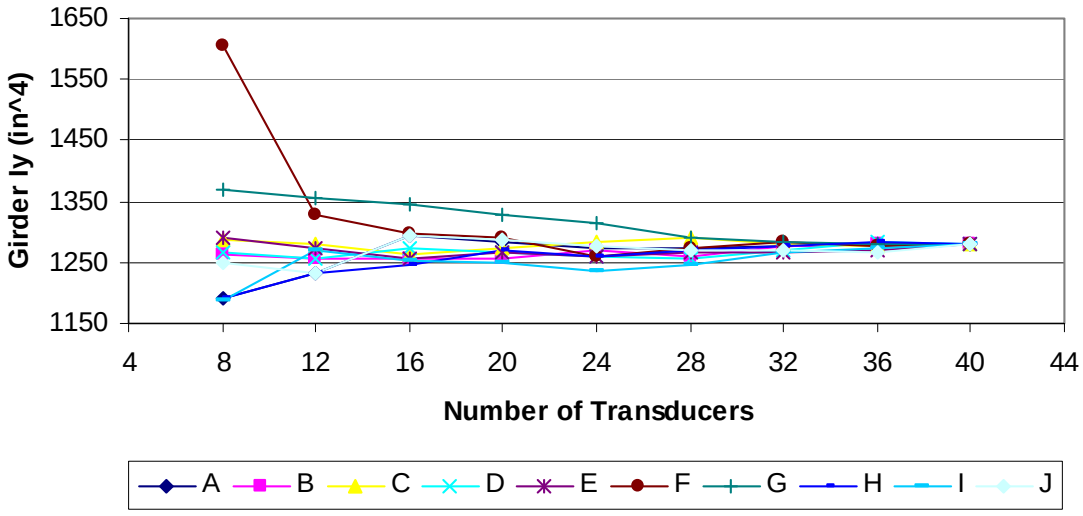

a. Bridge#1: Girder I_y versus number of transducers for additional modeling.

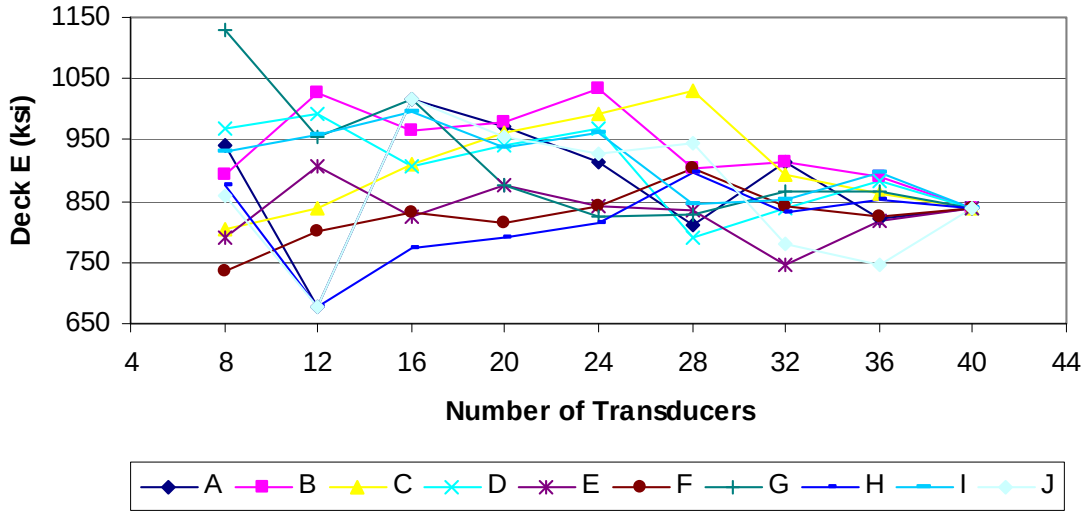

b. Bridge #1: Deck E versus number of transducers for additional modeling.

Figure B.3. Bridge #1: Results of additional modeling.

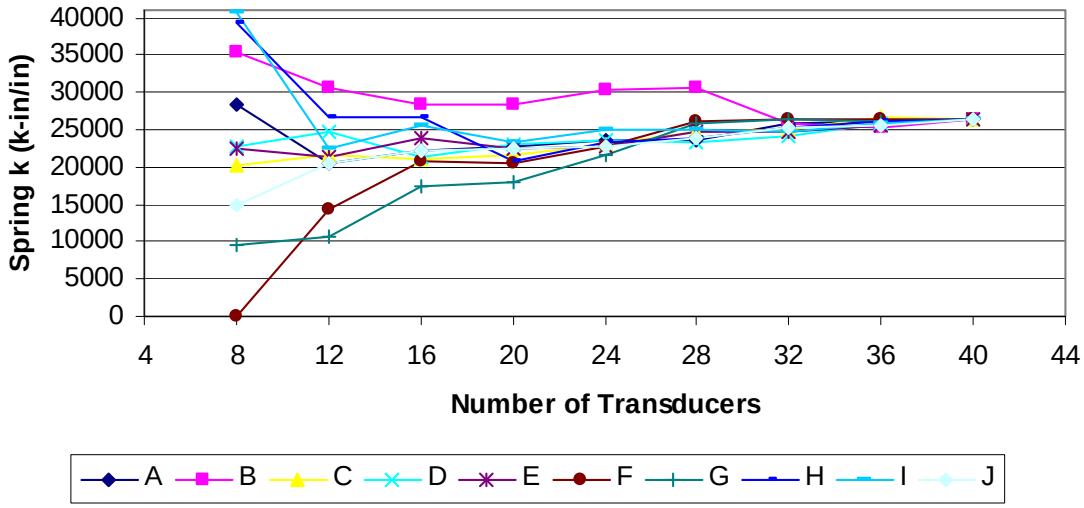

c. Bridge #1: Abutment spring k versus number of transducers for additional modeling.

Figure B.3. Continued.

As shown in Fig. B.3a and B.3c, the girder I_y values and spring k values are inversely related. As the girder I_y value increases, the spring k value decreases. This is expected given the simple span arrangement of Bridge #1. In most model groups, A through J in Fig. B.3a , where the I_y value of the girders is increasing from a full transducer layout down to only 8 transducers, the number of transducers near the abutments are decreasing. The case where I_y is a maximum is a model where no transducers near the abutments were used in the modeling. This is expected as the optimization program has only mid-span strain data to optimize the model properties. Without strain data at a number of locations along the length of the beam, the optimized I_y value is the value that fits the strain data available.

The change in the spread of the optimized model values are easily visible in the plots of the girder I_y values and spring k values as the number of transducers used in each model decreases. The deck E values are more variable and random when compared to the other two-optimization properties. There seems to be no correlation between the transducer layout and the deck E values.

B.3 Summary & Conclusion

This additional modeling created a trend line of data that one was able to follow from a full transducer layout of 40 strain transducers all the way to a reduced transducer layout of only eight strain transducers. The relationship between the girder I_y and the spring k values is easily visible in

the data plots. The increased girder Iy values were directly related to the quantity of strain transducer data at the abutments that were used in the modeling. The deck E values were more random and no distinguishable pattern between the transducer layout and the deck E values was discovered.

Given the simple layout of Bridge #1, single span with one steel girder cross-section and timber deck, it was ideal for an investigation of this type. The inclusion of abutment strain data in the modeling optimization process is important to ensure a final bridge model that accurately represents the bridge's behavior.